CR42-24, a Novel Colchicine Derivative, as a Therapy for Bladder Cancer

by

Clayton James Bell

A thesis submitted in partial fulfillment of the requirements for the degree of

Master of Science

in

Cancer Sciences

Department of Oncology

University of Alberta

Abstract

Colchicine is an anti-mitotic drug that targets unpolymerized tubulin, and inhibits microtubule polymerization. It is primarily used to treat gout but has been investigated in numerous clinical trials to treat conditions such as leukemia (ALL), prostate cancer, and inflammatory diseases. However, due to its narrow therapeutic window colchicine has had limited clinical translation. Previously, our lab has designed and synthesized a novel colchicine derivative (CR42-24) with a more favorable pharmacological profile compared to colchicine. This was accomplished by designing a structure with an increased affinity for βIII tubulin. βIII tubulin is a β-tubulin isotype that is incorporated into tubulin dimers that make up microtubules. βIII is an excellent target for novel therapies as it has low expression in healthy tissue, is overexpressed in metastatic cancers, and is a clinical marker of poor prognosis. Using cell line screening we demonstrate that CR42-24 is highly toxic to a variety of cancer types with IC50 values at low nanomolar concentrations. More specifically CR42-24 is shown to be highly effective against bladder cancer. Current chemotherapy for bladder cancer is a combination of gemcitabine and cisplatin (gem/cis). Although marginally successful, many patients develop resistance to gem/cis leaving them with limited options for a second line therapy, thus development of alternative therapies is highly desired. Using *in vitro* and *in vivo* assays we demonstrate that CR42-24 is highly effective on BC cell lines and xenografts. We also show that CR42-24 is highly synergistic with other chemotherapies, thereby increasing its therapeutic potential. Through our studies we have shown that CR42-24 is effective in treating aggressive BC and thus may serve as an alternative or second line therapy.

Preface

This thesis is an original work done by Clayton James Bell. The research project, of which this thesis is a part, were conducted with the approval of the University of Alberta Health Sciences Animal Care and Use Committee in accordance with guidelines from the Canadian Council for Animal Care under "Design of a new treatment for prostate cancer", AUP00000453, and "Oncolytic VACV in mouse models of bladder cancer", AUP00000390. In addition, patient derived models were conducted with human research ethics approval, from Health Research Ethics Board of Alberta protocol "HREBA.CC-16-0362".

Table of Contents

Table of Contents

List of Tables

List of Figures

List of Abbreviations

BC- Bladder cancer

Cis-cisplatin

Cis/gem-combination cisplatin gemcitabine

Ca/gem- combination carboplatin gemcitabine

Cys-Cysteine

DMSO-dimethyl sulfoxide

FBS-fetal bovine serum

FDA- Food and Drug Administration

ICIs- Immune checkpoint inhibitors

IC50= 50% inhibitory concentration

IV-intravenous

IP-intraperitoneal

NMIBC- non-muscle invasive bladder cancer

MAP-microtubule associated protein

mBC- metastatic bladder cancer

M-CAVI-chemotherapy combination consisting of methotrexate, carboplatin, and vinblastine

MIBC- muscle invasive bladder cancer

MT- Microtubules

MTA-microtubule targeting agent

MVAC- combination methotrexate, vinblastine, doxorubicin, and cisplatin

NAC-neoadjuvant chemotherapy

PD-1- programmed death receptor-1

PD-L1- programmed death receptor ligand 1

PI- prodium iodide

PDX-patient derived xenograft

P/S- penicillin/streptomycin

RC- radical cystectomy

ROS-reactive oxygen species

TURBT- transurethral resection of bladder tumor

Chapter 1-Introduction

1.1- Bladder Cancer

Worldwide, bladder cancer (BC) is the 9th most common cancer and is the 13th most common cause of cancer death (1). In Canada, BC is the 4th most common cancer in men and the 12th most common cancer in women; on average 9000 people are diagnosed every year with BC, and approximately 2400 people die each year (2). In the United States, the National Institute of Health (NIH) estimates that in 2018 approximately 82,000 people will be diagnosed with BC and there will be approximately 17,000 deaths (3). In Europe, in 2012 it was estimated that there were 118,000 new cases of BC diagnosed and 52,000 deaths (1). The significant incidence of BC around the world makes BC a significant problem to both patients and heath care systems.

Studies show incidence of BC is higher in men than in women occurring at a ratio of 3.2:0.9(4). Although more prevalent in men, women have a higher rate of more aggressive disease and on average have worse prognosis than men. BC incidence increases with age, and the most significant risk factor for developing BC is cigarette smoking. A recent study estimated that half of all reported cases are due to cigarette smoking (5). Other risk factors include chronic bladder inflammation due to recurrent urinary tract infections or persistent bladder stones (6).

BC originates from the epithelium (urothelium) of the inner surface of the bladder. The most common type of bladder cancer is urothelial carcinoma (90% of cases), however, squamous cell carcinoma, small-cell carcinoma, and adenocarcinoma have also been described (7). BC prognosis varies by type of disease. BC tumors that have not invaded into the muscle layers (lamina and muscularis propria) surrounding the bladder are classified as non-muscle invasive bladder cancer (NMIBC) and have a better prognosis (Figure 1.1). Disease that has breached beyond the muscle layers is classified as muscle-invasive bladder cancer (MIBC) and has a poorer prognosis (Figure 1.1).

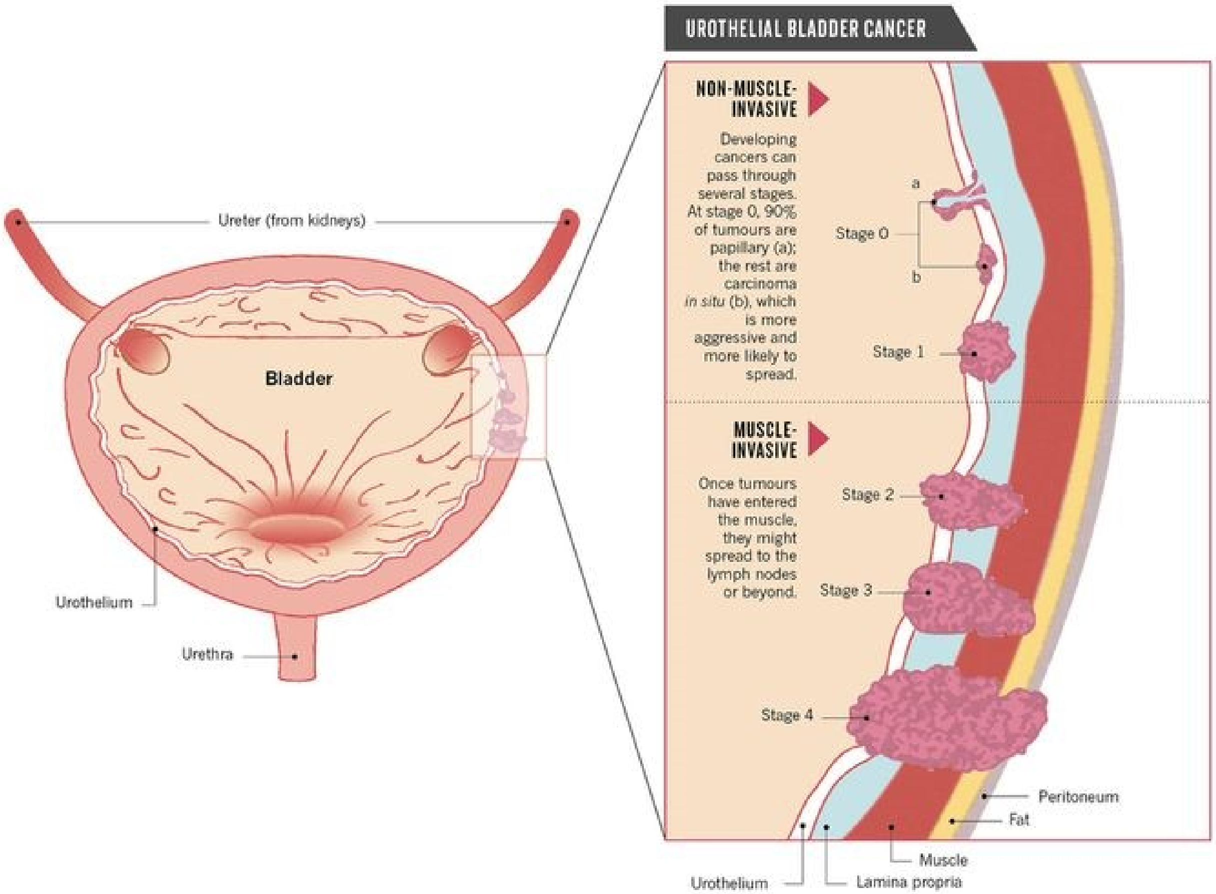

Figure 1.1- Classification of BC tumors by grade based on level of invasion into surrounding muscle layers. Stage 0 and 1 are classified as NMIBC which have not invaded into surround layers of the bladder. Stage 2-4 are classified as MIBC due to invasion into surround muscle layers of the bladder. Taken from "Unlocking Bladder Cancer" by Chris Berdik with permission from Springer Nature Publishing (2018).

Approximately 80% of patients are diagnosed with NMIBC and 20% with MIBC (4). NMIBC has an excellent prognosis with a 5-year survival rate of approximately 96% (Figure 1.2) (8). Prognosis for MIBC is poorer with a 5-year survival rate of 70% (Figure 1.2). The prognosis for MIBC patients further decreases with extent of localized invasion or the presence of lymph node metastasis. 5- year survival rate for patients with localized invasion or lymph node metastasis is 34%. Dismally, the presence of distant metastasis reduces 5- year survival rate to 5%. Of the patients diagnosed with BC only 4% are diagnosed with distant metastasis (6). Despite a relatively favorable prognosis, BC remains a severe problem for the health care system due to a high recurrence rate, inadequate response to therapies, and limited therapeutic options for patients.

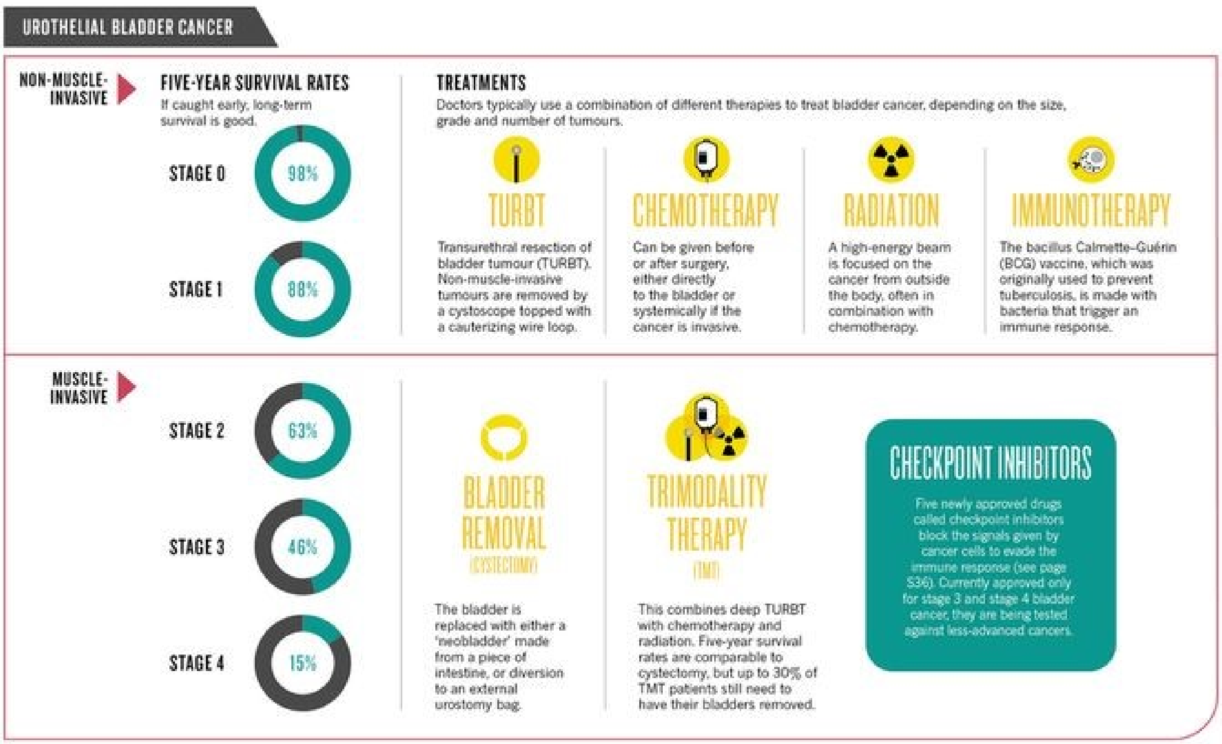

Figure 1.2- Breakdown of BC treatments for different stages of BC and their survival rates. Taken from “Unlocking Bladder Cancer” by Chris Berdik with permission from Springer Nature Publishing (2018).

1.2- Treatment of NMIBC

Treatment of BC is often multi-modal with patients receiving a combination of surgery, immunotherapy, chemotherapy, or radiation (summarized in Figure 1.2). Treatment plans vary depending on the type of disease at the time of diagnosis. Patients with NMIBC often undergo transurethral resection of bladder tumor (TURBT) in combination with other therapies. During TURBT all visible tumor is removed, underlying muscle layers are also removed to ensure complete resection of any residual disease and accurate staging of disease (9). Due to the high recurrence rate associated with TURBT alone (60-90%), patient treatments are often supplemented with intravesical adjuvant chemotherapy or immunotherapy (10). Adjuvant chemotherapy is single-agent mitomycin C, doxorubicin, or epirubicin (11). All patients receive a single adjuvant dose; however intermediate risk patients often receive multiple rounds of intravesical chemotherapy as maintenance treatment as it has been shown to reduce the risk of recurrence (11,12). Alternatively, intravesical BCG therapy can be used in place of chemotherapy and is the recommended maintenance therapy for high-risk patients (13,14). Bacillus Calmette–Guérin (BCG) therapy was established in 1976 and became FDA approved in 1990 (15). Although the mechanism of BCG treatment is not fully understood, BCG therapy has been shown to lead to the recruitment and activation of both innate and adaptive immune cells (16). Recruitment and activation of immune cells leads to the destruction of tumor cells by cytotoxic T cells (CTCs) (16). Additionally, BCG therapy has also been shown to cause tumor cell lysis directly (17,18). Treatment with BCG has been shown to significantly decrease progression rates, increase survival, and decrease rates of recurrence (9,15,19). Moreover, BCG has been shown to be superior compared to intravesical chemotherapy or TURBT alone for high-risk patients (13, 14). BCG therapy includes 4 to 6 weeks of induction therapy, followed by 3 weekly installations given every 3 months for 12-36 months (20). Although effective, failure of BCG therapy is still common, at which point patients have few therapeutic options. BCG failure is classified as the presence of disease at six months from the time of TUR or an increase in disease grade while on BCG treatment (21). The European Urology Association recommends that patients who have BCG-failure undergo radical cystectomy (RC) to have recurrent disease removed (9). Similarly, the Canadian Urology guidelines recommend RC for high-risk NMIBC patients who fail BCG therapy (15). Alternatively, intravesical chemotherapy or the use of BCG with interferon-α2a have been investigated clinically and may be used for patients who are unfit for surgery or refuse RC. In a phase II trial, intravesical gemcitabine has activity in patients and is more effective than mitomycin C; however, recurrence rate was high with only 28% of patients being recurrence-free at 1-year (22). Overall, NMIBC shows a favorable prognosis with well investigated therapeutic options. However, the high recurrence rate and disease progression make NMIBC a particularly burdensome disease to patients and to the health care system. Recently, immune checkpoint inhibitors are being investigated clinically as potential treatments for NMIBC (Table 1.3 and 1.4).

There are currently five ICIs that have been approved for the treatment of BC by the FDA. All of the five therapies: Pembrolizumab, Avelumab, Durvalumab, Atezolizumab, and Nivolumab, are of the Programmed death receptor (PD-1) or Programmed death receptor ligand-1 (PD-L1) inhibitor class which prevent the interaction of PD-1 and PD-L1 (mechanism reviewed in Pardoll, 2012 (23). The PD-1 receptor is expressed on the T-cell surface. When T-cells engage tumor cells, PD-L1 on the tumor cell surface binds to the PD-1 receptors on the T-cell inhibiting T-cell activity and preventing tumor cell lysis. By blocking the PD-1/PD-L1 interaction, ICIs prevent the inhibition of T-cells allowing the immune system to maintain the T-cell response to tumors. These therapies are breakthrough therapies for the treatment of BC and are dramatically changing the treatment paradigm of BC. These therapies are approved as both first line and second line therapies and show great promise in the treatment of both localized and metastatic bladder cancer (24) (Table 1.1 and 1.2). Compared to the current standard of care, ICIs have been shown to improve overall survival and have better safety profiles as compared to chemotherapy (25).

There are many clinical trials that are investigating ICIs as standalone treatments or in combination with other therapies (Table 1.3 and 1.4). Durvalumab (NCT02901548), atezolizumab (NCT02451423), and pembrolizumab (NCT0262596) are being tested in phase II or phase III clinical trials in BCG-refractory patients. ICIs are also being investigated in combination with many other therapies. Additionally, pembrolizumab (NCT02324582) and atezolizumab (NCT02792192) are both being examined in conjunction with BCG therapy in high-risk NMIBC patients. Results from these studies are expected in 2019. Although no results are yet available from these trials, the use of ICIs in other studies examining ICIs in advanced BC have been highly effective, which is encouraging for their use in NMIBC.

1.3-Treatment of MIBC

MIBC patients often undergo a combination of surgery, chemotherapy, and/or radiation therapy. During RC the bladder, adjacent distal ureters, surrounding fatty tissue, and nearby lymph nodes are removed. To improve patient outcomes, patients also receive neoadjuvant chemotherapy (NAC). NAC is recommended over adjuvant therapy since earlier delivery of chemotherapy is thought to prevent metastasis, treat micro-metastatic disease earlier, and patients have increased tolerance to chemotherapy (26). Based on this, it is recommended that MIBC patients undergo NAC irrespective of further treatment, even for lymph node and metastasis negative patients. Overall, meta-analysis indicates there to be a modest increase of 5% in patient survival when cisplatin-based combination therapy was used as compared to non-cisplatin based regimens (27). In another meta-analysis, it was found that pathological downstaging occurred in 72.1% of patients who underwent NAC (28). Wright et al. (2013) found that patients given cisplatin/gemcitabine (cis/gem) or methotrexate, vinblastine, doxorubicin, and cisplatin (MVAC) in the neoadjuvant setting had a higher complete response rate (CR; no detectable clinical disease) and a higher objective response rate (ORR; a reduction in tumor volume) than patients who did not receive chemotherapy (29). Overall, this data strongly supports the use of NAC for MIBC.

MVAC or cis/gem are two NAC chemotherapeutic regimens. Meta-analysis shows conflicting results as to whether MVAC or cis/gem is superior. Wright et al. (2013) found that cis/gem had a higher CR (29% vs. 22%) and ORR (56% vs. 45%) when compared to MVAC (30). However, a larger more updated meta-analysis by Drabick et al. (2016) found there was no statistically significant difference between CIS/GEM and MVAC when used as a NAC (26). Although it is not clear whether CIS/GEM or MVAC is superior, clinical data support the use of NAC before RC in the treatment of MIBC. Other therapies such as ICIs, oncolytic viruses, and targeting therapies are also currently being examined as treatments for MIBC.

As standalone treatments ICIs are being examined in both an adjuvant and a neoadjuvant setting for MIBC (Table 1.3). Additionally, other trials are currently examining ICIs in combination with other treatment modalities (Table 1.4). Although little data is available from these trials so far ICIs have been very promising as treatments for many different types of cancer and will likely be alternative treatments for patients.

1.4- Metastatic BC treatment

In patients with metastatic BC (mBC) systemic chemotherapy with platinum-based regimens is the current standard of care. However, trials with ICIs are showing great promise as a treatment for mBC (34). MVAC and cis/gem are the current chemotherapy regimens for mBC. MVAC and cis/gem increase patient survival up to 14.8 and 13.8 months respectively, with response rates of 46% and 49% (35). Despite similar response rates and OS survival rates, cis/gem is recommended due to a more favorable toxicity profile. In a phase III clinical trial cis/gem was found to have decreased adverse events and lower toxicity than MVAC (36). Based on this, it was recommended that cis/gem combination therapy be used over MVAC (6). Despite this recommendation, variability still exists with MVAC being the preferred standard of care in the US. Although cisplatin-based therapy has been found to result in increased patient survival with mBC, kidney toxicity is an undesirable side effect of cisplatin based therapy. Due to impaired kidney function and other comorbidities, as much as 50% of patients are ineligible for cisplatin-based chemotherapy (37). In the case of cisplatin-ineligibility, combination carboplatin and gemcitabine (ca/gem) is then recommended as the standard of care. Despite having a more favorable toxicity profile carboplatin-based regiments have been found to be less effective than cisplatin-based therapies (38,39). Many studies have demonstrated the superiority of cisplatin-based regimens over carboplatin-based ones. In a phase II trial, Dogliotti et al. (2007) showed that cis/gem was superior to ca/gem, with ORR being 9.1% higher in the cis/gem arm compared to ca/gem arm. Additionally, median overall survival was also increased from 9.8 months to 12.8 months in the cis/gem group. Another trial examined the use of ca/gem and compared to a modified MVAC regimen consisting of combination methotrexate, vinblastine, and carboplatin (M-CAVI) and found that ORR for M-CAVI and ca/gem were found to be 20% and 39.5%

respectively (40). As mentioned above, the 5-year survival rate of mBC patients is 5%. This is due to the high proportion of mBC patients that are unresponsive to primary therapy, ineligible for cisplatin-based therapy, the inferiority of carboplatin-based regimens, and limited second-line therapeutic options. Recently, many clinical trials have been conducted examining chemotherapy as second-line options.

Many small phase II clinical trials have investigated both single agent and combination chemotherapy as second-line therapies for mBC (41). A phase II clinical trial found that single-agent paclitaxel had a response rate of 10% and a median survival of 7.2 months (42). Other trials, however, have found that paclitaxel has a lower response rate (5-7%) and a median survival of only 6.5 months (43). In a phase III clinical trial, combination paclitaxel/gemcitabine was found to have good response rates (40%), making it a promising second-line therapy (44). Other combinations such as docetaxel, gemcitabine, and carboplatin have also been found to have an ORR rate of 56%, but this has not been investigated beyond small phase II trials (45). Despite these results, poor prognosis remain due to the lack of large phase III clinical trials in the second-line setting (46). This has left clinicians with no clear treatment guidelines and an underserved patient population. Therefore, the need for alternative therapies for mBC is highly desirable. Recently ICIs have become breakthrough therapies for a number of cancers including melanoma, non-small cell lung cancer, and recently mBC (summarized in table 1.2).

Two ICIs, pembroluzimab, and atezolizumab have been approved and are showing great promise as therapies for mBC. Atezolizumab was the first PD-1 inhibitor to be approved in BC (47). Atezolizumab is a monoclonal antibody against PD-L1 and is also approved for the treatment of melanoma, and NSCLC. In a phase I trial for metastatic BC patients atezolizumab showed an ORR rate of 21% and overall survival (OS) of 10.1 months (48). It is also undergoing a phase II clinical trial (ImVigor 210) in patients that were treatment-naïve, or cisplatin-ineligible mBC patients (49). In this trial, atezolizumab showed objective response rates (ORR) of 24% and median survival of 14.8 months. Based on these results atezolizumab was granted approval by the FDA as a treatment for metastatic bladder cancer. There are also a number of other trials examining ICIs in combination with other immune agents such as CPI-144, epacadostat, BCG, and varlilumab (Table 1.4). Together the number of combination trials currently underway and reports from other trials attest to the effectiveness of atezolizumab as a treatment for BC in both a first and second-line setting.

Pembrolizumab has also been and is currently investigated as both a first and a second line therapy for BC (50,51). A phase III trial (KEYNOTE-045) is currently underway in which pembrolizumab is being compared to single-agent chemotherapy in a second-line therapy setting. Interim reports show that compared to single-agent chemotherapy, pembrolizumab increases overall survival (10.3 months, vs. 7.4 months) and has fewer side effects. The interim results of this study make pembrolizumab the only ICI to show increased OS as compared to chemotherapy in a second-line treatment setting. Based on these studies pembrolizumab was approved as second-line therapy for mBC.

Pembrolizumab has also been investigated as first-line therapy in many clinical trials for mBC. In an ongoing multi-center phase III clinical trial (KEYNOTE-012) pembrolizumab was used as first-line therapy in cisplatin-ineligible patients and showed good ORRs (29%). Pembrolizumab is also being investigated in many phase I and II trials in combination with other agents such as radiation therapy (NCT02560635), the oncolytic virusCVA21 (NCT02043665), and other mAbs (see Table 1.4 for full list). Overall, pembrolizumab has shown great promise as both a second-line and a first-line therapy. These results continue to shape the landscape of BC treatment and provide much-needed alternatives for patients.

It is also worth mentioning that 3 other ICIs have been granted approval as therapies for mBC based on early phase I and II results. These 3 ICIs, avelumab, nivolumab, and durvalumab have approved for the treatment of mBC, and are currently being investigated in a number of phase I, II, and III clinical trials (Table 1.3 and 1.4). Little trial data are available for these therapies but preliminary data appear promising thus providing other much needed clinical options for mBC patients.

In conclusion, ICIs have been shown to be highly effective in the treatment of mBC with many different ICIs achieving clinical success (Table 1.1 and 1.2). With the recent success of ICIs in the ability to treat BC, ICIs provide much-needed alternatives to an underserved BC patient population. Although many trials are still underway, it is clear that ICIs have dramatically changed the current treatment paradigm. In addition to early clinical success, the number of clinical trials examining ICIs attests their effectiveness. With dozens of trials (extensive review in Apolo *et al*., 2017) currently underway exploring the use of ICIs as both single agents and in combination with other therapies, it is clear that ICIs will play a significant role in the treatment of BC. Despite the success of ICIs challenges still remain. Subsets of patient populations remain unresponsive to ICI therapy. Additionally, ICIs are only successful on a subpopulation of patients. For patients with low or no PD-L1 expression, ICIs are at best marginally effective. This unresponsive patient population is therefore still in need of other therapeutic options; thus, the continued development of novel BC therapies is necessary.

Overall, BC is a significant problem for patients and the health care system. NMIBC recurrence creates a difficult problem for both clinicians and patients as repeat treatments are often required. Moreover, disease recurrence creates a significant financial burden on the healthcare system. In MIBC and mBC, ineligibility for cisplatin-based chemotherapy, poor response to primary and secondary therapies, and few second-line therapeutics make these diseases particularly burdensome. Despite these challenges until recently, BC treatment has not progressed in recent decades. However, ICIs are showing great promise in both first and second-line settings and are providing much needed therapeutic alternatives. With extensive investigations into the use of ICIs in a number of patient populations, these treatments will change the treatment paradigm for all types of BC. However, patients that are PD-L1 low or PD-L1-negative respond poorly to ICI therapy and would require other treatment options. Patients with little to no PD-L1 expression have been found to have little response to ICIs.

Based on this clinical need for alternative therapies for BC and promising *in vitro* screening results, we chose to examine CR42-24's suitability to treat BC. We assessed CR42-24's effectiveness on BC using both *in vitro* and *in vivo* methods. In our studies, we found CR42-24 to be highly effective on BC. Importantly, *in vitro* CR42-24 was more effective than single-agent gemcitabine (gem) and cisplatin (cis). Moreover, CR42-24 was more effective than combination gem/cis *in vitro*. CR42-24 was highly effective *in vivo* and was able to significantly delay the growth of both cell line and patient-derived xenografts. Also, CR42-24 was as effective as combination gem/cis *in vivo*. Together, these results suggest that CR42-24 is highly effective on BC and provides a much-needed alternative therapy for BC patients.

Table 1.1: Clinical trials of ICIs as a second line therapy for BC.

Treatment name	Pembrolizumab		Atezolizumab		Nivolumab		Durvalumab	Avelumab
Reference	Plimack *et al*.	Bellmunt	Powles *et al*	Rosenberg et al.	Sharma *et al*.	Galsky *et al*.	Massard et al.	Apolo et al.
Phase	1b	III	I	II	I/II	II	I/II	I
ORR	27	21	21	15	24.4	19.6	31	18.2
PR	15	14.1	NR	10	18	17.4	NR	6.8
CR	11	7	7 (PD+)	5	6.4	2.3	NR	11.4
PFS	2	2.1	6	2.1	2.8	2	NR	2.9
OS	13	10.3	NR	11.4	9.7	8.7	NR	13.7

ORR, objective response rate; PR, partial response; CR, complete response; PFS, progression free survival; OS, overall survival; NR, not reported.

Table 1.2: Clinical trials of ICIs as a first line therapy for BC.

Treatment name	Pembrolizumab	Atezolizumab
Reference	Balar *et al*.	Balar *et al*.
Phase	II	II
ORR	23	24
PR	13	18
CR	9	6
PFS	2.7	NR
OS	15.9	NR

ORR, objective response rate; PR, partial response; CR, complete response; PFS, progression free survival; OS, overall survival; NR, not reported.

Table 1.3: Clinical trials with ICIs as single agent.

Study	Phase	Disease stage	Study notes
Atezolizumab			
Imvigor 210-Cohort 1	II	mBC-2nd line	NA
NCT02589717	IV	mBC-2nd line	NA
NCT02302807	III	mBC-2nd line	Vs. Single agent chemo
Imvigor 210-Cohort 2	II	mBC-1st line	NA
NCT02451423	II	NMIBC	BCG refractory and neoadjuvant
NCT02662309	II	NMIBC	Neoadjuvant
NCT02450331	III	NMIBC	Adjuvant
NCT02844816	III	NMIBC	BCG refractory
Pembrolizumab			
Keynote-025	III	mBC-1st line	Single agent chemo
NCT02500121	II	mBC-1st line	Maintenance therapy vs placebo
Keynote-052	II	mBC-1st line	Cisplatin-ineligable
NCT02736266	II	MIBC	Neoadjuvant
NCT 02625961	II	NMIBC	NA
Nivolumab			
NCT02387996	II	mBC-2nd line	NA
NCT02632409	III	MIBC	Adjuvant
Durvalumab			
NCT01693562	I/II	mBC-2nd line	Expansion study
NCT02901548	III	NMIBC	BCG refractory
Avelumab			
NCT01772004	I	mBC-2nd line	Expansion study
NCT02603432	III	mBC-1st line	Vs. best supportive care

mBC, metastatic bladder cancer; MIBC, muscle-invasive bladder cancer; NMIBC, non-muscle invasive bladder cancer. Refer to Clinicaltrials.gov

Table 1.4: Clinical trials examining ICIs in combination with other treatment modalities

ICIs + other immunotherapies			
NCT02528357	I	mBC-2nd line	Pemb +/- GSK3174998
NCT01968109	I	mBC-2nd line	BMS-986016 +/- Niv
NCT02318277	I/II	mBC-2nd line	Durv + epacadostat
NCT02443324	I	mBC-2nd line	Pemb +ramucirumab
NCT02614456	I	mBC-2nd line	Niv + IFN-G
NCT02994953	I	mBC-2nd line	Avel + NHS-IL12
NCT02381314	I	mBC-2nd line	Ipilu + enoblituzumab
NCT02636035	I	mBC-2nd line	Niv + Enadenotucirev
NCT02298153	I	mBC-2nd line	Atez + epacadostat
NCT02298153	I/Ib	mBC-2nd line	CPI-1444 +/- Atez
NCT02527434	II	mBC-2nd line	Trem + Durv
NCT01928394	I/II	mBC-2nd line	Niv + Ipilu
NCT02553645	I/II	mBC-1st line	Atez + Varlilumab
NCT02897765	Ib	mBC-1st line	Niv + Neo-PV-1
NCT02812420	I	MIBC	Durv + Trem
NCT02845323	II	MIBC	Niv + Urelumab
NCT02324582	I	NMIBC	Pemb + BCG
NCT02792192	I/II	NMIBC	Atez +/- BCG
ICIs + Chempotherapy			
NCT02437370	I	mBC-2nd line	Pemb + Doc or Gem
NCT02581982	II	mBC-2nd line	Pemb + Paclitaxel
NCT02853305	III	mBC-1st line	Pemb +/- plat
NCT01524991	II	mBC-1st line	ipilu + Gem/Cis
NCT02807636	III	mBC-1st line	Atez + Gem/Carbo
NCT02516241	III	mBC-1st line	Durv +/- Trem
NCT02690558	III	MIBC	Pemb + Gem/Cis
ICIs + Other			
NCT02546651	I	mBC-2nd line	Durv + multiple agents
NCT02643303	I/II	mBC-2nd line	PolyCLC + Durv + Temb
NCT02619253	I	mBC-2nd line	Pemb + verinostat
NCT02443324	I	mBC-2nd line	Pemb + Ramucirumab
NCT 02346955	I	mBC-1st line	Pemb +/- CM-24
NCT02043865	I	mBC-1st line	Pemb +/- CVA21
NCT02717156	I	mBC-1st line	Pemb + sEphb4-HAS
NCT02662052	II	MIBC	Pemb + Cis + XRT
NCT02621151	II	MIBC	Pemb + Gem + XRT
NCT02891161	I/II	MIBC	Durv + XRT
ICIs + tyrosine kinase inhibitors			
NCT02501096	Ib/II	mBC-2nd line	Pemb+ Levatinib
NCT02452424	II	mBC-2nd line	Pemb + PLX3397
NCT02351739	II	mBC-2nd line	Pemb +/- Acalabrutinib

Pemb, Pembrolizumab; Doc, Docetaxel; gem, gemcitabine; cis, cisplatin; Carbo, Carboplatin; Plat, platinum compound; Durv, Durvalumab; Ipilu, Ipilubumab; Atez, Atezolizumab; Niv, Nivolumab; BCG, Bacillus Calmette–Guérin; Temb, tremelimumab; IFN-G, interferon-gamma; XRT, External radiation treatment; GSK3174998(56);BMS-986016-NF-kB inhibitor;

epacadostat-Indolamine 2,3 dioxygenase inhibitor; ramucirumab; VEGFR2 antibody; NHS-IL12-fusion protein; enoblituzumab-B7-H3 antibody; Enadenotucirev- oncolytic adenovirus; epacadostat- Indolamine 2,3 dioxygenase inhibitor; CPI-1444-adenosine-A2A receptor antagonist, Varlilumab-CD27 antibody, Neo-PV-1-cancer vaccine, Urelumab-CD137 monoclonal antibody. Refer to Clinicaltrials.gov

1.5- Colchicine

Colchicine is a vinca alkaloid derived from *Colchicum* plants and is currently used to treat gout and Familial Mediterranean Fever (FMF). Additionally, investigations have examined colchicine as a therapy for several rheumatological and cardiovascular diseases (57). Colchicine's therapeutic effect comes from its high affinity for tubulin, protein heterodimers that make up the microtubules (MTs) of cells. MTs are long cylindrical proteins that are components of the cell's cytoskeleton and are essential for cellular function (58). Colchicine binds to unpolymerized tubulin and acts as a MT poison by blocking microtubule dynamics (assembly). It has been found that at high concentrations colchicine induces MT depolymerization and at low concentrations inhibits MT elongation (59). By causing MT depolymerization and inhibiting polymerization, colchicine blocks cells from completing metaphase, therefore, inhibiting mitosis causing cell cycle arrest in mitosis and entry into apoptosis (60). Despite being examined extensively, colchicine has had limited clinical success due to its high toxicity profile and low therapeutic index.

1.5.1- Clinical Uses of Colchicine

Dose limitations have restricted colchicine to use as a therapeutic compound (60). Despite having significant anti-proliferative properties, colchicine is only used clinically as an anti-inflammatory. The anti-inflammatory properties of colchicine come from its ability to disrupt MTs and cell signaling in leukocytes thereby blocking pro-inflammatory processes (57). Colchicine primarily inhibits neutrophil chemotaxis, adhesion, and mobilization (61,62). Research has also demonstrated that colchicine inhibits secretion of cytokines and other immunomodulators from macrophages. Together, the inhibition of neutrophils and macrophages make colchicine a potent anti-inflammatory drug. Even in an anti-inflammatory capacity colchicine dosing is limited. At low doses, common side effects of colchicine include diarrhea, nausea, vomiting, myelosuppression, and in severe cases renal, and hepatic toxicity.

Beyond its use in treating gout and FMF, colchicine has been investigated as a treatment for rheumatoid arthritis, osteoarthritis, Bechet's disease, pericarditis, atherosclerosis, cardiovascular disease, and cirrhosis (57,63). As a highly potent anti-inflammatory colchicine has been shown to be an effective treatment for many inflammatory diseases. In addition to its anti-inflammatory properties colchicine has been shown to be highly anti-proliferative (64). As such, a large body of research has investigated colchicine as a treatment for cancer. Indeed, colchicine has been found to be an anti-proliferative on cancer cells. In preclinical models, colchicine is an effective treatment for gastric, thyroid, colon, and lung cancer (65–68). Additionally, prospective studies have demonstrated that treatment with colchicine for acute gout flare-ups significantly reduces the risk of cancer (69). Together, this data supports the use of colchicine as an anti-cancer drug. Despite this potential benefit, colchicine's use in the clinic is limited due to its severe toxicity and low therapeutic index.

1.5.2- Colchicine derivatives

To overcome the low therapeutic index of colchicine, many groups have investigated colchicine derivatives, with a number of them being effective anti-cancer treatments. There are several derivatives patented with some progressing as far as clinical trials. One particular compound, ZD6126, has been shown to be a potent anti-angiogenic compound and inhibits vascularization of tumors inducing necrosis at the center of tumors (70–73). Preclinical studies using ZD6126 have found it to have a significantly reduced toxicity profile as compared to colchicine with a maximum tolerated dose of 400mg/kg in xenografted mice (70). In one study ZD6126 was used at a therapeutic dose of 200mg/kg and was found to cause 70-100% tumor necrosis (73). Another colchicine derivative identified as compound 40 by Vishwakarma et al. (2015) was found to have increased anti-cancer effects as compared to colchicine (74). Interestingly, compound 40 also has reduced Multi-drug resistance protein-1 (MDR-1) induction, suggesting colchicine derivatives may be alternative treatments for cancers that have established resistance due to MDR-1 expression. Another colchicine derivative, CT20126 was shown to have potent anti-cancer activity, indicating induction of apoptosis in many cancerous cell lines in the low nanomolar (nM) range (75).

The Tuszynski lab has also published papers on a number of colchicine derivatives that demonstrate increased anti-cancer activity (64). Through *in silico* and *in vitro* screening, the Tuszynski lab identified some colchicine derivatives; of these derivatives, a number of thio-colchicine derivatives showed increased potency as compared to colchicine and other derivatives tested. One particular compound, CR42-24, showed great promise as a cancer therapeutic.

1.6-Microtubules and Tubulin

1.6.1- Microtubules

Microtubules (MTs) are long cylindrical proteins that are essential to many cellular processes (58). Microtubules form tracks for intracellular transport, facilitate chromosome separation during mitosis, regulate cell polarity, and form the structure for cilia and flagella (76). Microtubules are polymerized tubulin heterodimers consisting of an $\alpha\beta$ dimer. Tubulin dimers with GTP bound to both monomers are called assembly competent and they can be added onto existing microtubules to facilitate elongation of MTs (77). MTs consist of a plus end and a minus end; the plus end grows much more rapidly than the minus end and is characterized by more frequent depolymerization called microtubule catastrophe (78). The mechanism controlling the transition between growth and catastrophe is poorly understood but most likely involved GTP hydrolysis taking place in the plus end of a microtubule at a rate faster than MT polymerization. Research has found that older MTs are more prone to catastrophe. It is not known what molecular events trigger catastrophe to occur, but it has been proposed that MT defects or increasing taper at the tip of older MTs may be responsible for inducing catastrophe (79,80). MT dynamics change throughout the cell cycle and during cell differentiation, which is primarily controlled by factors that promote MT polymerization or depolymerization. MT-associated proteins (MAPs) aid in regulating the dynamics of MTs (81). MAP proteins can bind to MTs and change MT dynamics by altering polymerization or depolymerization rates. The MAP, MT polymerase, can increase the rate of MT polymerization by attaching to the plus-end of MTs and recruiting tubulin dimers. MAPs also regulate MT depolymerization. MT depolymerases which belong to the kinesin family of proteins can increase MT depolymerization rates through different mechanisms (82). The role of kinesin motor proteins in MT dynamics is important for MT-organization within cells and is vital for cellular function (81,83,84).

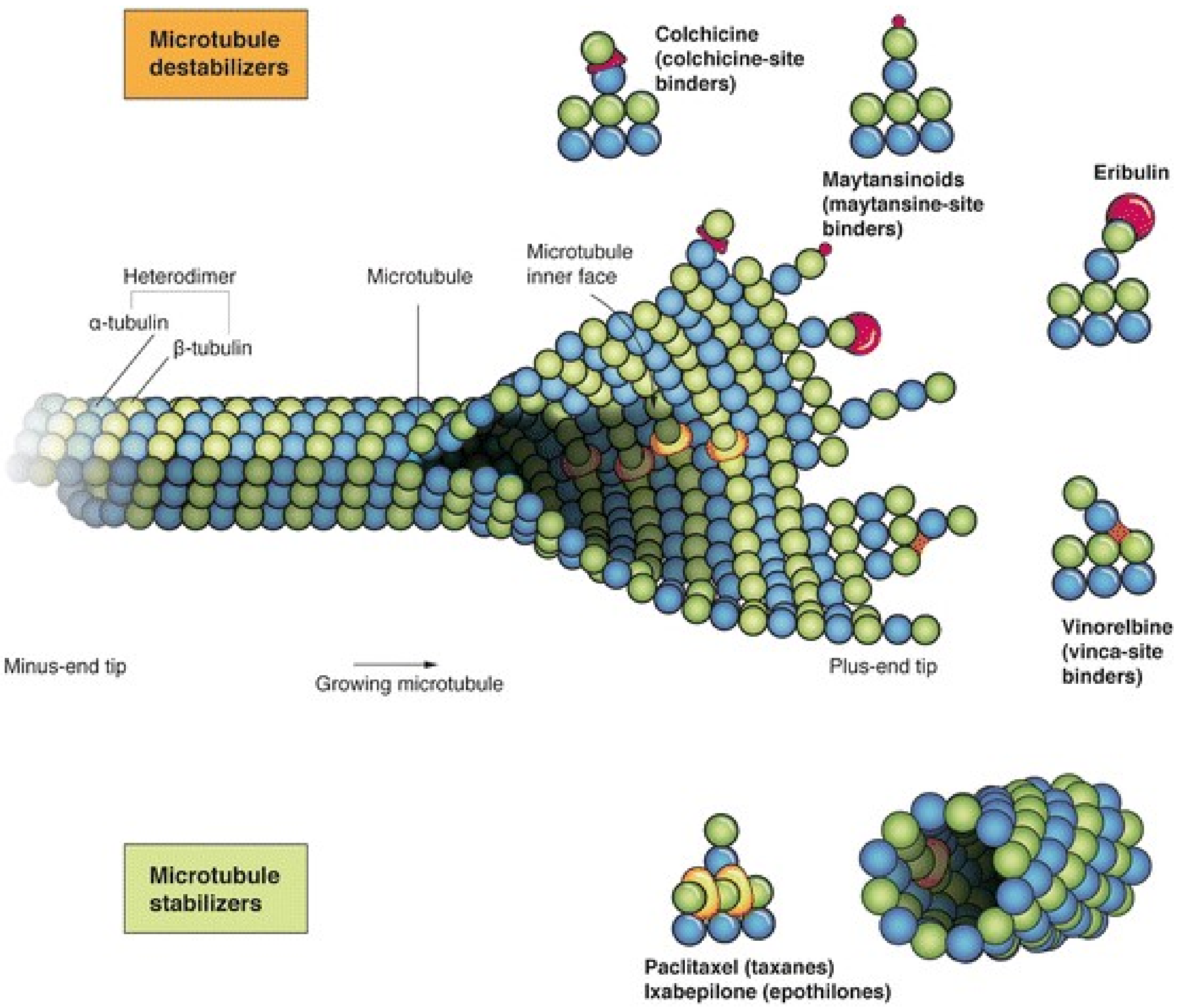

Figure 1.3- Binding sites of multiple MT inhibitors. MT-targeting agents bind to multiple sites on MTs and either stabilize or destabilize MTs. MT stabilizers, taxanes and epothilones bind to β-tubulin and bridge adjacent β-tubulin dimers leading to stabilization of microtubule structure. Microtubule destabilizers bind to either the colchicine site or the vinca alkaloid site and induce MT depolymerization. Eribulin is a halichondrin B synthetic analogue and inhibits MT polymerization by binding to the plus-end of MTs causing mitotic arrest. Maytansinoids bind to b-tubulin dimers at the plus-end of MTs and inhibit MT dynamics, preventing both polymerization and depolymerization. Adapted from "Clinical Development of Anti-Mitotic

Drugs in Cancer" by Olziersky and Labidi-Galy with permission from Springer Nature, copyright (2018).

Due to their essential function in cell division, MTs have been the target of many cancer agents (Figure 1.3) (85). MTs are critical for alignment of chromosomes during mitosis: during prometaphase, mitotic spindle MTs attach to chromosomes at their kinetochores after the nuclear envelope breaks down. MTs then extend, pushing chromosomes to the metaphase plate and allowing the cells to progress through metaphase and into anaphase. In anaphase, MTs contract to pull sister chromatids apart. Cancer cells are more sensitive to MT targeting agents (MTAs) as they enter mitosis more frequently than healthy cells (86,87). A large number of MTAs have been discovered and are currently used clinically (Figure 1.3, and 1.4) including drugs such as paclitaxel, epothilones, and vinca alkaloids (reviewed extensively in (85,88)). There are two classes of MTAs: microtubule destabilizers and microtubule stabilizers. MT-destabilizers inhibit MT polymerization at high concentrations and include drugs such as vinblastine, vincristine, estramustine, colchicine, and cytophycins. Conversely, MT-stabilizing agents such as paclitaxel and epothilones stimulate polymerization but also prevent further MT polymerization. Although stabilizers and destabilizers affect MTs through different mechanisms, both classes of compounds block cells in mitosis. Blockage of cells in mitosis leads to induction of apoptosis or exit from mitosis making them highly effective anti-cancer agents.

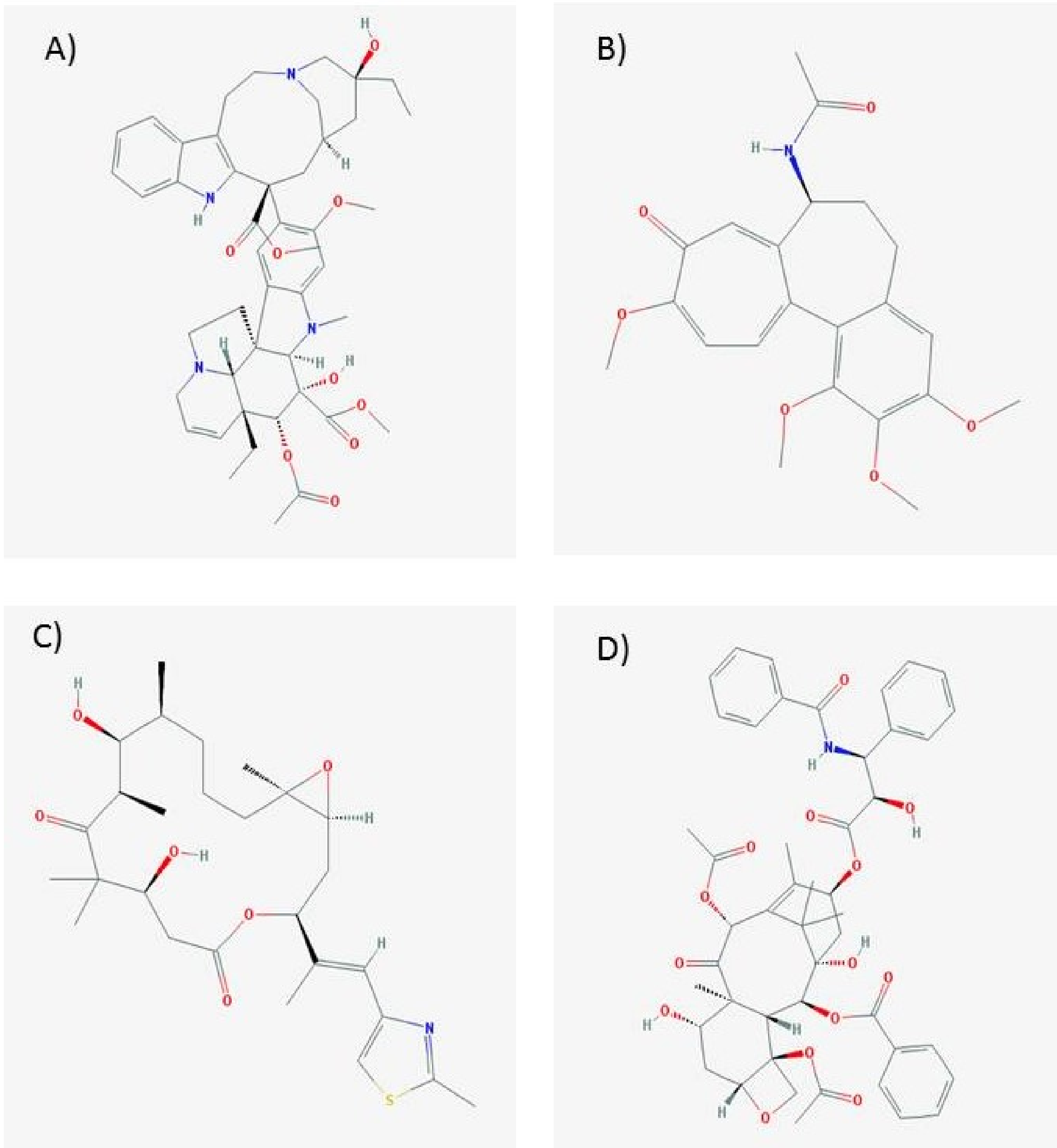

Figure 1.4- Structure of MTAs. A-C shows structures of MT-destabilizing agents vinblastine (a, CID 13342), vincristine (b, CID 5978), colchicine (c, CID 6167). C and D show images of MT-stabilizing agents paclitaxel (d, CID 36314) and epothilone B (e, CID 448799). Images taken from PubChem compound database. https://www.ncbi.nlm.nih.gov/pccompound/.

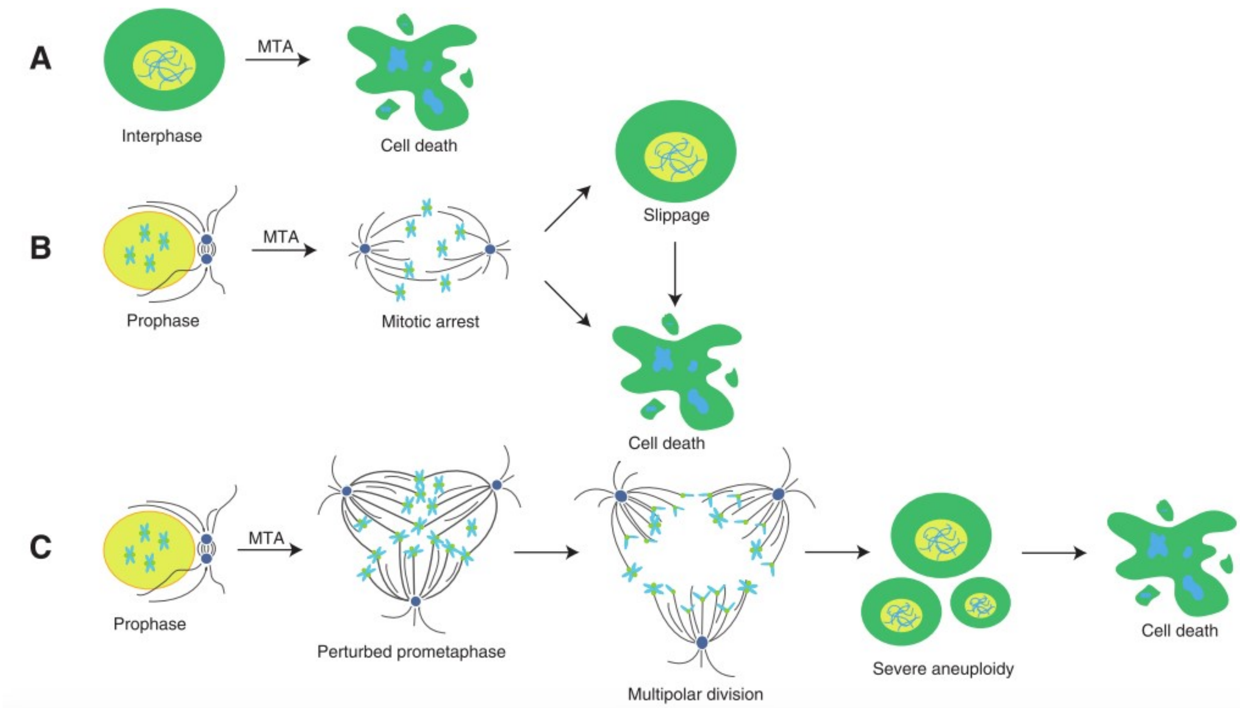

Figure 1.5-Different mechanisms of action of MTAs. MTAs are hypothesized to induce cell death through disruption of cell signaling during interphase (a). MTAs also cause cell death via disruption of mitosis (b). MTAs induce mitotic arrest which can cause lead directly to cell death or after mitotic slippage (exit from mitosis without cell division). MTAs also can cause aberrant chromosomal division leading to severe abnormalities in daughter cells which may lead

to cell death (c). Adapted from "Clinical Development of Anti-Mitotic Drugs in Cancer" by Olziersky and Labidi-Galy with permission from Springer Nature, copyright (2018).

Mitotic poisons can induce cell death via different mechanisms (see Figure 1.5, reviewed in ref. (86,89)). Mitotic arrest is believed to be the main mechanism by which mitotic poisons induce cell death. During mitosis interference with chromosome alignment causes mitotic arrest. Arrested cells then enter into apoptosis or exit mitosis without dividing (mitotic slippage) after which cells enter into apoptosis (Figure 1.5C). Other mechanisms by which MTAs induce cell death have also been described. During interphase, mitotic poisons can affect cell signaling and intracellular transport which may lead to cell death (Figure 1.5A). In prostate cancer, Taxol has been shown to inhibit nuclear translocation of the androgen receptor which is required for castration-sensitive prostate cancer (90–92). Additionally, Paclitaxel and vincristine, have been shown to be synergistic with DNA damaging agents by inhibiting the transport of DNA repair proteins to the nucleus (93). Recently it has been shown that paclitaxel also causes mis-segregation of chromosomes during mitosis (94) (Figure 1.5B). Daughter cells undergo subsequent cell death in interphase.

1.6.2- Tubulin Isotypes

As mentioned above, MTs consist of tubulin heterodimers comprised of an α and β subunit. In eukaryotic cells, there are several isoforms of tubulin: α, β, and γ. These isoforms are found in all eukaryotic cells and are conserved throughout evolution. Recently, other isoforms: δ, ε, ζ, and η have been discovered in prokaryotic cells but are not found in eukaryotic cells (95). α and β subunits dimerize to form tubulin dimers which serve as the subunits for MT polymerization. γ -tubulin forms a ring structure which provides the foundation for MT elongation. γ-tubulin is also found at centrioles which form the basis of the MT organizing center (94). In total, in human cells there are seven γ-tubulin proteins, eight α-tubulin proteins, and eight β-proteins, each of which is encoded by a separate gene. Little is known about γ and α isotypes or if any functional differences exist between them. The focus of much research has been on the β isotypes which show variable tissue distribution and have been found to have some functional differences. In the human body, there are eight β-tubulin isotypes (96). Isotype I (βI), IVb (βIVb), and V (βV) are ubiquitous throughout healthy tissues. Isotype 6 (βVI) is hematopoietic specific, and IIa (βIIa), IIb (βIIb), III (βIII), and IVa (βIVa) are expressed in the brain. Multiple genes encode β-tubulin isotypes (TUBB), many of which show high homology and are conserved across species. The isotypes vary primarily in the last 15 amino-acids at the C-terminus of the proteins (97). Differences at the C-termini of β-tubulin isotypes alter their ability to interact with MAPs (98). At the transcriptional level, isotypes also vary in their 3' untranslated region (UTR) which is involved in regulating transcriptional and translational modifications. The variable expression pattern and conservation throughout evolution suggest functional differences between isotypes (99).

1.6.3- βI and II

There has been some research showing functional differences between β-tubulin isotypes. However, this does not apply to all isotypes as research has demonstrated that isotypes can be functionally redundant. Narishige et al. (1999) found that increases in βI and βII expression accompanied hypertrophy of cardiac muscle. The authors suggest that increased expression of βI and βII may result in increased microtubule stability (100). Lezama et al. (2001) propose that βI prevents interaction of tubulin and actin filaments as experiments showed that βI is depleted in cortical regions of MDCK cells which are regions rich in actin filaments (101). Although these data suggest a possible functional role of βI, it is not yet clear and requires further research. βII has been proposed to play a specific role in anchoring microtubules to the centrosome during mitosis and cell periphery. Experiments examining Hela cells undergoing mitosis have shown that βII is isolated to the centrosome and the cell periphery (102). The specific localization of βII suggests that it may play a role in cell division and centrosome function. However, it has been pointed out that the high concentration of βII in neuron cells is contradictory to its involvement in mitosis as neuronal cells do not undergo cell division.

1.6.4- βIV

βIV is localized to axonemes which are MT-based structures that aid in cilia and flagella movement (103,104). BIV tubulin has also been shown to be essential for flagellar stability, and function (105,106). The axoneme is the inner core of cilia and flagella in eukaryotic cells. There are two centralized MTs (the central doublet) and nine outer MT doublets (the outer doublets). Each pair is composed of a complete MT and an incomplete MT. During motility, the motor protein dynein attaches to the complete MT and slides along the incomplete MT on the adjacent doublet. By moving along the MTs dynein proteins produce the force necessary to form cilia and flagella movement. Based on this evidence, it has been suggested that βIV is functionally different from other isotypes.

1.6.5- βV

Little is known about β V. Similar to βIII, βV lacks the cysteine 239 residue which may serve to protect cells from oxidation by reactive oxygen species (ROS). However, there is little research on βV tubulin.

1.6.6- βVI

βVI tubulin is hematopoietic specific (107). Research into the function of βVI has demonstrated that inhibition of βVI expression affects platelet morphology, causing platelets to become spherical rather than discoid shaped. Additionally, decreased expression of βVI in platelets also impairs formation of the marginal band that resides on the periphery of cells (108). Additionally, βVI inhibition appears to impair blood coagulation (109,110). Together, this data suggests that βVI plays a specific role in the cytoskeleton of platelets and is therefore crucial for platelet function.

1.6.7-βIII

Of all the β-tubulin isotypes βIII appears to have the most functional differences and is one of the most heavily researched isotypes. βIII is less sensitive to reactive oxygen species and free radicals. Although the mechanism is not yet clear, Ludueña and Banerjee (2008) hypothesize that the lack of cysteine 239 (Cys 239) in βIII tubulin makes it less sensitive to free radicals and ROS (111–113). Cys 239 is highly conserved among tubulin isotypes and throughout evolution. In βIII (and in βV) Cys 239 is substituted with serine. Since sulfhydryl groups are highly reactive species and react with ROS, the substitution of Cys with serine could decrease the reactivity of βIII. Functional studies have lent support to this hypothesis as it has been that found that α/βIII reacts less with alkylating agents than other isotypes (112). Moreover, βIII is overexpressed in tissues with increased exposure to ROS and oxygen free radicals (96,114–116). βIII is only expressed in neuronal and testicular tissue, both of which are oxidative tissues. In this context, cells with increased susceptibility to ROS would upregulate βIII allowing cellular MTs to be protected from oxidative damage, thereby protecting cells. Carré et al. (2002) have also supported this theory showing that βIII tubulin dimers localize at the mitochondria of cells; since the mitochondria are the primary producers of ROS in cells, the presence of βIII at the mitochondrial membrane would serve to neutralize ROS produced by the mitochondria (117). The presence of βIII in tumors also supports this protectionist hypothesis. Tumors which are under increased oxidative stress have upregulated βIII as compared to non-cancerous tissues (118,119). Overexpression of βIII in cancer cells would, therefore, give cells a survival advantage by protecting them from ROS. Altogether this data supports the hypothesis that βIII has a protectionist role in cells.

In addition to protecting cells from ROS, βIII also plays a role in embryogenesis (116). During development of the cerebral cortex, in post-mitotic, pre-migratory neuron cells βIII is expressed. In particular, βIII is expressed in granule, stellate, and basket cells in the developing cortex. βIII is one of the earliest cytoskeletal proteins to be expressed by central nervous system cells. βIII may play a role in neurite extension by enhancing MT polymerization and stability through phosphorylation. The phosphorylation of αβIII tubulin dimers in neurite MTs is essential for neurite development as phosphorylated tubulin is associated with highly stable MTs, which allows neurons to develop (120–124). The importance of βIII in neural development is confirmed by congenital brain syndromes in which mutations in βIII result in impairment in brain development. CFEOM3 is a group of disorders of the eye caused by dysfunction of the oculomotor nerve. Symptoms of CFEOM3 include neuropathy, facial paralysis, and mental and behavioral abnormalities. In-vivo mutational studies have demonstrated that mutations in βIII result in impaired axon guidance of oculomotor neurons (125–127). Other mutations in βIII are found in patients with pontocerebellar hypoplasia (PCH) (126,127). βIII mutations lead to cortical disorganization and nerve axon abnormalities associated with PCH. The mutations in βIII associated with CFEOM3 and PCH are substantial evidence to support the hypothesis that βIII has a significant functional role in neurogenesis.

βIII also exhibits altered dynamic behavior compared to other tubulin isotypes (104). Ludena and Lu (2002) found that MTs formed from αβIII dimers assemble after a long lag time (128,129). The long lag-time of αβIII is in contrast to MTs formed from αβII and αβIV dimers which assemble rapidly with no lag-time. Another study found that when βIII is transfected into cells, MT assembly decreases (130). Based on these results it appears that βIII may polymerize to a lesser extent than other isotypes. Moreover, MTs formed from αβIII dimers decay more slowly *in vitro* when compared to αβII MTs (130). Based on these results Banerjee and Ludena (2008) have proposed a model for βIII functions. In the embryonic nervous system, more dynamic MTs formed from αβIII dimers aids in cell growth, migration, and differentiation. As cells reach terminal differentiation, they begin to express other isotypes such as II and IV which exhibit more stability which is more advantageous for proliferative cells. However, in non-proliferative neuronal cells, ROS and oxidative stress can compound over time; thus, βIII expression remains in those cells to serve a protective role against ROS.

1.7- βIII tubulin in cancer

Research has shown that βIII is both a predictive and a prognostic marker for a number of cancers (116,131). However, the role of βIII in cancer is not yet clear as contradictory evidence has been published. Many studies have found that upregulation of βIII is a mechanism of paclitaxel resistance and a marker for poor response to taxanes (114,115,130–133). Taxanes induce MT stabilization, preventing depolymerization arresting cells in mitosis which leads to cell death. Upregulation of a less dynamic isotype such as βIII may counteract the stabilizing effects of taxanes. In a clinical setting, research shows that upregulation of βIII in multiple cancers is a marker for poor response to Taxol therapy (115,134–139). However, in some studies, βIII tubulin expression has been found to be a marker for sensitivity to taxane therapy and not a marker of resistance (140–142). A phase-II clinical trial found that βIII did not serve as a predictive marker for the success of paclitaxel-based regiments in non-small cell lung cancer (NSCLC) patients (143). Due to these contradictory results, it is not yet clear whether or not βIII serves as a marker for taxane sensitivity and requires further research.

In addition to being upregulated in cancerous tissue, increased βIII expression has also been shown to be associated with more aggressive and metastatic types of cancer and serves as a marker of poor prognosis (58,115,137). Many studies have found that βIII expression is a marker for poor prognosis in multiple types of cancer (131,134,144,145). βIII tubulin expression has been found to be significantly upregulated in more-aggressive breast, prostate, and colorectal cancer when compared to less aggressive forms of disease (115,138,146). Specifically, βIII tubulin expression has been shown to be localized to the invasive margins of colorectal tumors, and there is a significant upregulation in invasive tumors as compared to non-invasive tumors (147). βIII tubulin also has been found to correlate with TNM staging of tumors in NSCLC (148). Together this data supports that βIII is a prognostic marker for many different cancers.

Overall, it is clear βIII serves as a prognostic marker, and its use as a predictive marker has yet to be elucidated. Ferlini et al. (2015) suggest that βIII only serves as a prognostic marker in tissues that in a differentiated state lack βIII expression (145). In this context, βIII would serve as a marker for dedifferentiation and therefore poor prognosis. This hypothesis is supported by evidence showing that TUBB3 expression is upregulated in hypoxic and poor nutrient conditions. Ferlini et al. (2007) found that hypoxia-induced factors (HIF) 1 and 2 bind upstream of TUBB3 and that βIII expression is found in hypoxic areas within tumors (149–151). The upregulation of TUBB3 would, therefore, passively accompany increases in pro-survival signaling, dedifferentiation and increased cell-proliferation through HIF-1 and 2 transcription (152–154). This theory also supports how βIII may act as a predictive marker for taxane resistance. HIF transcription has been found to induce dedifferentiation, and upregulation of a stem cell-like phenotype. The protectionist factors, such a MDR-1 upregulation and increased resistance to apoptosis that are associated with a stem-cell phenotype would confer resistance to Taxol. Therefore, the expression of βIII may serve as a surrogate marker for sensitivity to Taxol. However, this could only be the case in hypoxic tumors in which HIF gene transcription is induced. Therefore, just in severely hypoxic and poorly vascularized tumors does βIII serves as a surrogate marker for taxane sensitivity.

In summary, βIII serves as a prognostic marker for cancer patients. Overall, increased βIII expression has been found to be associated with more aggressive and metastatic disease. The predictive power of βIII for taxane sensitivity is still debated and is an area of active research. In some contexts, it appears that βIII may serve as a marker for taxane resistance and as a marker for poor response to taxane therapy. However, this is contracted by studies that show βIII as a positive predictor of sensitivity to taxane therapy. These findings are complicated by βIII expression being under HIF transcriptional control, which coordinates multiple resistance factors that work to protect cancer cells. Further research will be needed to clarify the predictive value of βIII as a biomarker for taxane response.

1.8- βIII as a Drug Target

Research on βIII's role in drug resistance and prognosis have made it a desirable and promising drug target. High-throughput screening has identified compounds such as IDN5390 and other seco-taxanes (Pepe et al., 2009) that have increased affinity for βIII (155,156). These taxane derivatives were found to be highly effective on cell lines overexpressing βIII. These derivatives have been found to be more effective than paclitaxel and were effective on subcultured cell lines that were resistant to other therapeutics. Moreover, experiments found that they are effective irrespective of βIII tubulin levels, and modulation of βIII tubulin levels did not affect cells sensitivity to βIII compounds. Interestingly, IDN5390 and other derivatives such as CST-10202 and Yg-3-46a were found to be poor substrates for MDR-1 and were active on paclitaxel-resistant cell lines with increased MDR-1 expression (156–158). Together these results support that βIII specific compounds are highly active agents and may overcome established mechanisms of resistance.

Recently our lab also characterized and synthesized many colchicine derivatives with increased affinity for βIII tubulin (64). Using in-silico screening some colchicine derivatives with increased affinity for βIII were identified. The most promising hits were synthesized and screened for affinity for βIII and their cytotoxic effects. From these derivatives, our lab identified CR42-24 as the most promising patentable compound for further development. CR42-24 is a thio-colchicine derivative and has been modified in a number of positions to increase its affinity for βIII. Previously, the Tuszynski group characterized CR42-24s cytotoxic profile on some cancer and normal cell lines. In order to assess the effectiveness of CR42-24 we performed an *in vitro* cell line screen. In this cell line screen, we found that CR42-24 was highly active on many different cancers (Figure 3.1 and 3.2). Not only was CR42-24 effective on most cell lines screened, but CR42-24 was also much more cytotoxic compared to current standard of care agents. Specifically, CR42-24 was highly effective on a high-grade bladder cancer cell line. Based on the clinical need for alternative therapies for bladder cancer, we chose to examine further whether or not CR42-24 would be an effective treatment for bladder cancer. To this end we assessed CR42-24's effectiveness on BC using both in-vitro and in-vivo methods. In our studies, we found CR42-24 to be highly effective on BC. In-vitro CR42-24 was more effective than single-agent gemcitabine (Gem) and cisplatin (Cis). Moreover, CR42-24 was more effective than combination Gem/Cis in-vitro. CR42-24 was highly effective in-vivo and was able to significantly delay the growth of both cell line and patient-derived xenografts. Also, CR42-24 was as effective as combination Gem/Cis in-vivo. Together, these results suggest that CR42-24 is highly effective on BC and provides a much-needed alternative therapy for BC patients.

Chapter 2-Materials and Methods

2.1-Compounds and drug dilutions

Paclitaxel (T7191-25MG), gemcitabine (G6423-10MG) and cisplatin (PHR1624-200MG) were purchased from Millipore-Sigma and stored in manufacturer recommended conditions. CR42-24 was purchased and synthesized by ChemRoutes (Edmonton, Canada) achieving 98% purity. CR42-24, gemcitabine, and Paclitaxel were weighed on a calibrated scale and dissolved in 100% DMSO to a concentration of 5mM. 5mM master stocks of compounds were aliquoted into 10µL aliquots and stored at -20°C. Cisplatin was weighed on a calibrated scale and dissolved in DMSO to a concentration of 5mM). Cisplatin was aliquoted into 50µl aliquots and stored at -80°C. On the day of cell viability experiments aliquots of compound were taken and let thaw at room temperature. Once thawed, compounds were serially diluted in dimethyl sulfoxide (DMSO) (gem, CR42-24, and paclitaxel) or PBS (cis) by one-half to desired concentrations. 10µl of compound were then added to 10 mL of DMEM medium containing 10% fetal bovine serum, and 1% penicillin/streptomycin. Drug-containing medium was then added to cells according to experimental procedures.

2.2-Cell culture

All cell lines were purchased from American Type Culture Collection (ATCC) with the exception of the UM-UC-3, UM-UC-14, and 253J cell lines which were graciously gifted by Dr. Ronald Moore (Faculty of Medicine and Dentistry, University of Alberta). All cell lines were cultured in DMEM supplemented with 10% FBS, and 1% penicillin/streptomycin. Cell cultures were maintained at 37°C, 5% CO_2, and in a humidified incubator. Cells were cultured until approximately 90% confluent at which point they were subcultured based on cell growth rates, or harvested for experimentation. Cells were subcultured or harvested for experimentation by trypsinization (TrypLE express, ThermoFisher Scientific). Trypsinized cells were harvested, and diluted with growth medium. Cells were counted using stained using trypan blue and counted with a hemocytometer to estimate cell numbers. Cells were then diluted to desired concentrations for experimentation.

2.3-Cell Viability Determinations

Cell viability in the presence of paclitaxel, CR42-24, cisplatin, or gemcitabine was determined using resazurin. Cells seeded in 96-well plate at concentrations proportional to their growth rate, ranging from 2 to 5,000 cells per well in a volume of 100 uL. After plating, cells were allowed to adhere to the plate overnight. The following day 100 µL medium containing 2x final drug concentrations (in 0.1 % DMSO) was added to each well (total volume 200 µl). Each drug concentration was administered to three wells. Treatment was maintained for a 72-hour period. Following 72 hours, each well is administered 22µl of resazurin reagent (440 µM). The plates were incubated at 37℃ for 4 hours. Absorbance of plates were then read using BMG Labtech Fluostar Omega plate reader set to 540 nm excitation and emission 590 nm. Relative cell viability is determined by comparing cell viability to DMSO treated cells (0.05%). Experimental results are an average of at least n=3 experiments. Cell viability (% DMSO treated control) was input into GraphPad Prism 6 software. Graphs were generated by transforming drug concentrations (in molarity) to log concentration. Curves were then analyzed by 4-parameter analysis to determine IC50 values for each compound.

2.4-Combination Drug studies

Viability of T24 cells incubated with both gem and cis was determined by co-incubating cells with IC20 concentrations (determined using GraphPad Prism 6) of cisplatin (2µM), plus increasing concentrations of gemcitabine. $2x10^3$ cells were plated in a 96-well plate and left to adhere overnight. The following day cells were treated with 100µl of medium containing increasing concentrations of CR42-24 or 2µM cisplatin (in PBS) and increasing concentrations of gemcitabine. Cells were treated in triplicate and left for 72 hours; at which point cell viability was determined by resazurin assay as described above. Mean cell viability was determined from at least 3 independent experiments. For drug synergy experiments T24 cells were plated as described above. After adhering overnight cells were treated for 24 hours with medium containing IC20 concentrations of gem (10nM), cis (2µM), or CR42-24 (3nM). After 24 hours cells were washed 2x with phosphate-buffered saline, and then incubated with medium containing gem, cis or CR42-24 at increasing concentrations. After 48 hours of treatment (72 hours total) cell viability was determined as described above. Single agent comparison was performed as described above, incubating cells with drugs for 72 hours. Combinatory index values were calculated using ComboSyn software (ComboSyn, Inc). For full description of Combosyn methods see Chou TC and Martin N. CompuSyn for Drug Combinations: PC Software and User's Guide (2005)

2.5-*In vivo* studies

All animal care and experimental procedures were approved and performed in accordance with Canadian Council on Animal Care (CCAC) guidelines. Experimental procedures were approved by the University of Alberta Health Sciences Animal Care and Use Committee under protocol number AUP00000453 (Dr. John Lewis) and AUP00000390(Dr. Mary Hitt). Patient derived samples were obtained by Dr. Ronald Moore, with approval from Health Research Ethics Board of Alberta under protocol HREBA.CC-16-0362 (Dr. Ronald Moore).

For T24 xenograft experiments $2x10^7$ T24 cells were suspended in 50µl of PBS and mixed with an equal volume of Matrigel (BD Biosciences, Bedford, MA, USA). 100µl of cell/matrigel mixture was injected subcutaneously into the right-flank of 8-12-week-old NOD SCID gamma (NSG) [NOD.Cg-Prkdcscid Il2rgtm1Wjl/SzJ] mice (mean body weight of 33 g) which were obtained from Dr. Lynne Postovit (University of Alberta). Tumors were left to grow to 50 mm^3, at which point mice were separated into groups, and treatment was initiated. For all studies mice were weighed every second day for the duration of the studies. CR42-24 treated mice received injections of CR42-24 intravenously via tail-vein every second day for 12 days or 18 days. Mice were injected with either 75 uL (3 mg/kg) or 150 µl (6 mg/kg) of CR42-24. CR42-24 solution was prepared immediately before injection by diluting 10 µl of CR42-24 (20 mg/ml in 100% DMSO) in 10 µl of DMSO and 180 µl of PBS to create a final concentration of 1mg/ml. Vehicle control treated mice were injected IV via tail-vein injections with either 75 or 150 µl of 10% DMSO in PBS. Injections were given every second day for a total of 12 or 18 days depending on the study. Vehicle control mice received the same volume as CR42-24 injected mice. In the case of two doses of CR42-24 used control mice received injections with the higher volume. When comparing CR42-24 and cis/gem combination therapy mice received a CR42-24 (3 mg/kg) in the same manner as described earlier. In this study mice received 2 cycles of CR42-24, vehicle control, or cis/gem combination therapy. CR42-24 and vehicle control cycles consisted of IV injections of CR42-24 every second day for 12 days. Following 18 days of no treatment another cycle of treatment was initiated. A single cis/gem cycle is as follows: On day 0 mice were given a dose of gem (40 mg/kg), and 4 hours later a dose of cisplatin (3 mg/kg) was given. On day 3, 6, 9, and 12 mice were given gem alone (40 mg/kg). After Day 12 mice were not injected for 18 days. On day 30 a second cycle of cis/gem therapy began. Cisplatin doses were given intraperitoneally by injecting 130uL of 0.75mg/ml of cisplatin in PBS. Gemcitabine doses were given intraperitoneally (IP) by injecting 265uL of gemcitabine (5mg/ml) dissolved in PBS. Tumors were measured every second day using calipers and tumor volume was calculated using the formula: (longest measurement x shortest measurement^2)/2. At endpoint tumors were excised, photographed, weighed, and fixed in 20% formaldehyde/5% sucrose solution.

Patient derived xenograft models were generated as follows. Primary bladder cancer tissues were obtained from consenting patients undergoing surgery with the approval of the University of Alberta Health Research Ethics Board. Samples were received in saline and processed within 2 h of surgery. Submucosal and necrotic tissues were stripped from the tumor tissue and the remaining tumor was cut into ~3x3x3 mm pieces and placed in Hanks Balanced Salt Solution containing 100 U/ml penicillin, 100 U/ml streptomycin, and 0.25 ng/ml Fungizone (Gibco).

Male NSG mice were 6-12 weeks old and at least 20 g in weight at the time of tumor implantation. To establish subcutaneous PDX tumors, mice were anesthetized with 2% isoflurane and site of implantation was sterilized with 70% isopropanol. A small incision (3-4 mm in length) was made in the right flank of the mice and the connecting tissue was separated via blunt dissection. Tumor tissue from patients, or from mice when performing passages, was then placed into the incision and the tissue was closed with Vetbond™ Tissue Adhesive (3M). Initial implanted tumors were grown to ~500 mm3 and then were processed as described above for primary patient tissue and implanted into additional NSG mice. This process was performed again to have enough tumor bearing mice for experimentation (These PDX tumors were referred to as Passage 3).

When passage 3 tumors reached a volume of 200 mm^3 mice were randomized into groups. Mice in the CR42-24 treatment group were injected IV with CR42-24 (3 mg/kg) and control group mice received an equal volume of vehicle control (10% DMSO in PBS) as described above. Injections were given every second day for 18 days. After 18 days tumors were measured every second day until end-point (tumor volume 1500 mm3). Upon endpoint mice were then euthanized. Tumors were then excised, and fixed in 20% formaldehyde/5% sucrose.

2.6-Cell imaging experiments

$5x10^4$ T24 cells were plated on glass coverslips and left to adhere overnight. The following day cells were treated with medium containing Hoechst 33342 dye (H1399, ThermoFisher Scientific), 5 μM CR42-24 (0.1% DMSO), or medium with DMSO (0.1%). Cells were treated for increasing time intervals. After specified time interval medium was aspirated, and coverslips were washed twice with PBS. Cells were then fixed with 100% ice-cold methanol. After fixation cells were blocked for 1 hour using PBS with 1% Tween-20 (PBST) with 1% BSA. Cells were then incubated with rabbit β-tubulin antibody overnight (1:500). The following morning coverslips were washed 3 times with PBST for 5 minutes per wash. Coverslips were then incubated for 1 hour with goat anti-rabbit secondary antibody (1:500) conjugated with AlexaFluor 546 dye. After incubation coverslips were washed 3 times 10 minutes with PBST. After washing coverslips were fixed with ProLong Gold Antifade mounting medium (P101444, ThermoFisher Scientific). Slides were imaged using upright Zeiss Examiner Z1 microscope, equipped with 63x 1.4 oil DIC 420782-990 objective lens, and a Hammatsu EM-CCD digital camera. Images were taken using Velocity 6.1 imaging software. Images from at least 20 separate cells were taken per slide. Images were quantified using ImageJ software.

2.7-Cell cycle analysis

Serum starvation was used to synchronize cells in G0. $5x10^5$ T24 cells were plated in a 6-well plate in serum-free medium and left to adhere overnight. The following morning cells were incubated with DMEM supplemented with increasing concentrations of CR42-24 (0.1% DMSO), 50 nM paclitaxel (0.1% DMSO), or medium containing 0.1% DMSO. Cells were treated for 24 hours. After 24 hours cells were washed with PBS, trypsinized, and spun down at 300g for 5 minutes. Cell pellets were washed twice with PBS. After washing cells were fixed with ice-cold 100% methanol and spun down at 850g for 10 minutes. Cells were suspended in 400 µl of PBS containing Hoechst 33342. Cells were incubated for 30 minutes at room temperature, washed 2x with PBS. Cells were transferred to flow cytometry tubes and analyzed on BD FACSCANTO II (BD Bioscience). Cell cycle analysis was done using methods reported previously by Pozarowski, and Darzynkiewicz (2004). Cell cycle analysis data was analyzed using FlowJo software (FlowJo, LLC).

2.8-Annexin V flow cytometry

Annexin V staining was done using Annexin V-FITC apoptosis detection kit (APOAF-20TST; Millipore Sigma). Protocol was performed as per manufacturer instructions. Flow cytometry on cells was performed using BD FACSCANTO II (BD Bioscience). Flow cytometry data was analyzed using FlowJo software (FlowJo, LLC).

2.9-Western blot analysis

Cell lysates were harvested from cell lines by growing cells in T25 flasks. When cells reached 90% confluence cells were lysed using RIPA lysis and extraction buffer (89900, Millipore Sigma). Lysates were incubated on ice for 30 minutes, then flasks were scraped using cell scraper. Cell lysates were then harvested and added to a 1.5 ml eppendorf tube and spun in a centrifuge at 10,000g for 10 minutes at 4°C. After spinning cell lysates were transferred to another eppendorf tube and pellets were discarded. Protein concentration was determined using a Bicinchoninic Acid Protein Assay (B9643; Millipore Sigma). Cell lysates were resolved on an 8-10% sodium dodecyl sulphate (SDS) polyacrylamide gel electrophoresis (PAGE). Cell lysates analyzed for βIII protein expression were run on 10% SDS-PAGE gel, and cell lysates for examining MDR-1 expression levels were ran on an 8% Gel. Resolved lysates were transferred to a polyvinylidene difluoride (PVDF) membrane overnight at 4°C at 20V. After transferring membranes were blocked using 50% rockland blocking buffer (MB-070) in PBS for 1 hour. Membranes were hybridized with rabbit anti-MDR-1 (1:500) (EPR10364-57; AbCam) or rabbit Anti-βIII antibodies (1:1000) (Abcam, ab18207) overnight. The following morning membranes were washed using PBST for 3x 10 minutes. After washing membranes were incubated with goat anti-rabbit secondary antibody (1:1000) conjugated with AlexFluor 680 fluorophore for 1 hour. After 1 hour membranes were washed 3x 10 minutes in PBST. Membranes were than scanned using Li-Cor Bioscience Odyssey imager. Membranes were than incubated with Rabbit anti-actin antibody (1:10,000) for 1 hour. Membranes were washed 3x 10 minutes in PBST. after washing membranes were incubated with goat anti-rabbit secondary antibody (1:10,000) for 1 hour. Membranes were washed 3x 10 minutes in PBST and scanned as mentioned above. Membrane images were analyzed using imageJ quantification software as described.

2.10-MDR-1 inhibition experiments

CAPAN-1, U87, UM-UC-14, and Hela cells were plated in a 96-well plate as described in cytotoxicity experiments above. After adherence, overnight 100 µl of medium containing 5 µM CR42-24, with and without CyA (10 µM) to 3 wells. Media containing only CyA with no

CR42-24 was also added to wells in triplicate. Cells treated with medium containing 0.1% DMSO was used as a control. Cells were incubated in 24-hour time intervals. At time intervals 24, 48, 72, 96, and 120, 22 μl of resazurin was added to each well. Plates were incubated at 37ºC. After 4 hours cell viability was determined using plate reader as described in cytotoxicity experiments.

2.11-MDR-1 gene expression and IC50 correlational analysis

To perform correlation analysis between MDR-1 gene expression and IC50, ABCB1 gene expression values were taken from the CCLE (Broad Institute). IC50 values were taken from cytotoxicity experiments performed and determined using analysis stated above. Correlational analysis was done using GraphPad prism software.

2.12-βIII knockdown

5x 10^3 T24 cells per well were plated in a 96-well plate and left to adhere overnight. The following morning cells were transduced as per manufacturer's instructions using βIII shRNA (sc-105009-V; Santa Cruz biotech) or Control shRNA Lentiviral Particles (sc-108080; Santa Cruz Biotech). After 24 hours of transduction cells were left to rest for 24 hours. After 24 hours cells were selected using puromycin (10 μg/ml). Cells were passaged in puromycin containing medium, changing medium was done every 3 to 5 days. Puromycin resistant cells were scaled up to a T75 flask. Once cells reached 90% confluency cells were harvested and cytotoxicity analysis was performed.

2.13-Statistical analysis

All statistical analysis comparing two groups was done using a student's t-test. p-values less than 0.05 were considered significant. Statistical analysis comparing more than two groups was done using two-way ANOVA. p-values less than 0.05 were considered significant. Kaplan-meier survival curve analysis for *in vivo* survival studies were done using Log-rank (Mantel-Cox) test, p-value < 0.05 was considered statistically significant.

Chapter 3-Results

3.1-CR42-24 decreases cell viability at low nanomolar concentrations *in vitro*

In-vitro screening was used to assess the efficacy of CR42-24 on both human and mouse cancer cell lines. Cell lines were grown in culture and treated with various concentrations of either CR42-24, or paclitaxel. CR42-24 was active on multiple prostate, bladder, skin, breast, pancreatic, and kidney cancer cell lines. CR42-24 had IC50 values in the low nanomolar range (0.8-10 nM) across all cancer cell lines tested (Figure 3.1, and 3.2, and Table 3.1 and 3.2). CR42-24 was most effective on the prostate cell line LNCap with an IC50 of 0.9 nM. CR42-24 was least effective on the Caki-1 cell line with an IC50 of 10.5 nM. For all cell lines tested, CR42-24 was more effective than paclitaxel with the exception of the 786-0 kidney cancer cell line (Figure 3.1D). In addition to being active against cancer cell lines, CR42-24 was cytotoxic to healthy GM38 fibroblast cells. CR42-24 treatment resulted in a 40% reduction in cell viability at concentrations higher than 8nM (Figure 3.1C). Conversely, Paclitaxel was not cytotoxic to GM38 cells at concentrations lower than 1250 nM. It is worth noting that at higher concentrations CR42-24 was less cytotoxic than paclitaxel. Although the majority of the cell lines tested were sensitive to CR42-24, some cell lines were resistant to the compound. Resistant cell lines included the cervical cancer cell line Hela, the prostate cancer cell line PC3, and the glioblastoma cell line U87 (Figure 3.2A-C). These cell lines showed no reduction in IC50 after treatment with CR42-24 after 72 hours. We also compared CR42-24 to gem in pancreatic cancer cell lines. CR42-24 was more effective on MiaPaCa-2 and PANC-1 cell lines showing IC50s of 4.42 nM, and 3.28 nM, respectively compared to gem which had IC50s of 2190 nM for the MiaPaCa-2 cell line, and 18.1 nM for the PANC-1 cancer cell line (Table 3.1). Overall, CR42-24 was found to be highly cytotoxic to cancer cells *in vitro*. CR42-24 was more cytotoxic than paclitaxel and had effect on non-cancerous fibroblast cells, but was less cytotoxic at micromolar doses. Of all the cell lines tested in the cell line panel, CR42-24 was highly effective against the T24 bladder cancer cell line. Due to the high clinical need for alternative therapies for bladder cancer we chose to examine further if CR42-24 would be an effective therapy for bladder cancer.

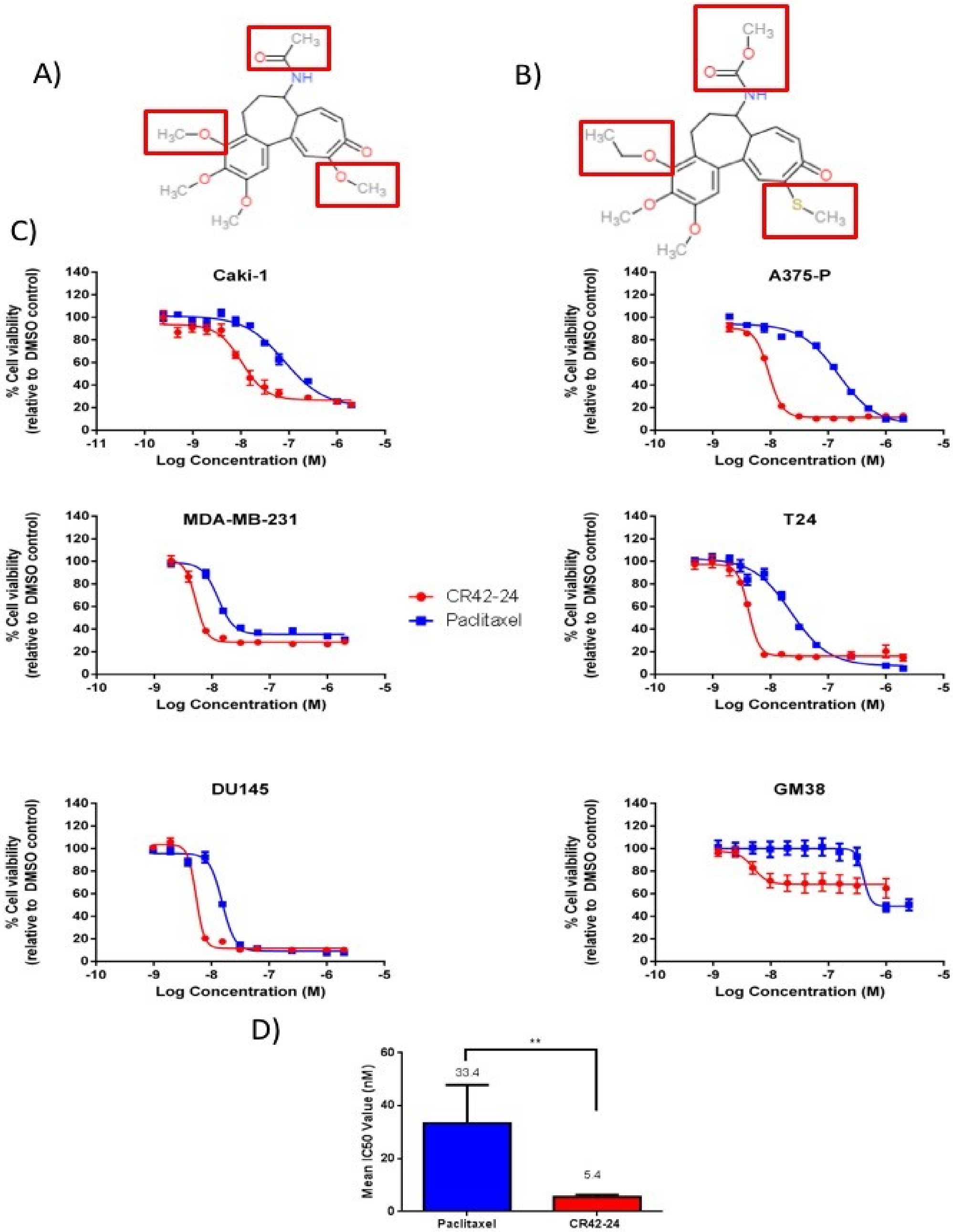

Figure 3.1- CR42-24 is highly effective on cancer cell lines *in vitro* and is more cytotoxic than paclitaxel. Panels A and B show the chemical structure of colchicine, and CR42-24 respectively. Panel C shows representative graphs of the cell viability of cell lines incubated with CR42-24 (red circles) and paclitaxel (blue squares). Graphs indicate the cell viability (mean +/- SD) of cells from three independent experiments run in triplicate. Panel D is a summary graph of the mean IC_{50} values for cell lines. Together this shows that CR42-24 is highly effective on many different cancer cell lines.

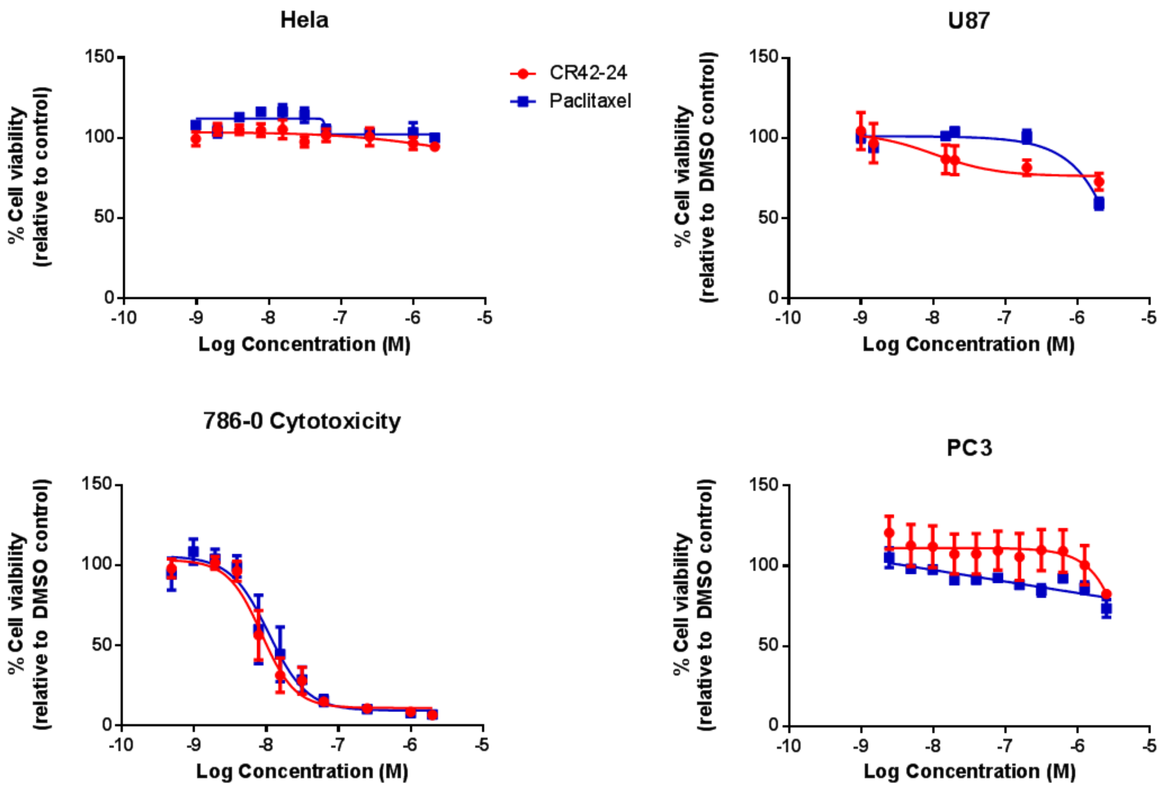

Figure 3.2- Effects of CR42-24 on cancer cell lines *in vitro*. Panels shows representative graphs of the cell viability of Hela, U87, 786-0, and PC3 cell lines incubated with increasing concentrations of CR42-24 (red circles) and paclitaxel (blue squares). Graphs indicate the cell viability (mean +/- SD) of cells from three independent experiments run in triplicate. Overall CR42-24 was not effective on Hela, U87, and PC3 cells. CR42-24 was effective on 786-0 cell line, and was as effective as paclitaxel.

Table 3.1: IC_{50} values of CR42-24 and paclitaxel on cancer cell lines.

Cell line	CR42-24 (nM)	PAC (nM)
Kidney Cancer		
786-0	8.00	10.8
Caki-1	10.5	81.1
Melanoma		
A375-P	9.34	148.0
MDA-MB-435	4.67	9.43
Prostate cancer		
Du145	5.27	15.5
LnCap	9.77	9.75
PC3	> 5000	> 5000
Breast Cancer		
MCF-7	1.80	9.94
MDA-MB-231	5.25	12.7
MDA-MB-468	4.672	14.3
Bladder Cancer		
T24	4.29	27.2
Glioblastoma		
U87	> 5000	> 5000

Table 3.2: IC_{50} values of CR42-24 and gemcitabine on pancreatic cancer cell lines

Pancreatic Cancer		
Cell line	**CR42-24 (M)**	**Gem (nM)**
MiaPaCa-2	4.47	1940
Panc-1	3.28	18.1
CAPAN-1	> 5000	> 5000

3.2-CR42-24 is highly effective on BC cell lines *in vitro*

We tested CR42-24 on a panel of bladder cancer cell lines and compared to single-agent gem and cis. In all cell lines tested (T24, 253J, UM-UC-3, UM-UC-14) CR42-24 had low nanomolar IC50s ranging from 10 nM to 1.9nM (Figure 2.3A-E). CR42-24 also performed better than both single agent gem, and cis. The UM-UC-3 and UM-UC-14 cell lines were largely resistant to gemcitabine showing minimal reductions in IC50 after incubation of 72 hours (20% and 25% reduction in cell viability respectively). In addition to being effective on high grade BC cell lines, CR42-24 was also effective on the low-grade bladder cancer cell lines RT4 (T0) and RT112 (G1) (Figure 2.4). It is worth noting however that after incubation with CR42-24 for 72 hours the RT4 cell line still had a viability of 43% even at 5μM suggesting a subpopulation of the treated cells are still metabolically active. Lastly, we examined if CR42-24 was as effective as combination gem/cis treatment. Cell viability analysis showed that CR42-24 was more effective than combination cis/gem in the T24 cell line when gem/cis was used concurrently (Figure 2.3F). This further supports that CR42-24 may serve as an effective alternative therapy for BC. Altogether data shows that CR42-24 is highly effective on BC. This supports the hypothesis that CR42-24 would be an effective treatment for BC.

A)

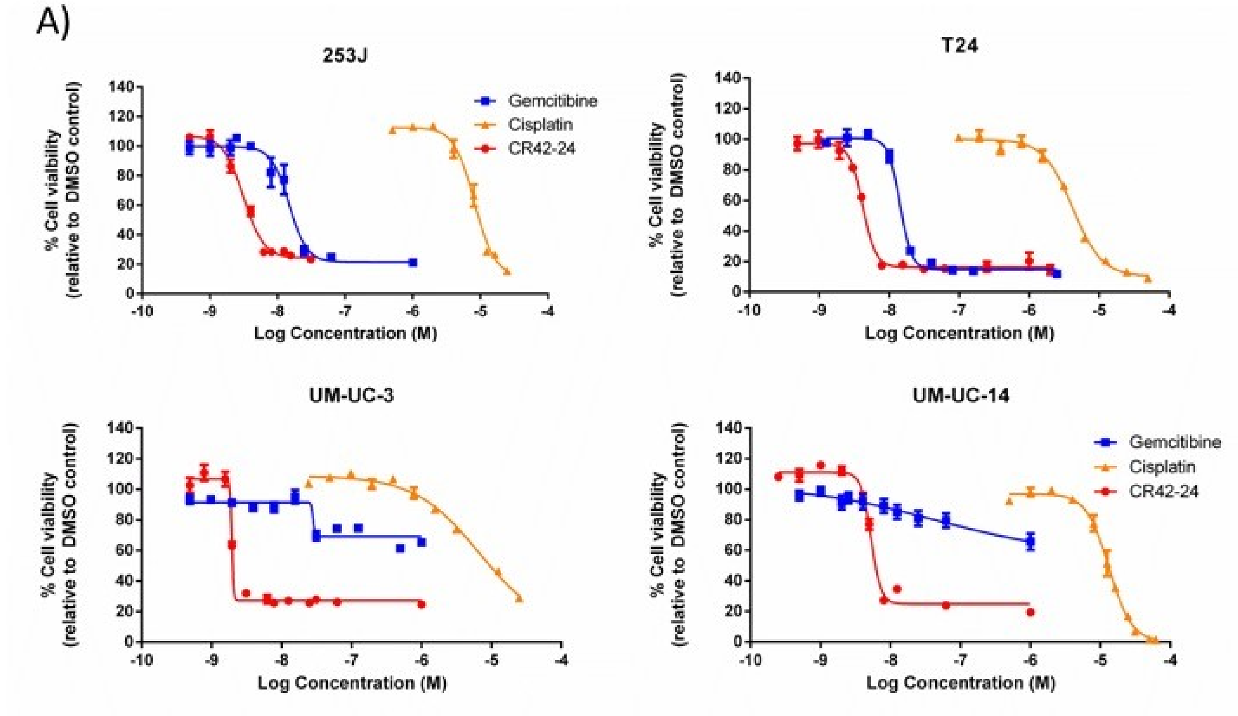

E)

Cell line (grade)	CR42-24 IC50 (nM)	Gemcitabine IC50 (nM)	Cisplatin IC50 (nM)
253J (4)	3.09	37.8	8150
T24 (3)	4.29	13.9	4180
UM-UC-3 (3)	1.9	N/A	8890
UM-UC-14 (4)	5.27	N/A	9100

F)

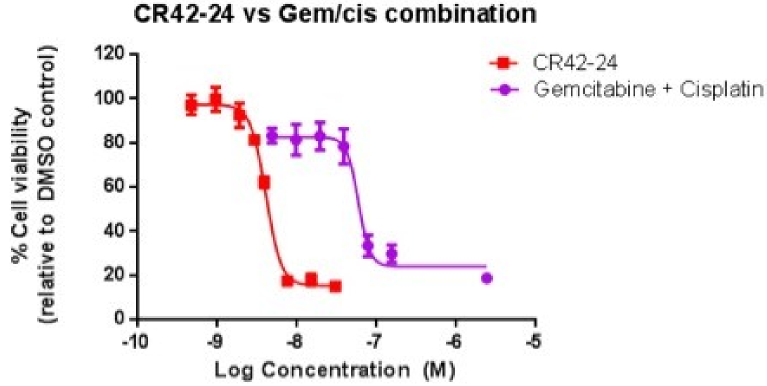

Figure 3.3- CR42-24 active on BC cell lines and is more effective than Gem and Cis *in vitro*. Panel A shows representative graphs of cell viability for bladder cancer cell lines incubated with increasing concentrations of CR42-24 (red), gemcitabine (blue), and cisplatin (orange). Graphs show cell viability (mean +/- SD) for 3 independent experiments done in triplicate. Panel B is a summary table of the IC_{50} values for all of the cell lines used in the bladder cancer cell line panel. Panel C shows a graph of cell viability for T24 cells incubated with CR42-24 (Red) or combination gemcitabine/cisplatin (Purple). Overall, CR42-24 was more effective than single agent and combination gemcitabine/cisplatin in a range of high grade BC cell lines. This demonstrates that *in vitro* CR42-24 is highly effective on BC and supports the hypothesis that it may be an alternative therapy for BC.

3.3-CR42-24 Causes microtubule depolymerization, apoptosis G2/M phase arrest

Because CR42-24 is a colchicine derivative, we hypothesized that the mechanism of action of CR42-24 would be similar to that of colchicine. To investigate this hypothesis, we performed flow cytometry and microscopy on CR42-24 treated cells. Figure 3.5A shows histograms of PI staining in cells treated with increasing concentrations of CR42-24. CR42-24 treatment caused an increase in S-phase and G2/M phase in a dose-dependent manner as shown by the increased the proportion of cells in the G2/M phase of the cell cycle (summarized in Figure 3.5C). Annexin V flow cytometry analysis was also performed to examine for the induction of apoptosis after CR42-24 treatment. Experiments found that there was also an increase in annexin V positive cells in a dose-dependent manner (Figure 3.5B and D). The increase in annexin V and PI positive cells suggests apoptosis induction in CR42-24 treated cells. Together these data suggest CR42-24 acts similarly to other MT targeting agents inducing G2/M phase arrest leading to the induction of apoptosis. We also performed cell imaging experiments on T24 cells treated with 5μM CR42-24. Images show that increased exposure to CR42-24 induces microtubule depolymerization and causes loss of microtubule integrity. Together these data support the hypothesis that CR42-24 behaves like colchicine, inducing depolymerization of microtubules and cause a G2/M phase arrest causing cells to enter into apoptosis.

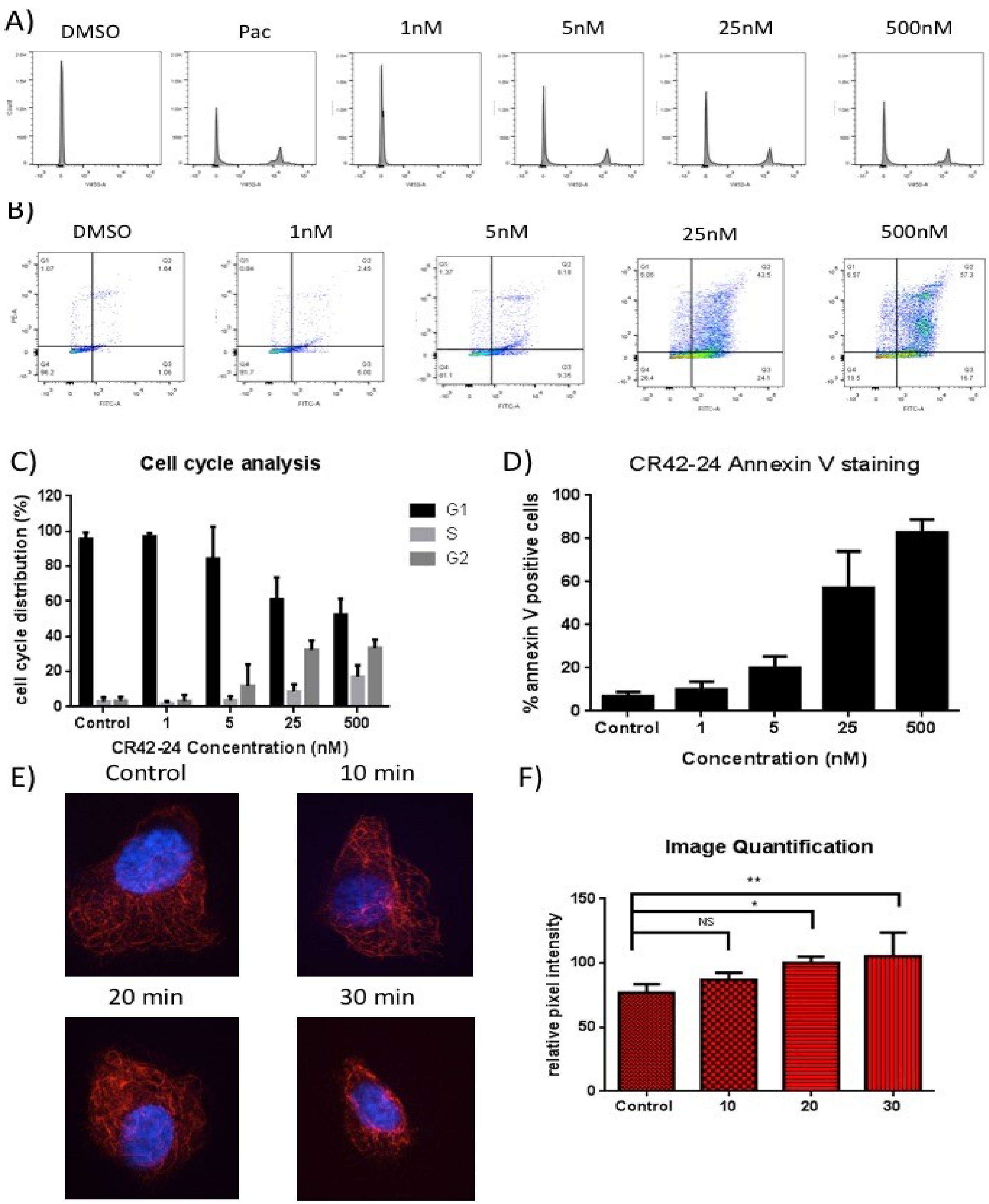

Figure 3.4- CR42-24 induces G2/M phase arrest and induces apoptosis in T24 cells. Panel A shows representative histograms of T24 cells treated with CR42-24 for 48 hours. Stained cells were then analyzed by flow cytometry for analysis of DNA content within cells. Panel B shows representative flow cytometry plots of cells treated with increasing concentrations of CR42-24 for 48 hours. Panel C summarizes cell cycle analysis data from 3 independently performed experiments done in duplicate. Panel D summarizes 3 independently performed experiments analyzing annexin V flow cytometry data for T24 cells treated with CR42-24. The graph indicates an increase in Annexin V, both early and late apoptotic cells, in a dose dependent manner. Panel E shows representative images of T24 cells treated for various time intervals. Top left shows a control cell treated with media containing 1% DMSO for 30 minutes. Top right shows a cell treated for 10 minutes, bottom left shows a cell treated for 20 minutes and bottom right shows a cell treated for 30 minutes. Panel F shows a graph summarizing 3 independent cell imaging experiments. Pixel intensity was measured for 5 cells from each experiment using imageJ. Together this data shows that treatment with CR42-24 induces microtubule catastrophe and causes loss of microtubule integrity. * $p < 0.05$; ** $p < 0.01$

3.4-CR42-24 decreases xenograft tumor growth *in vivo*

To further investigate the applicability of CR42-24 to treat BC we then examined CR42-24 *in vivo*. T24 xenografted NOD/SCID/γ mice were treated with either CR42-24 (3 mg/kg or 6 mg/kg) or vehicle control every second day for 18 days (10 injections total). Overall, CR42-24 was able to block T24 tumor growth (Figure 3.6A) without any overt signs of toxicity, assessed by change in body weight (Figure 3.6B). Treatment at doses of 3 and 6 mg/kg were able to completely negate tumor growth in treated mice. There was a statistically significant difference between control and both treatment groups ($p < 0.01$, one-way ANOVA). There was no statistically significant difference between 3 and 6 mg/kg doses of CR42-24. Overall, CR42-24 was able to slow the growth of T24 xenografts in vivo, and was able to prevent tumor growth at a dose of 3 mg/kg. To test a more clinical situation we tested CR42-24 on mice bearing larger T24 xenografts. CR42-24 was not able to control tumor growth as shown by the increase in tumor volume over the course of the treatment period (Figure 3.6C). Most mice only received 5 injections of CR42-24 at which point they had to be euthanized due to tumor burden end-point being reached. Although CR42-24 did not stop tumor growth, CR42-24 was able to slow the

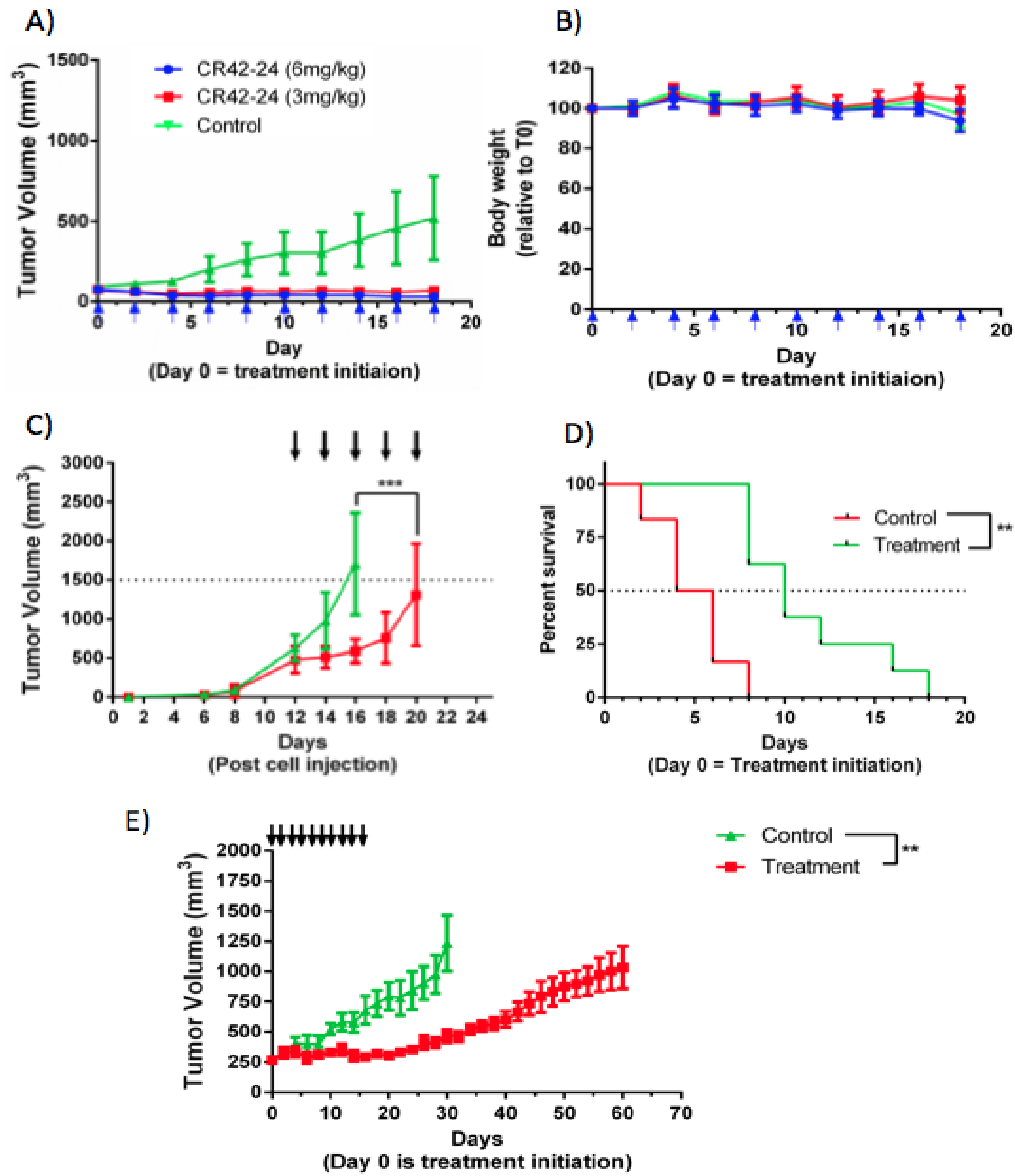

Figure 3.5- CR42-24 inhibits growth of T24 cell line and patient derived xenografts *in vivo*. Panel A, Graph of tumor volume for CR42-24 treated mice and vehicle control mice. Control mice (n=4) were treated with vehicle control (10.5% DMSO in PBS, shown in green) and CR24-24 treated mice treated at 3 or 6 mg/kg (red, and blue respectively). Panel B shows the change in body weight for the treatment groups shown in A. Panel C shows tumor volume for

T24 xenograft bearing mice that were injected when tumors reached a volume of 500 mm^3. Mice were injected every second day at 3 mg/kg of CR42-24 or vehicle control. Panel D shows a Kaplan-Mayer survival curve of the mice shown in panel C. Panel E shows tumor growth of PDXs in NSG mice. Overall CR42-24 significantly delays both cell line derived xenografts and patient derived xenografts *in vivo*. ** $p < 0.01$; *** $p < 0.001$

growth of xenografts. There was a significant difference between the growth curves of control mice and CR42-24 treatment groups ($p< 0.001$, one-way ANOVA). Moreover, treatment with CR42-24 was able to double the time to tumor burden end-point relative to the control group (Figure 3.6D). Mice treated with vehicle control had a median survival of 5 days after initiation of treatment whereas mice treated with CR42-24 had a median survival of 10 days ($p< 0.01$, Wilcoxon-Gehan test). Together this data shows that CR42-24 has the ability to treat larger tumors *in vivo*, further supporting its utility as a treatment for BC patients. We also tested the effect of CR42-24 on a patient-derived xenograft model (PDX). Tissue from a high-grade (T3b) chemo-naive patient was xenografted into NOD/SCID/γ mice. Once tumors reached 200 mm^3 treatment was initiated. CR42-24 was able to negate tumor growth for the duration of the treatment period (Figure 3.6 and 3.5E). Treatment with CR42-24 significantly reduced tumor growth as compared to vehicle control ($p< 0.01$, one-way ANOVA). Specifically, CR42-24 was able to significantly extend the median survival of CR42-24 treated mice relative to control mice ($p < 0.05$). The ability of CR42-24 to treat PDX models further supports the utility of CR42-24 as a treatment for BC.

Lastly, we compared the effects of CR42-24 against combination cis/gem. Mice bearing T24 xenografts were treated with CR42-24 (3 mg/kg, red), cis/gem (40 and 3 mg/kg respectively, blue), or vehicle control (10.5% DMSO in PBS, green). Overall, CR42-24 performed as well as combination cis/gem and negated tumor growth for the duration of the experiment (Figure 3.5A). There was no significant difference in tumor volume between CR42-24 and gem/cis groups ($p > 0.05$). There was a significant difference between control and CR42-24 ($p < 0.01$, one-way anova) and control and gem/cis groups ($p < 0.01$, one-way anova). Panel B shows the body weight for the mice over the injection period. Mice were weighed once a week over the course of the experiment to ensure there were no signs of toxicity associated with treatment. There was no significant difference between control, CR42-24, and gem/cis groups body weight over the injection period ($p > 0.05$, one-way anova). This suggests that at a dose of 3 mg/kg CR42-24 was not toxic to mice. Moreover, cis/gem at doses of 3 mg/kg and 40 mg/kg, respectively, are non-toxic. Figure 3.5C shows a graph of tumor weights on day 43 24 hours following the last treatment day. As with tumor volume there was a significant difference between control and CR42-24 ($p <0.001$, one-way anova) and control and gem/cis groups ($p < 0.01$, one-way anova). There was no significant difference between CR42-24 and gem/cis group ($p > 0.05$, one-way anova). Panel D shows representative images of tumors excised from mice on day 43. Overall, this data suggests that CR42-24 is as effective as cis/gem combination therapy. The ability of CR42-24 to negate tumor growth *in vivo* as effectively as cis/gem at a safe dose further lends support to CR42-24 being an effective treatment on BC.

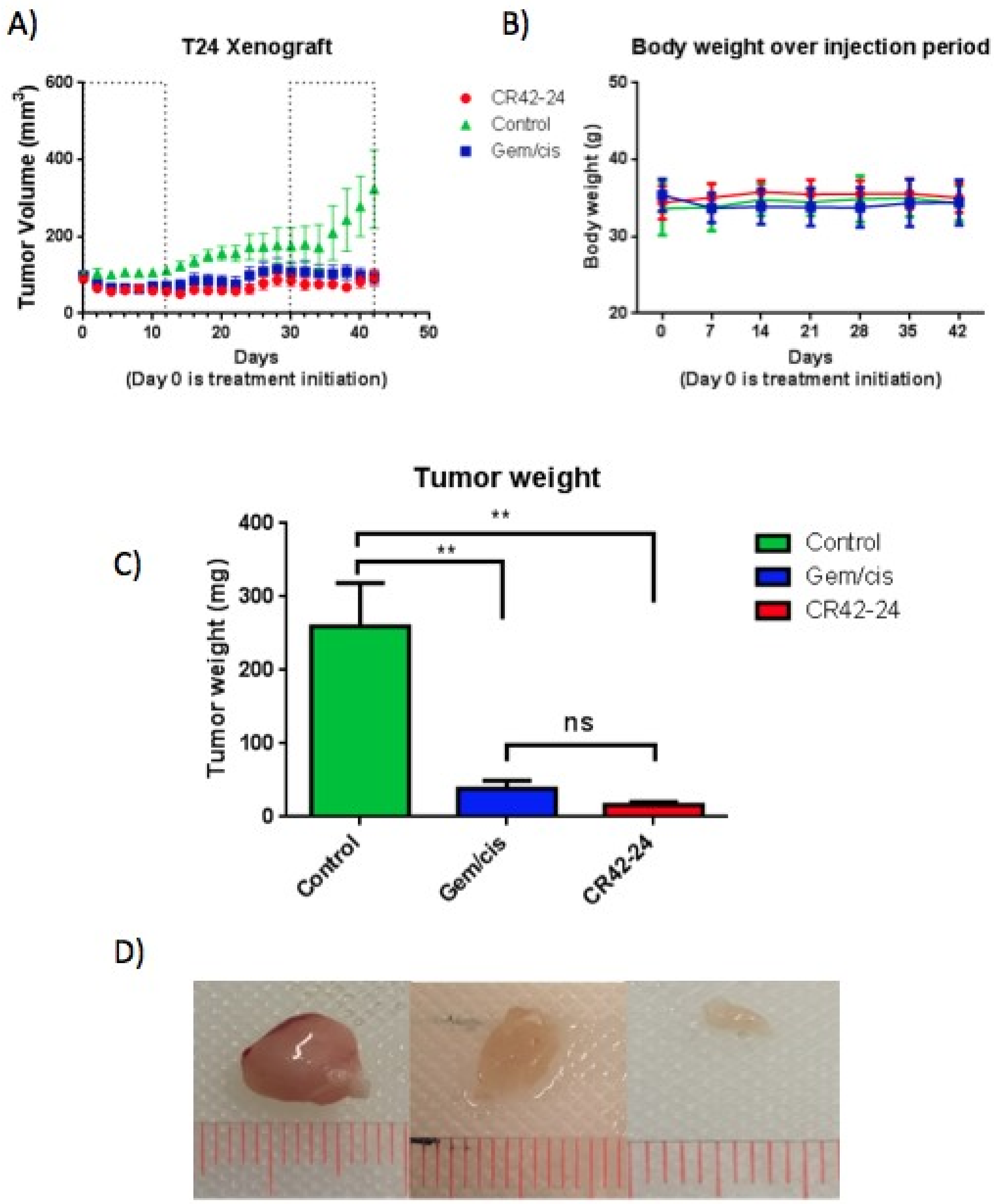

Figure 3.6- Effects of CR42-24 as compared to Gemcitabine/cisplatin combination therapy *in vivo*. Panel A shows the growth of T24 xenografts when treated with CR42-24 (red), gemcitabine/cisplatin (blue), or vehicle control (green). Treatment cycles as described in materials and methods are represented by dashed boxes. Panel B shows the body weight for the mice over the injection period. There were no significant differences observed between control,

CR42-24, and gemcitabine/Cisplatin groups' body weight over the injection period ($p > 0.05$, one-way ANOVA). Panel C shows a graph of tumor weights on day 43, 24 hours following the last treatment day. As with tumor volume there was a significant difference between control and CR42-24 ($p < 0.001$, one-way ANOVA) and control and gemcitabine/cisplatin groups ($p < 0.01$, one-way ANOVA). There was no significant difference between CR42-24 and gemcitabine/Cisplatin group ($p > 0.05$, one-way

3.5-CR42-24 resistance in MDR-1 mediated in a cell line dependent manner

It has been shown that colchicine is a substrate of multidrug resistance protein 1 (MDR-1), which has been found to be a mechanism of resistance to a number of compounds. We examined if MDR-1 was responsible for mediating resistance to CR42-24(159). PC3, U87, and CAPAN-1 cell lines were found to be insensitive to CR42-24, with IC50s being higher than 5 μM (Table 1) using resazurin assay. We hypothesized that these cell lines would have increased expression of MDR-1 therefore conferring resistance to CR42-24. To test this hypothesis, we began by performing a correlational analysis of MDR-1 gene expression using the Cancer Cell Line Encyclopedia (CCLE) and the IC50 values for each of the cell lines tested. We found that there was a weak ($r2=0.16$) but significant ($p =0.0016$) correlation between MDR-1 gene expression and IC50 (Figure 3.7A). We then examined cell lysates from the resistant cell lines and sensitive cell lines. Figure 3.7B shows western blot data of cell lysates from several cell lines. Cell lysates were harvested from the resistant CAPAN-1, U87, Hela, and PC3 cells, as well as the sensitive cell lines PANC-1, MDA-MB-468, UM-UC-3, and UM-UC-14. There was no trend observed in the resistant cell lines as only Hela contained detectable amounts of MDR-1 whereas CAPAN-1, PC3 and U87 cells did not. In the sensitive cell lines, Panc-1, MDA-MB-468, and UM-UC-3 cell lines had no detectable quantities of MDR-1. Surprisingly, UM-UC-14, one of the most sensitive cell lines had the greatest MDR-1 gene expression. Due to the gene expression data, and western blot data conflicting we performed functional analysis on both resistant and sensitive cell lines. We incubated cell lines with CR42-24 with and without cyclosporine A (CyA). Cyclosporine A has been found to be a competitive inhibitor of MDR-1 and is the basis for many clinical inhibitors of MDR-1 that have entered clinical trials (160,161). Incubating cells with CyA made Hela and UM-UC-14 cells much more sensitive to CR42-24 killing, showing a more rapid reduction in cell viability when combined with CyA as compared to CR42-24 alone (Figure 3.7C, D). Incubating CAPAN-1 and PC3 cells with CyA did not sensitize the cells to CR42-24 (Figure 3.7E, F). Overall, this data suggests that MDR-1 gene expression does confer sensitivity to CR42-24 in cell line dependent manner. When cell lines are MDR-1 positive, cell lines show increased sensitivity to CR42-24 when MDR-1 is inhibited. However, when MDR-1 is absent, such as in the PC3 and CAPAN-1 cell lines, MDR-1 does induce resistance to CR42-24. In this case, other mechanisms of resistance are likely responsible for insensitivity to CR42-24. In conclusion, MDR-1 is not the sole determinant of sensitivity to CR42-24, and other mechanisms, such as off-target interactions, may determine resistance to CR42-24.

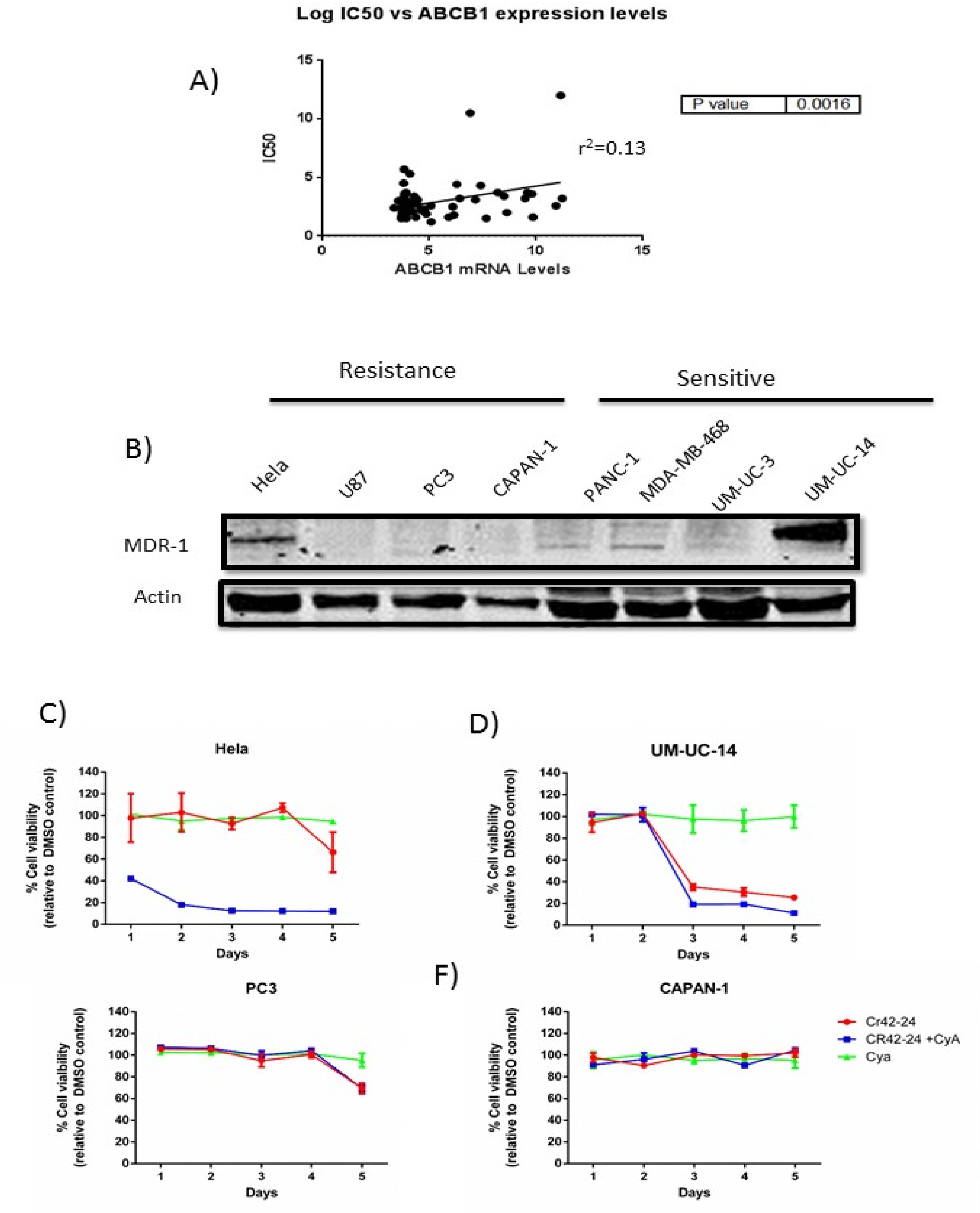

Figure 3.7- MDR-1 meditates CR42-24 resistance in a cell dependent manner. Panel A shows a correlation graph of MDR-1 gene expression and IC50 value for all sensitive cell lines screened in vitro. Panel B shows western blot results of cell lysates from different cell lines. Hela, U87, PC3, and CAPAN-1 cells

which were Panel C shows graphs of cell lines incubated with CR42-24 and or without cyclosporine A. Graphs indicate the cell viability of cells (mean +/- SD) from 3 independent experiments. Cells were then incubated with CR42-24 with (blue) and without (red) cyclosporine A. Cells were incubated with cyclosporine alone as a control (green). Overall MDR-1 appears to mediate resistance to CR42-24 but in a cell line dependent manner.

3.6-Decreases in βIII tubulin levels do not affect sensitivity to CR42-24

Since CR42-24 was found to have increased affinity for βIII we also examined whether or not changes in βIII tubulin levels changed sensitivity to CR42-24. We began by performing a western blot on cell lysates harvested from cell lines tested for CR42-24 activity (Fig 3.8A). Cell lines were selected based on their level of sensitivity to CR42-24. Pairs from each type of cancer tested were selected, one cell line that was most sensitive to CR42-24 (lowest IC50, black) and one that was most resistant (highest IC50, red). Overall there was no trend in βIII levels in cell lysates. Most cell lines were positive for βIII expression. However, MDA-MB-468 and CAPAN-1 had almost no βIII tubulin. Western blot results are summarized in Figure 3.8B. The lack of a trend in βIII tubulin levels between resistant and sensitive cell lines suggests that βIII levels do not determine sensitivity to CR42-24. To confirm this hypothesis βIII knockdown in T24 cells was performed and sensitivity to CR42-24 and paclitaxel was assessed. Stable transduction of T24 cells resulted in a 20% reduction in βIII tubulin levels (Figure 3.8C). Viability of cells transduced with βIII or scramble shRNA and treated with CR42-24 are shown in Figure 3.8D. Decreasing βIII tubulin levels appeared not to affect sensitivity to CR42-24 (Figure 3.8D, left). However, knockdown of βIII sensitized the cells to paclitaxel (Figure 3.8D, right). There was a significant difference ($p < 0.05$) in cell viability for shTUBB3 cells as compared to shControl cells when incubated with paclitaxel at 50, 25, and 12.5nM of paclitaxel. There was no significant difference in cell viability (as assessed by alamar blue assay) for shβIII knockdown cells as compared to shControl cells. The lack of a trend in βIII levels among cell lines with varying degrees of sensitivity to CR42-24 and knockdown experiments corroborating this data together suggest CR42-24 sensitivity is not determined by βIII levels. It should be noted, however, that CR42-24 binds to all tubulin isotypes at various binding affinities, with the highest affinity for βIII. Consequently, the resultant toxicity of CR42-24 is a combination of all individual isotype affinities weighted by the expression levels of these isotypes in a given cell line.

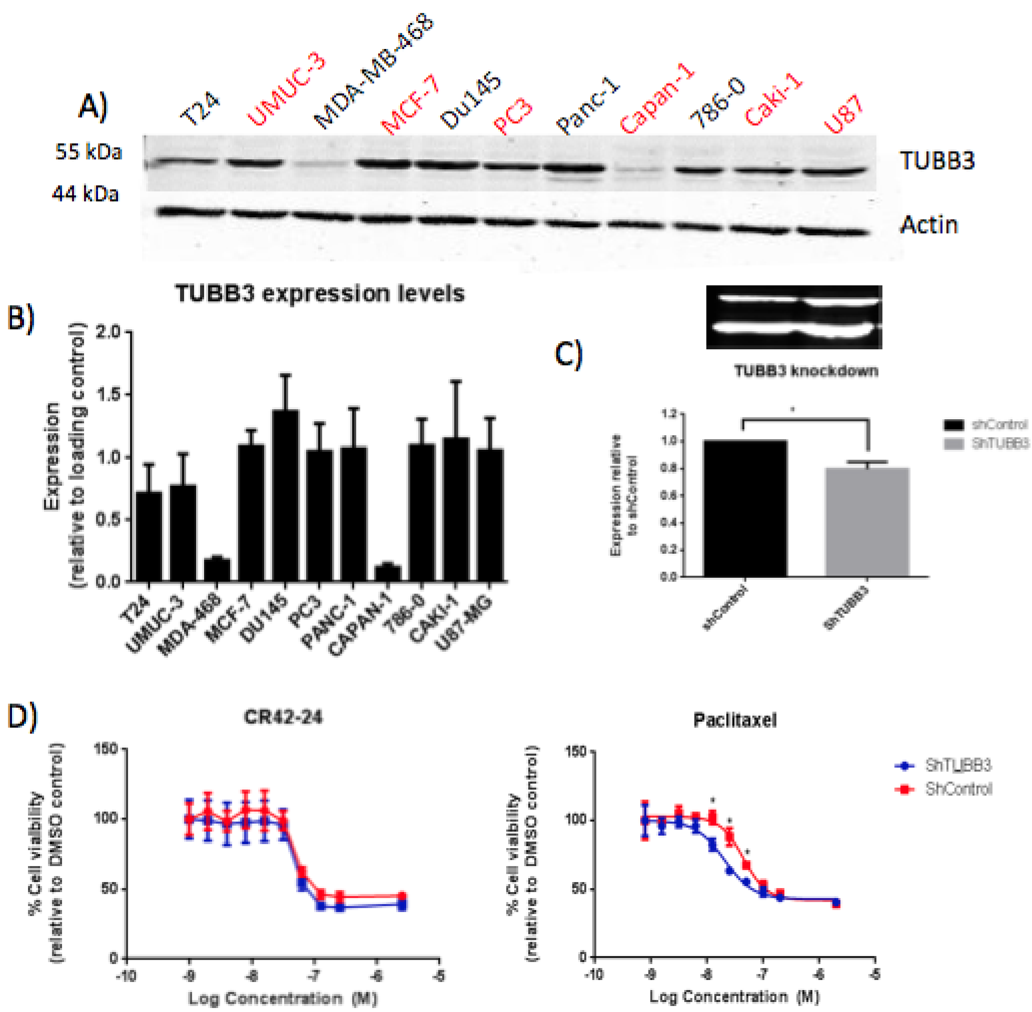

Figure 3.8-βIII tubulin knockdown does not affect sensitivity to CR42-24. Panel A shows western blot data for cells lines that were tested for sensitivity to CR42-24 and data is summarized in panel B showing a graph of expression for cell lines (N=3 +/- SD). Panel C shows western blot knockdown results using shRNA. Graph in lower panel C summarizes western data from 3 separate passages of T24 cells passaged in medium containing 5μM puromycin. Panel D shows cell viability data from T24 cells transduced with shTUBB3 or

shControl. Overall βIII knockdown cells showed increased sensitivity to paclitaxel but not to CR42-24. This data suggests that changes in βIII levels do not affect sensitivity to CR42-24.

Lastly, we examined whether CR42-24 could be used in combination with gem or cis. Since new therapies that are introduced into a clinical setting are often combined with current standard of care therapies we wanted to test whether or not CR42-24 could be combined with current therapies for BC. To test this, we combined CR42-24 with gemcitabine or cisplatin and sequentially treated cells. First T24 and 253J cells were incubated with gemcitabine, cisplatin, or with CR42-24 for 24 hours. After 24 hours cells were washed and then treated with the combinational drug for 48 hours. After a total of 72 hours, cell viability was tested using resazurin. Overall, CR42-24 was synergistic with both cisplatin and gemcitabine when given sequentially (Figure 3.9). Pre-treating cells with CR42-24 highly sensitized the cells to cisplatin killing. Doses above 2 μM cisplatin were found to be effective on CR42-24 pre-treated cells whereas cisplatin alone did not affect cell viability (Figure 3.9A and 3.10A). In the T24 cell line treatment with 2 μM cisplatin reduced cell viability to 71%, thus the addition of cisplatin further reduced cell viability by 9%. 4 μM cisplatin was able to reduce cell viability to 67%, in contrast to cisplatin alone which did not reduce cell viability relative to DMSO control treated cells at doses lower than 4 μM. To determine whether or not these combinations were synergistic we performed combinatory index calculations. 2, 4, and 50 μM cisplatin were found to be highly synergistic with CI values of 0.11, 0.07, and 0.05 respectively (Figure 3.9B). In both T24 and 253J cell lines CR42-24/gemcitabine combination treatment was also found to be effective (Figure 3.9C, D, and 3.10B). In both cell lines when cells were pre-treated with gemcitabine for 24 hours, cells were sensitized to killing by CR42-24. Incubating cells with CR42-24 following gemcitabine treatment sensitized the cells to killing at all doses tested (Figure 3.9C). In the T24 cell line doses of CR42-24 as low as 0.5 nM were significantly more active on gemcitabine pre-treated cells than cells treated with CR42-24 alone. We also calculated CI values for these

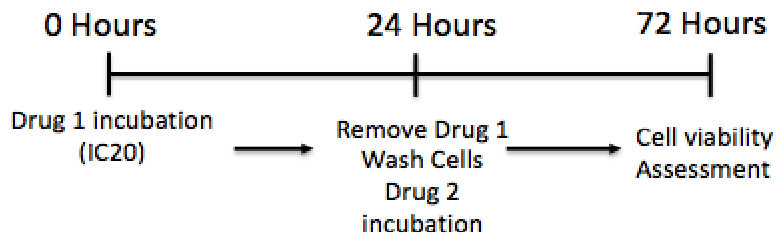

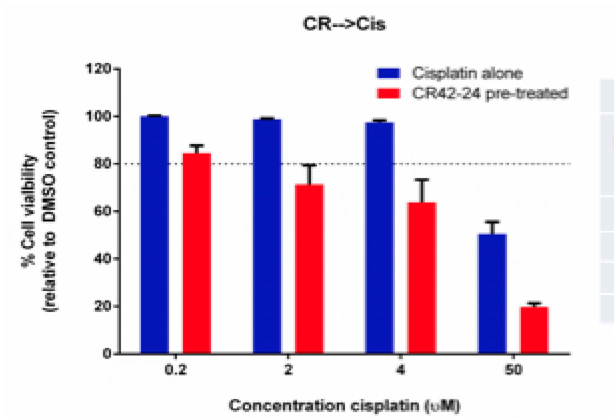

CR42-24 → Cisplatin			
Dose Cr (nM)	Dose Cis (uM)	Effect (% cells killed)	CI
4.0	0.2	0.15	1.2
4.0	2.0	0.29	0.11
4.0	4 .0	0.37	0.07
4.0	50	0.8	0.05

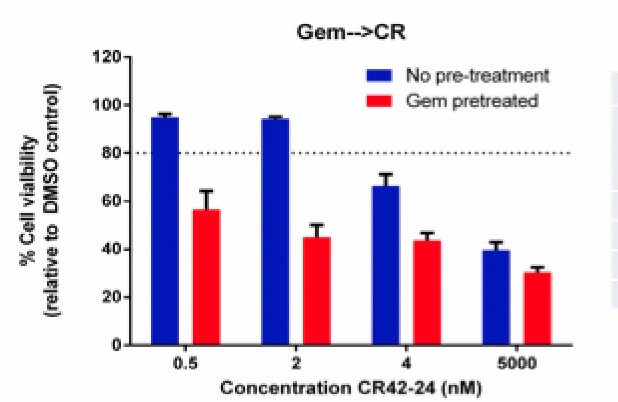

Gemcitabine → CR42-24			
Dose CR42-24 (nM)	Dose GEM (nM)	Effect (% cells killed)	CI
0.5	10	0.44	0.86
2.0	10	0.56	0.61
4.0	10	0.57	0.59
5000	10	0.70	0.86

Figure 3.9-CR42-24 is synergistic with Gemcitabine and Cisplatin in a sequence specific manner. Panel A shows a schematic of the experimental design for drug synergy studies. Panel B shows a graph of cell viability for cells either pre-treated with CR42-24 followed by incubation with cisplatin (red) or treated with cisplatin alone for 72 hours at the same concentrations (blue). The combinatory index values for the drug combinations is summarized in the table on the right of panel B. Panel C shows the cell viability of cells pretreated with gemcitabine followed by treatment with CR42-24 compared to cells treated with CR42-24 alone for 72 hours. Panel D right shows CI values calculated for each of the concentrations of drug

used in the synergy testing. Dotted lines indicate the cell viability of cells treated with only IC20 concentration of CR42-24 (A) and Gem (B). Together this evidence shows that CR42-24 is synergistic with both gemcitabine and cisplatin in a schedule dependent manner.

combinations and found that values ranged from 0.86 to 0.59, suggesting that gemcitabine/CR42-24 has a mild additive effect (Figure 3.9D). In the 253J cell line pretreating cells with gem sensitized cells to CR42-24 killing. Low doses of CR42-24 show increased reduction in cell viability, whereas CR42-24 alone did not cause reductions in cell viability (Figure 3.10B). Synergy was only seen when cells were pre-treated with CR42-24 followed by cis, and pretreated with gem followed by CR42-24. In T24 cells, pre-treating cells with CR42-24 followed by gem was not synergistic, and pre-treated cells were as sensitive to gem as non-pretreated cells (Figure 3.11A). Additionally, when cells were pretreated with cis followed by CR42-24, treatment was not synergistic and pretreated cells showed no sensitization to CR42-24 killing (Figure 3.11B). Together this data suggests that CR42-24 can be effectively combined with other chemotherapy drugs. However, the synergy of CR42-24, gem, and cis only occurs in a sequential manner, and is dependent on proper sequence of administration. Overall, it suggests that combining CR42-24 with current BC chemotherapy drugs may be beneficial and make other drugs more efficacious.

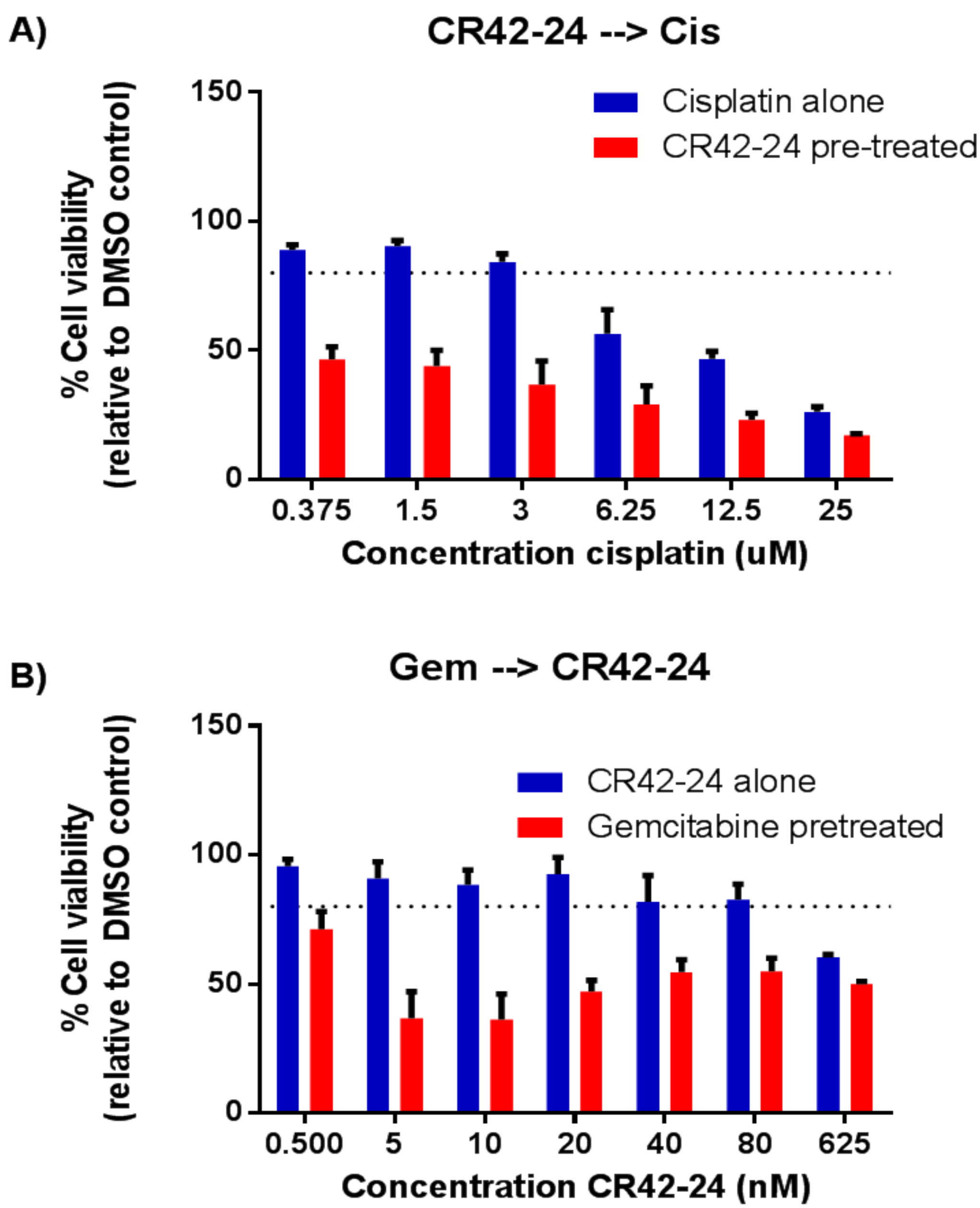

Figure 3.10- Synergy of CR42-24, Gem, and Cis on 253J cells. 253J cells were incubated for 24 hours with an IC20 concentration of CR42-24 (a) or gem (b). Panel A shows a graph of cell viability for cells either pre-treated with CR42-24 followed by incubation with cisplatin

(Red). As a control cells were treated with cisplatin alone for 72 hours at the same concentrations as those used in the sequential treatment condition (blue). Panel B shows the cell viability of cells pretreated with gemcitabine (red), followed by treatment with CR42-24 compared to cells treated with CR42-24 alone (blue) for 72 hours. Dotted lines indicate the cell viability of cells treated with only IC20 concentration of Gem. Overall, CR42-24 is synergistic with both gem and cis in a schedule dependent manner.

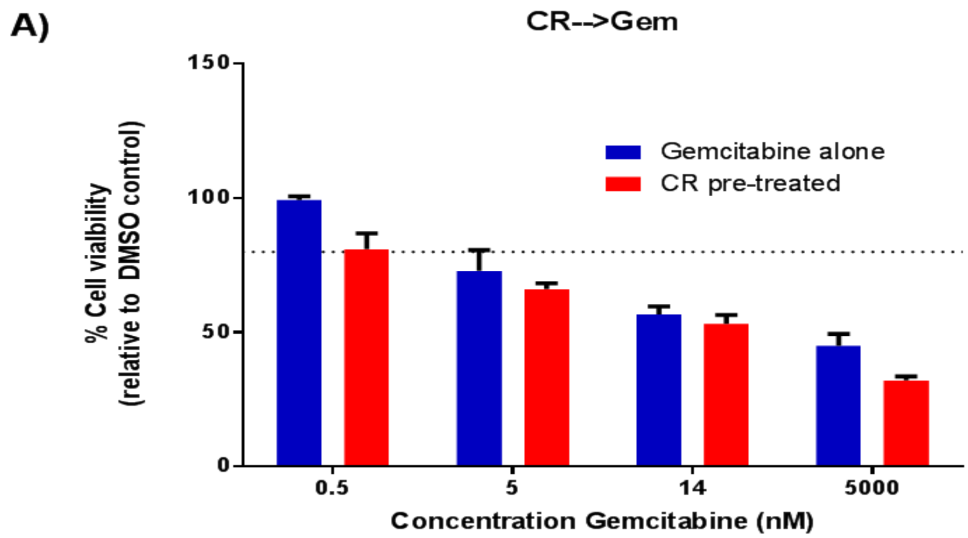

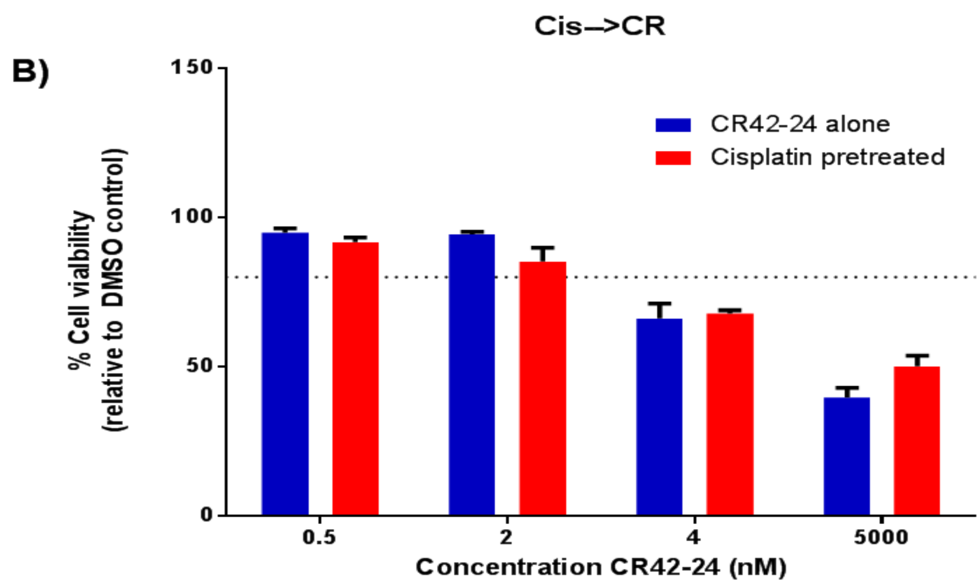

Figure 3.11- Sequence dependent synergy of CR42-24 and Gem, and Cis. Panel A shows a graph of cell viability for cells either pre-treated with CR42-24 followed by incubation with gem (Red) or treated with gem alone for 72 hours at the same concentrations (blue). Pre-treating cells with CR42-24 does not sensitizes cells to gem killing. Panel B shows the cell viability of

cells pretreated with cis (red), followed by treatment with CR42-24 compared to cells treated with CR42-24 alone (blue) for 72 hours. Dotted lines indicate the cell viability of cells treated with only IC20 concentration of CR42-24 (A) and Cis (B). Pre-treating cells with cis does not sensitizes cells to CR42-24 killing. Together this data suggests a sequence dependent synergy between CR42-24, gem, and cis.

Chapter 4-Discussion and Conclusion

4.1-Discussion and conclusion

Here we have demonstrated that CR42-24, a novel colchicine derivative, is a promising new cancer therapy agent. CR42-24 showed increased performance compared to other clinically used chemotherapy drugs *in vitro* (Figure 3.1, 3.2, Table 3.1). In particular, CR42-24 was highly effective against BC. Assessment of CR42-24 *in vitro* and *in vivo* showed that CR42-24 is highly effective against both BC cell line xenografts and PDXs (Figure 3.3, 3.4, and 3.6). CR42-24 is also as effective as combination cis/gem *in vivo* (Figure 3.5). Together data supports that CR42-24 is a promising therapy agent for BC.

Initially, we began by assessing CR42-24's activity on a number of cell lines. We found that CR42-24 had IC50 values in the low nanomolar range (1 nM to 10 nM) for most of the cell lines tested. CR42-24 was more cytotoxic than paclitaxel in all cell lines tested with the exception of the kidney cancer cell line 786-0 (Figure 3.2). Interestingly, CR42-24 was highly effective on another kidney cancer cell line Caki-1, and had increased effectiveness compared to paclitaxel (Figure 3.1). These conflicting results may be due to insensitivity of 786-0 cells to MTAs. Clinically renal clear cell carcinoma (RCC) is unresponsive to chemotherapy, and patients see little benefit with chemotherapy treatment (162,163). Moreover, mechanisms of resistance to chemotherapy have been found to extend beyond that of MDR-1 expression, suggesting RCC has multiple mechanisms of resistance to chemotherapeutics (164).

Few cell lines screened were resistant to CR42-24. However, Hela, PC3, CAPAN-1, and U87 cells were found to have IC50s above 5 μM. A possible hypothesis for these results that was not examined could be that CR42-24 is inducing cellular senescence. Cells that have entered into senescence have been shown to be still metabolically active but remain in a non-proliferative state (165,166). The induction of senescence may, therefore explain why these cells showed little reduction in cell viability using resazurin assay. In support of this it has been shown that prostate cancer, glioblastoma, and pancreatic cancer cell lines are all capable of entering senescence (167–172). In this context, CR42-24 may still be active against these cell lines, but does not cause apoptosis induction.

CR42-24 was also highly effective against BC cell lines *in vitro*. CR42-24 had IC50s in the low nanomolar range for the cell lines tested. CR42-24 was more effective than single-agent gem and cis, showing lower IC50s in all cell lines tested (Figure 3.3). CR42-24 was also highly effective on the UM-UC-3 and UM-UC-14 cell lines, which showed little reduction in cell viability after gem treatment for 72 hours (Figure 3.3C, and D). This suggests CR42-24 may serve as an effective treatment for BC that is insensitive to gem. In addition to being more effective than single agents, CR42-24 was more effective than concurrent cis/gem treatment in the T24 cell line. These results may only hold in this context as the synergy of cis/gem has been reported to work in both a schedule and a cell line-dependent manner (173–175). Broader results regarding the comparison between CR42-24 and combination cis/gem cannot be made without further investigation. However, these results are encouraging and further support the effectiveness of CR42-24 on BC.

In addition to being active *in vitro*, CR42-24 was highly effective *in vivo*. CR42-24 was able to negate the tumor growth of both T24 xenografts, as well as BC PDXs. CR42-24 was effective at both 3 mg/kg and 6 mg/kg and was able to inhibit tumor growth for the duration of treatment (Figure 3.6A). CR42-24 was also able to slow tumor growth of larger T24 tumors although it was unable to inhibit tumor growth completely. This may have been a consequence of the dosage used as only 3 mg/kg. More efficacious results may have been obtained with a higher dose. Most encouraging was CR42-24s ability to treat high-grade patient-derived xenografts *in* *vivo*. CR42-24 was able to delay growth of PDXs and able to extend survival of the mice from 31 to 82 days. These results are very encouraging as PDX models are much more representative of a clinical setting and provide further support that CR42-24 would be a good candidate for a BC therapy.

We also investigated CR42-24's mechanism of action and found it to act similarly to microtubule destabilizers such as colchicine and other vinca alkaloids (60,176). CR42-24 induces a G2/M phase arrest, and apoptosis in treated cells. Moreover, CR42-24 acts as a MT destabilizer with treated cells showing loss of MT structure after treatment for 20 minutes (Figure 3.5E and F). These results show that CR42-24, acts in a similar manner to other MT destabilizers. It has been shown that both colchicine and other vinca alkaloids cause microtubule depolymerization and induce G2/M phase arrest (60, 173). Also, other novel colchicine derivatives have been reported in the literature to exhibit a similar mechanism of action. The derivative CT20126, which shows immunosuppressive activity, has been reported to have a similar mechanism of action inducing microtubule depolymerization and G2/M phase arrest (177).

We then examined possible mechanistic explanations for sensitivity to CR42-24. MDR-1 protein expression has been shown to mediate resistance to multiple chemotherapeutics. Specifically, colchicine has been shown to be a MDR-1 substrate and MDR-1 expression has been shown to confer resistance to colchicine treatment (159,178,179). Thus, we investigated whether or not MDR-1 conferred resistance to CR42-24 as well. Overall, MDR-1 appears to affect sensitivity to CR42-24 in a cell line dependent manner. The UM-UC-14 and Hela cells, both of which were positive for MDR-1, showed increased sensitivity to CR42-24 when MDR-1 was inhibited by CyA. However, PC3 and CAPAN-1 cells were not sensitized to CR42-24 when

MDR-1 was inhibited. Overall, this this suggests other mechanisms of resistance are also responsible for conferring insensitivity to CR42-24. In addition to MDR-1, there are multiple multi-drug resistance proteins (MRP) expressed by cancer cells (180). There are nine MRP proteins that have been found to be expressed by cancer cells and induce resistance to a number of anti-cancer agents. Little is known about MRP protein functions, substrate specificities, and their role in cancer cell resistance (180–182). A possible hypothesis is that other MRP proteins have increased affinity for CR42-24 over MDR-1 increasing resistance to CR42-24. It is worth noting that these results do agree with published literature which has shown that other βIII targeting compounds are poor substrates for MDR-1 and overcome MDR-1 mediated resistance (74,156,158). βIII specific Taxol derivatives have been shown to have reduced affinity for MDR-1 and are effective on cell lines with increased MDR-1 gene expression. Other colchicine derivatives have also been shown to have reduced affinity for MDR-1 and can overcome colchicine resistance (74).

In addition to examining MDR-1 as a determinant for CR42-24 sensitivity, βIII tubulin levels were also examined. Based on our results it appears that βIII level does not determine sensitivity to CR42-24. In-vitro screening demonstrated that CR42-24 was effective on cell lines irrespective of βIII tubulin expression levels (compare Table 2.1, and 2.2 and Figure 2.8A). This suggests that despite increased βIII tubulin expression CR42-24 is still highly effective. A similar trend was also found for the Taxol derivative Yg-3-46a which was shown to be affected little by changes in βIII tubulin levels, despite having increased affinity for βIII (158). Overall, our data agree with published literature that shows βIII specific compounds are not exclusively affected by βIII expression levels. Since these compounds also bind to other tubulin isotypes, albeit with different affinities, a combined effect should be taken into account with the weights determined by the individual expression levels of the various tubulin isoforms in the cell line studied.

Lastly, we assessed if CR42-24 was synergistic with gem and cis. CR42-24 was synergistic with both gem and cis when given in a sequential manner. CR42-24 pretreatment of T24 cells sensitized them to CR42-24 killing. CR42-24/cis was highly synergistic showing CI values as low as 0.05. In addition, CR42-24 was also synergistic with gem. Gem pretreatment sensitized cells to CR42-24 killing. Surprisingly, low doses of CR42-24 were more highly effective on gem pretreated cells. The synergy of low dose CR42-24 and gem may be highly beneficial in a clinical setting. The pairing of CR42-24 and gem may allow for dose reduction of both drugs. The use of low dose CR42-24 and gem may be advantageous in patients with low tolerance for chemotherapy. These results are highly encouraging as pairing of novel compounds is necessary when moving into a clinical setting.

Overall, CR42-24 was highly effective against many different types of cancer. Specifically, CR42-24 was effective *in vitro* and *in vivo* on BC. This data supports that CR42-24 is be a promising therapeutic for BC. In addition, CR42-24s synergy with other compounds further supports the applicability of CR42-24 to be used in a clinical setting, since it is necessary to combine novel compounds with existing therapeutics. Overall BC has a poor prognosis, especially in the advanced disease setting. This is in part due to ineligibility for cisplatin-based therapy, inadequate response to therapies and limited second-line therapy options. This leaves a significant unmet clinical need for alternative therapies for bladder cancer. In this context, CR42-24 may provide a much-needed alternative for a neglected patient population.

4.2-Future work

Future work into CR42-24 could include examining CR42-24 in other animal models, in combination with other therapeutics, and researching the possibility of senescence induction in CAPAN-1, U87, and PC3 cell lines. To better represent a clinical setting, orthotopic animal models should be generated. As the majority of BC patients are diagnosed with NMIBC and undergo intravesical chemotherapy, assessment of CR42-24 in this setting would be beneficial. If effective, CR42-24 may provide an alternative therapy for patients who have disease recurrence or may serve as a better alternative treatment to mitomycin C or BCG. To perform these experiments orthotopic bladder tumors in mice or rats would be used as an experimental model. Intravesical instillation of CR42-24 could be performed and assessment of the effectiveness of CR42-24 as an intravesical therapy would be tested. Mitomycin C or BCG therapy would serve as beneficial control groups as it would provide insight into CR42-24s performance relative to currently used therapies. This assessment would be beneficial as it represents a more clinical setting, and it would indicate whether CR42-24 would be beneficial for NMIBC patients.

In addition to assessing CR42-24 as a treatment for NMIBC, CR24-24 also showed great promise as a therapy for pancreatic cancer. In-vitro screening indicated that CR24-24 was much more effective than gem on pancreatic cancer cell lines. As pancreatic cancer currently has the very poor prognosis and patients are in desperate need of alternative therapies, CR42-24 could be very beneficial to this patient population. Using xenograft models, the effects of CR42-24 on pancreatic tumors could be assessed. These experiments would support whether CR42-24 is an effective treatment for pancreatic cancer. Comparison to gem should also be performed as it is the current standard of care for pancreatic cancer. If *in vivo* data indicates CR42-24 is active against pancreatic cancer in animal models it could serve as an alternative therapy for an underserved patient population.

Further investigation into CR42-24 combination therapy would also be beneficial. In-vitro investigation showed that CR42-24 was highly synergistic with both gem and cis. Future experiments could investigate the optimal delivery schedule for CR42-24 with cis and gem. Since it has been shown that drug synergy is both schedule and cell line dependent, it would be beneficial to examine various schedules and doses of each compound to find the most synergistic combinations. Building on *in vitro* optimization, *in vivo* experiments should also be performed. In-vivo experiments comparing to published cis/gem schedules would allow for assessment of the effectiveness of CR42-24 combinations in animal models. In-vivo work would give further support using CR42-24 in a clinical setting as a treatment for BC. Moreover, it should give critical information moving forward into clinical trials. Clinical trials could be better informed and optimal scheduling and drug combinations could be employed moving forward into clinical trials.

In addition to synergy with chemotherapeutics, assessment of combination therapy with ICIs would also be very beneficial. ICIs have been found to be highly effective on BC and have started providing alternative therapies for patients. Moreover, ICIs are currently in multiple clinical trials in combination with chemotherapeutics and other agents. Assessment of CR42-24 and ICI synergy would be very beneficial as it could provide insight into the suitability of CR42-24 be used with ICIs. With the rapid expansion of ICIs in the treatment of BC, they will undoubtedly be employed in the treatment of BC patients. If CR42-24 would be effective in combination with ICIs it may be that CR42-24 can substitute currently used chemotherapy/ICI combinations. The benefit of CR42-24 substitution may be that of a reduced toxicity profile, or increased effectiveness.

In-vitro screening indicated that a number of cell lines were resistant to CR42-24 when assessed by resazurin assay. The cell lines U87, CAPAN-1, and PC3 all showed no reduction in cell viability when treated with CR42-24 for 72 hours. Moreover, PC3 and CAPAN-1 cell lines did not show significant reductions after 5 days of incubation with CR42-24. The addition of CyA did not sensitize these cell lines to CR42-24 killing suggesting that resistance is not mediated by MDR-1. A possible explanation for this is that CR42-24 is inducing cellular senescence. When in senescence, cells are still metabolically active but are non-proliferative. This is therefore a possible explanation as to why there was no reduction in cell viability in the resazurin assay. Several experiments could be performed to investigate the hypothesis that in these cell lines CR42-24 is inducing senescence. Clonogenic assays could be performed on these cell lines to confirm that cells when treated with CR42-24 are non-proliferative. If no colonies are formed than this would suggest that CR42-24 is still active against these cell lines and that they are not resistant. To corroborate further investigation could be done to examine treated cells for b-Galactosidase activity which is a marker for cellular senescence. Both luminescent and cell imaging based experiments could be performed to assess for B-Gal activity. Lastly, western blot analysis on p16, or p21 levels should be performed on cell lysates from cells treated with CR24-24. p16 and p21 have been found to be upregulated in senescent cells (183,184). The increased expression of p16 and p21 would confirm on a molecular level the induction of senescence in these cell lines.

To build on these experiments examination as to why CAPAN-1, PC3, and U87 cells become senescent while other cancer cell lines from similar types of cancer enter into apoptosis would be enlightening. Possible hypothesis may be that due to genetic or protein alterations these cell lines enter into senescence rather than apoptosis. It has been shown that alteration in apoptosis signaling result in the induction of senescence rather than apoptosis (185). Experiments have demonstrated that changes in the pro-apoptotic protein Bcl-2 or Caspases results in cells entering senescence rather than apoptosis (186). Similarly, telomerase expression in these cell lines may explain this phenomenon as telomerase overexpression has been found to protect cells from apoptosis (187). Investigation into cell line differences may allow identification of mechanisms of resistance to CR42-24. Identification of resistance mechanisms would allow the selection of patients that would not benefit from CR42-24 treatment, thereby sparing patients from undergoing unnecessary treatment.

References

1. Ribal MJ. Bladder Cancer Epidemiology. In: Bladder Tumors: [Internet]. Totowa, NJ: Humana Press; 2011 [cited 2018 Apr 30]. p. 1–22. Available from: http://link.springer.com/10.1007/978-1-60761-928-4_1

2. Bladder Cancer Facts | Bladder Cancer Canada [Internet]. [cited 2018 May 30]. Available from: https://bladdercancercanada.org/en/bladder-cancer-facts/

3. Bladder Cancer - Cancer Stat Facts [Internet]. [cited 2018 May 30]. Available from: https://seer.cancer.gov/statfacts/html/urinb.html

4. Sanli O, Dobruch J, Knowles MA, Burger M, Alemozaffar M, Nielsen ME, et al. Bladder cancer. Nat Rev Dis Prim. 2017;

5. Siegel RL, Jacobs EJ, Newton CC, Feskanich D, Freedman ND, Prentice RL, et al. Deaths Due to Cigarette Smoking for 12 Smoking-Related Cancers in the United States. JAMA Intern Med [Internet]. 2015 Sep 1 [cited 2018 May 17];175(9):1574. Available from: http://archinte.jamanetwork.com/article.aspx?doi=10.1001/jamainternmed.2015.2398

6. Alfred Witjes J, Lebret T, Compérat EM, Cowan NC, De Santis M, Bruins HM, et al. Updated 2016 EAU Guidelines on Muscle-invasive and Metastatic Bladder Cancer. Eur Urol [Internet]. 2017 Mar 1 [cited 2018 May 1];71(3):462–75. Available from: http://www.ncbi.nlm.nih.gov/pubmed/27375033

7. Willis D, Kamat AM. Nonurothelial Bladder Cancer and Rare Variant Histologies. Hematol Oncol Clin North Am [Internet]. 2015 Apr [cited 2018 May 30];29(2):237–52. Available from: http://www.ncbi.nlm.nih.gov/pubmed/25836932

8. Bladder Cancer: Statistics | Cancer.Net [Internet]. [cited 2018 Apr 3]. Available from: https://www.cancer.net/cancer-types/bladder-cancer/statistics

9. Babjuk M, Böhle A, Burger M, Capoun O, Cohen D, Compérat EM, et al. EAU Guidelines on Non-Muscle-invasive Urothelial Carcinoma of the Bladder: Update 2016. Eur Urol [Internet]. 2017 Mar 1 [cited 2018 May 30];71(3):447–61. Available from: http://www.ncbi.nlm.nih.gov/pubmed/27324428

10. Kamat AM, Bağcıoğlu M, Huri E. What is new in non-muscle-invasive bladder cancer in 2016? Turkish J Urol [Internet]. 2017 Mar [cited 2018 Apr 3];43(1):9–13. Available from: http://www.ncbi.nlm.nih.gov/pubmed/28270945

11. Porten SP, Leapman MS, Greene KL. Intravesical chemotherapy in non-muscle-invasive bladder cancer. Indian J Urol [Internet]. 2015 [cited 2018 May 30];31(4):297–303. Available from: http://www.ncbi.nlm.nih.gov/pubmed/26604440

12. Perlis N, Zlotta AR, Beyene J, Finelli A, Fleshner NE, Kulkarni GS. Immediumte Post–Transurethral Resection of Bladder Tumor Intravesical Chemotherapy Prevents Non–Muscle-invasive Bladder Cancer Recurrences: An Updated Meta-analysis on 2548 Patients and Quality-of-Evidence Review. Eur Urol [Internet]. 2013 Sep 1 [cited 2018 May 30];64(3):421–30. Available from: https://www.sciencedirect.com/science/article/pii/S0302283813006076?via%3Dihub

13. Sylvester R, Vandermeijden A, Witjes J, Kurth K. Bacillus Calmette-Guerin Versus Chemotherapy for The Intravesical Treatment Of Patients With Carcinoma In Situ Of The Bladder: A Meta-Analysis Of The Published Results Of Randomized Clinical Trials. J

Urol [Internet]. 2005 Jul [cited 2018 May 30];174(1):86–91. Available from: http://www.ncbi.nlm.nih.gov/pubmed/15947584

14. Shelley MD, Wilt TJ, Court J, Coles B, Kynaston H, Mason MD. Intravesical bacillus Calmette-Guérin is superior to mitomycin C in reducing tumour recurrence in high-risk superficial bladder cancer: a meta-analysis of randomized trials. BJU Int [Internet]. 2004 Mar [cited 2018 May 30];93(4):485–90. Available from: http://www.ncbi.nlm.nih.gov/pubmed/15008714

15. Zlotta AR, Fleshner NE, Jewett MA. The management of BCG failure in non-muscle-invasive bladder cancer: an update. Can Urol Assoc J [Internet]. 2009 Dec [cited 2018 Apr 3];3(6 Suppl 4):S199-205. Available from: http://www.ncbi.nlm.nih.gov/pubmed/20019985

16. Redelman-Sidi G, Glickman MS, Bochner BH. The mechanism of action of BCG therapy for bladder cancer—a current perspective. 2014 Mar 4 [cited 2018 Apr 3];11. Available from: http://www.nature.com/articles/nrurol.2014.15

17. Jackson A, Alexandroff A, Fleming D, Prescott S, Chisholm G, James K. Bacillus-calmette-guerin (bcg) organisms directly alter the growth of bladder-tumor cells. Int J Oncol [Internet]. 1994 Sep [cited 2018 May 30];5(3):697–703. Available from: http://www.ncbi.nlm.nih.gov/pubmed/21559633

18. Chen F, Zhang G, Iwamoto Y, See WA. BCG directly induces cell cycle arrest in human transitional carcinoma cell lines as a consequence of integrin cross-linking. BMC Urol [Internet]. 2005 Dec 12 [cited 2018 May 30];5(1):8. Available from:

http://bmcurol.biomedcentral.com/articles/10.1186/1471-2490-5-8

19. Han RF, Pan JG. Can intravesical bacillus Calmette-Guérin reduce recurrence in patients with superficial bladder cancer? A meta-analysis of randomized trials. Urology [Internet]. 2006 Jun [cited 2018 May 30];67(6):1216–23. Available from: http://www.ncbi.nlm.nih.gov/pubmed/16765182

20. Akaza H. Advancing NMIBC treatment beyond current BCG formulations. Nat Rev Urol [Internet]. 2017 Jan 6 [cited 2018 May 30];14(1):12–3. Available from: http://www.nature.com/articles/nrurol.2016.248

21. Kamat AM, Flaig TW, Grossman HB, Konety B, Lamm D, O'Donnell MA, et al. Consensus statement on best practice management regarding the use of intravesical immunotherapy with BCG for bladder cancer. Nat Rev Urol [Internet]. 2015 Apr 24 [cited 2018 May 31];12(4):225–35. Available from: http://www.nature.com/articles/nrurol.2015.58

22. Brooks NA, O'Donnell MA. Treatment options in non-muscle-invasive bladder cancer after BCG failure. Indian J Urol [Internet]. 2015 [cited 2018 May 31];31(4):312–9. Available from: http://www.ncbi.nlm.nih.gov/pubmed/26604442

23. Pardoll DM. The blockade of immune checkpoints in cancer immunotherapy. Nat Rev Cancer [Internet]. 2012 Apr 1 [cited 2018 Apr 3];12(4):252–64. Available from: http://www.nature.com/articles/nrc3239

24. Jamy O, Sonpavde G. Expert Opinion on Emerging Drugs Emerging first line treatment

options for bladder cancer: a review of phase II and III therapies in the pipeline Emerging first line treatment options for bladder cancer: a review of phase II and III therapies in the pipeline. 2017 [cited 2018 Apr 3]; Available from: http://www.tandfonline.com/action/journalInformation?journalCode=iemd20

25. Davarpanah NN, Yuno A, Trepel JB, Apolo AB. Immunotherapy: a new treatment paradigm in bladder cancer. Curr Opin Oncol [Internet]. 2017 Mar 16 [cited 2018 Apr 3];29(3):184. Available from: http://www.ncbi.nlm.nih.gov/pubmed/28306559

26. Yin M, Joshi M, Meijer RP, Glantz M, Holder S, Harvey HA, et al. Neoadjuvant Chemotherapy for Muscle-Invasive Bladder Cancer: A Systematic Review and Two-Step Meta-Analysis. Oncologist [Internet]. 2016 Jun 1 [cited 2018 May 18];21(6):708–15. Available from: http://www.ncbi.nlm.nih.gov/pubmed/27053504

27. Vale CL. Neoadjuvant Chemotherapy in Invasive Bladder Cancer: Update of a Systematic Review and Meta-Analysis of Individual Patient Data: Advanced Bladder Cancer (ABC) Meta-analysis Collaboration. Eur Urol [Internet]. 2005 Aug 1 [cited 2018 May 31];48(2):202–6. Available from: https://www.sciencedirect.com/science/article/pii/S0302283805002137?via%3Dihub

28. International Collaboration of Trialists IC of, Medical Research Council Advanced Bladder Cancer Working Party (now the National Cancer Research Institute Bladder Cancer Clinical Studies Group) the EO for R and T of CG-UTC, European Organisation for Research and Treatment of Cancer Genito-Urinary Tract Cancer Group the ABCS, Australian Bladder Cancer Study Group the NCI of CCT, National Cancer Institute of

Canada Clinical Trials Group, Finnbladder NBCS, et al. International phase III trial assessing neoadjuvant cisplatin, methotrexate, and vinblastine chemotherapy for muscle-invasive bladder cancer: long-term results of the BA06 30894 trial. J Clin Oncol [Internet]. 2011 Jun 1 [cited 2018 May 31];29(16):2171–7. Available from: http://www.ncbi.nlm.nih.gov/pubmed/21502557

29. Yuh BE, Ruel N, Wilson TG, Vogelzang N, Pal SK. Pooled Analysis of Clinical Outcomes with Neoadjuvant Cisplatin and Gemcitabine Chemotherapy for Muscle Invasive Bladder Cancer. JURO [Internet]. 2013 [cited 2018 May 31];189:1682–6. Available from: https://ac.els-cdn.com/S0022534712054298/1-s2.0-S0022534712054298-main.pdf?_tid=e1b6238c-3900-4d66-835f-52c3e7ded821&acdnat=1527783464_b8cc2f8b68f3a0b27cd5bfc96b526917

30. Lee FC, Harris W, Cheng HH, Shenoi J, Zhao S, Wang J, et al. Pathologic Response Rates of Gemcitabine/Cisplatin versus Methotrexate/Vinblastine/Adriamycin/Cisplatin Neoadjuvant Chemotherapy for Muscle Invasive Urothelial Bladder Cancer. Adv Urol [Internet]. 2013 Dec 8 [cited 2018 May 18];2013:317190. Available from: http://www.ncbi.nlm.nih.gov/pubmed/24382958

31. Hellmann MD, Ciuleanu T-E, Pluzanski A, Lee JS, Otterson GA, Audigier-Valette C, et al. Nivolumab plus Ipilimumab in Lung Cancer with a High Tumor Mutational Burden. N Engl J Med [Internet]. 2018 May 31 [cited 2018 May 31];378(22):2093–104. Available from: http://www.nejm.org/doi/10.1056/NEJMoa1801946

32. Gandhi L, Rodríguez-Abreu D, Gadgeel S, Esteban E, Felip E, De Angelis F, et al.

Pembrolizumab plus Chemotherapy in Metastatic Non–Small-Cell Lung Cancer. N Engl J Med [Internet]. 2018 May 31 [cited 2018 May 31];378(22):2078–92. Available from: http://www.nejm.org/doi/10.1056/NEJMoa1801005

33. Dwary AD, Master S, Patel A, Cole C, Mansour R, Mills G, et al. Excellent response to chemotherapy post immunotherapy. Oncotarget [Internet]. 2017 Oct 31 [cited 2018 May 31];8(53):91795–802. Available from: http://www.ncbi.nlm.nih.gov/pubmed/29207685

34. Massari F, Di Nunno V, Cubelli M, Santoni M, Fiorentino M, Montironi R, et al. Immune checkpoint inhibitors for metastatic bladder cancer. Cancer Treat Rev [Internet]. 2018 Mar 1 [cited 2018 May 1];64:11–20. Available from: http://www.ncbi.nlm.nih.gov/pubmed/29407369

35. Von Der Maase H, Sengelov L, Roberts JT, Ricci S, Dogliotti L, Oliver T, et al. Long-Term Survival Results of a Randomized Trial Comparing Gemcitabine Plus Cisplatin, With Methotrexate, Vinblastine, Doxorubicin, Plus Cisplatin in Patients With Bladder Cancer. J Clin Oncol [Internet]. [cited 2018 May 31];23:4602–8. Available from: http://citeseerx.ist.psu.edu/viewdoc/download?doi=10.1.1.1006.1004&rep=rep1&type=pf

36. Bamias A, Dafni U, Karadimou A, Timotheadou E, Aravantinos G, Psyrri A, et al. Prospective, open-label, randomized, phase iii study of two dose-dense regimens MVAC versus gemcitabine/ cisplatin in patients with inoperable, metastatic or relapsed urothelial cancer: A hellenic cooperative oncology group study (HE 16/03). Ann Oncol. 2013;

37. Bozovic-Spasojevic I, Azim HA, Paesmans M, Suter T, Piccart MJ, De Azambuja E. A consensus definition of patients with metastatic urothelial carcinoma who are unfit for

cisplatin-based chemotherapy. 2011 [cited 2018 May 31]; Available from: https://ac.els-cdn.com/S1470204510702758/1-s2.0-S1470204510702758-main.pdf?_tid=32bb5e72-505b-407a-8914-db4cb60e9681&acdnat=1527785054_7d9e78ee127d56d1f55f18dfaf23140c

38. Galsky MD, Chen GJ, Oh WK, Bellmunt J, Roth BJ, Petrioli R, et al. Comparative effectiveness of cisplatin-based and carboplatin-based chemotherapy for treatment of advanced urothelial carcinoma. Ann Oncol [Internet]. 2012 Feb 1 [cited 2018 May 31];23(2):406–10. Available from: https://academic.oup.com/annonc/article-lookup/doi/10.1093/annonc/mdr156

39. Ho GY, Woodward N, Coward JIG. Cisplatin versus carboplatin: comparative review of therapeutic management in solid malignancies. Crit Rev Oncol Hematol [Internet]. 2016 Jun 1 [cited 2018 May 1];102:37–46. Available from: http://linkinghub.elsevier.com/retrieve/pii/S1040842816300555

40. De Santis M, Bellmunt J, Mead G, Kerst JM, Leahy M, Maroto P, et al. Randomized phase II/III trial assessing gemcitabine/ carboplatin and methotrexate/carboplatin/vinblastine in patients with advanced urothelial cancer "unfit" for cisplatin-based chemotherapy: phase II--results of EORTC study 30986. J Clin Oncol [Internet]. 2009 Nov 20 [cited 2018 May 1];27(33):5634–9. Available from: http://ascopubs.org/doi/10.1200/JCO.2008.21.4924

41. Yafi Md FA, North S, Kassouf Md W. U R O L O G I C O N C O L O G Y First-and second-line therapy for metastatic urothelial carcinoma of the bladder. Curr Oncol. 18(1).

42. Joly F, Tchen N, Chevreau C, Henry-Amar M, Priou F, Chinet-Charrot P, et al. Clinical benefit of second line weekly paclitaxel in advanced urothelial carcinoma (AUC): A GETUG phase II study. J Clin Oncol [Internet]. 2004 Jul 15 [cited 2018 May 31];22(14_suppl):4619–4619. Available from: http://ascopubs.org/doi/10.1200/jco.2004.22.14_suppl.4619

43. Vaughn DJ, Broome CM, Hussain M, Gutheil JC, Markowitz AB. Phase II Trial of Weekly Paclitaxel in Patients With Previously Treated Advanced Urothelial Cancer. J Clin Oncol [Internet]. 2002 Feb 15 [cited 2018 May 31];20(4):937–40. Available from: http://www.ncbi.nlm.nih.gov/pubmed/11844814

44. Albers P, Park S-I, Niegisch G, Fechner G, Steiner U, Lehmann J, et al. Randomized phase III trial of 2nd line gemcitabine and paclitaxel chemotherapy in patients with advanced bladder cancer: short-term versus prolonged treatment [German Association of Urological Oncology (AUO) trial AB 20/99]. Ann Oncol [Internet]. 2011 Feb 1 [cited 2018 May 1];22(2):288–94. Available from: http://www.ncbi.nlm.nih.gov/pubmed/20682548

45. Bellmunt J, de Wit R, Vaughn DJ, Fradet Y, Lee J-L, Fong L, et al. Pembrolizumab as Second-Line Therapy for Advanced Urothelial Carcinoma. N Engl J Med [Internet]. 2017 [cited 2018 Apr 3];376(11):1015–26. Available from: http://www.ncbi.nlm.nih.gov/pubmed/28212060

46. Tsuruta H, Inoue T, Narita S, Horikawa Y, Saito M, Obara T, et al. Combination therapy consisting of gemcitabine, carboplatin, and docetaxel as an active treatment for advanced

urothelial carcinoma. Int J Clin Oncol [Internet]. 2011 Oct 23 [cited 2018 May 31];16(5):533–8. Available from: http://link.springer.com/10.1007/s10147-011-0224-4

47. Aydin AM, Woldu SL, Hutchinson RC, Boegemann M, Bagrodia A, Lotan Y, et al. Spotlight on atezolizumab and its potential in the treatment of advanced urothelial bladder cancer. Onco Targets Ther [Internet]. 2017 [cited 2018 Apr 3];10:1487–502. Available from: http://www.ncbi.nlm.nih.gov/pubmed/28331342

48. Petrylak DP, Powles T, Bellmunt J, Braiteh F, Loriot Y, Morales-Barrera R, et al. Atezolizumab (MPDL3280A) Monotherapy for Patients With Metastatic Urothelial Cancer. JAMA Oncol [Internet]. 2018 Feb 8 [cited 2018 Apr 3]; Available from: http://oncology.jamanetwork.com/article.aspx?doi=10.1001/jamaoncol.2017.5440

49. Rosenberg JE, Hoffman-Censits J, Powles T, van der Heijden MS, Balar A V, Necchi A, et al. Atezolizumab in patients with locally advanced and metastatic urothelial carcinoma who have progressed following treatment with platinum-based chemotherapy: a single-arm, multicentre, phase 2 trial. Lancet (London, England) [Internet]. 2016 May 7 [cited 2018 Apr 3];387(10031):1909–20. Available from: http://www.ncbi.nlm.nih.gov/pubmed/26952546

50. Balar A V, Castellano D, O'Donnell PH, Grivas P, Vuky J, Powles T, et al. First-line pembrolizumab in cisplatin-ineligible patients with locally advanced and unresectable or metastatic urothelial cancer (KEYNOTE-052): a multicentre, single-arm, phase 2 study. Lancet Oncol [Internet]. 2017 Nov 1 [cited 2018 Apr 3];18(11):1483–92. Available from: http://www.ncbi.nlm.nih.gov/pubmed/28967485

51. Plimack ER, Bellmunt J, Gupta S, Berger R, Chow LQM, Juco J, et al. Safety and activity of pembrolizumab in patients with locally advanced or metastatic urothelial cancer (KEYNOTE-012): a non-randomised, open-label, phase 1b study. Lancet Oncol [Internet]. 2017 Feb [cited 2018 Apr 3];18(2):212–20. Available from: http://www.ncbi.nlm.nih.gov/pubmed/28081914

52. Patel MR, Ellerton J, Infante JR, Agrawal M, Gordon M, Aljumaily R, et al. Avelumab in metastatic urothelial carcinoma after platinum failure (JAVELIN Solid Tumor): pooled results from two expansion cohorts of an open-label, phase 1 trial. Lancet Oncol. 2018;19(1).

53. Alsaab HO, Sau S, Alzhrani R, Tatiparti K, Bhise K, Kashaw SK, et al. PD-1 and PD-L1 Checkpoint Signaling Inhibition for Cancer Immunotherapy: Mechanism, Combinations, and Clinical Outcome. Front Pharmacol [Internet]. 2017 [cited 2018 Apr 3];8:561. Available from: http://www.ncbi.nlm.nih.gov/pubmed/28878676

54. Powles T, O'Donnell PH, Massard C, Arkenau H-T, Friedlander TW, Hoimes CJ, et al. Efficacy and Safety of Durvalumab in Locally Advanced or Metastatic Urothelial Carcinoma. JAMA Oncol [Internet]. 2017 Sep 14 [cited 2018 Apr 3];3(9):e172411. Available from: http://oncology.jamanetwork.com/article.aspx?doi=10.1001/jamaoncol.2017.2411

55. Durvalumab in Stage III Non–Small-Cell Lung Cancer. N Engl J Med [Internet]. 2018 Mar 28 [cited 2018 Apr 3];378(9):868–70. Available from: http://www.nejm.org/doi/10.1056/NEJMc1716426

56. Infante J, Ahlers CM, Hodi FS, Postel-Vinay S, Schellens JH, Heymach J V., et al. Abstract CT027: A phase I, open-label study of GSK3174998 administered alone and in combination with pembrolizumab in patients (pts) with selected advanced solid tumors (ENGAGE-1). Cancer Res [Internet]. 2016 Jul 15 [cited 2018 Apr 3];76(14 Supplement):CT027-CT027. Available from: http://cancerres.aacrjournals.org/lookup/doi/10.1158/1538-7445.AM2016-CT027

57. Leung YY, Yao Hui LL, Kraus VB. Colchicine--Update on mechanisms of action and therapeutic uses. Semin Arthritis Rheum [Internet]. 2015 Dec [cited 2018 May 1];45(3):341–50. Available from: http://www.ncbi.nlm.nih.gov/pubmed/26228647

58. Fojo T. The Role of Microtubules in Cell Biology, Neurobiology, and Oncology [Internet]. 2008. Available from: http://link.springer.com/10.1007/978-1-59745-336-3

59. Hastie SB. INTERACTIONS OF COLCHICINE WITH TUBULIN. Pharmac Ther [Internet]. 1991 [cited 2018 May 1];51:377–401. Available from: https://ac-els-cdn-com.login.ezproxy.library.ualberta.ca/016372589190067V/1-s2.0-016372589190067V-main.pdf?_tid=9b447bd4-b950-490f-9fe0-48b80babe09e&acdnat=1525206791_29724d18172fd3427c2f671888f735a6

60. Bhattacharyya B, Panda D, Gupta S, Banerjee M. Anti-Mitotic Activity of Colchicine and the Structural Basis for Its Interaction withTubulin. Med Res Rev Med Res Rev [Internet]. 2007 [cited 2018 Apr 27];28(1):155–83. Available from: https://onlinelibrary.wiley.com/doi/pdf/10.1002/med.20097

61. Cronstein BN, Molad Y, Reibman J, Balakhane E, Levin RI, Weissmann G. Colchicine

alters the quantitative and qualitative display of selectins on endothelial cells and neutrophils. J Clin Invest [Internet]. 1995 Aug [cited 2018 May 31];96(2):994–1002. Available from: http://www.ncbi.nlm.nih.gov/pubmed/7543498

62. Phelps P. Polymorphonuclear leukocyte motility in vitro: IV. Colchicine inhibition of chemotactic activity formation after phagocytosis of urate crystals. Arthritis Rheum [Internet]. 2008 Feb [cited 2018 May 31];58(S2):S25–33. Available from: http://www.ncbi.nlm.nih.gov/pubmed/18240263

63. Slobodnick A, Shah B, Pillinger MH, Krasnokutsky S. Colchicine: old and new. Am J Med [Internet]. 2015 May [cited 2018 May 1];128(5):461–70. Available from: http://www.ncbi.nlm.nih.gov/pubmed/25554368

64. Johnson L, Goping IS, Rieger A, Mane JY, Huzil T, Banerjee A, et al. Novel Colchicine Derivatives and their Anti-cancer Activity. Curr Top Med Chem [Internet]. 2017 Jul 26 [cited 2018 Apr 27];17(22). Available from: http://www.eurekaselect.com/148965/article

65. Lin Z-Y, Kuo C-H, Wu D-C, Chuang W-L. Anticancer effects of clinically acceptable colchicine concentrations on human gastric cancer cell lines. Kaohsiung J Med Sci [Internet]. 2016 Feb 1 [cited 2018 May 1];32(2):68–73. Available from: http://linkinghub.elsevier.com/retrieve/pii/S1607551X1500282X

66. Zhang L, Yang Z, Granieri L, Pasculescu A, Datti A, Asa SL, et al. High-throughput drug library screening identifies colchicine as a thyroid cancer inhibitor. Oncotarget [Internet]. 2016 Apr 12 [cited 2018 May 31];7(15):19948–59. Available from: http://www.ncbi.nlm.nih.gov/pubmed/26942566

67. Bhattacharya S, Das A, Datta S, Ganguli A, Chakrabarti G. Colchicine induces autophagy and senescence in lung cancer cells at clinically admissible concentration: potential use of colchicine in combination with autophagy inhibitor in cancer therapy. Tumor Biol [Internet]. 2016 Aug 11 [cited 2018 May 31];37(8):10653–64. Available from: http://www.ncbi.nlm.nih.gov/pubmed/26867767

68. HUANG Z, XU Y, PENG W. Colchicine induces apoptosis in HT-29 human colon cancer cells via the AKT and c-Jun N-terminal kinase signaling pathways. Mol Med Rep [Internet]. 2015 Oct [cited 2018 May 31];12(4):5939–44. Available from: http://www.ncbi.nlm.nih.gov/pubmed/26299305

69. Kuo M-C, Chang S-J, Hsieh M-C. Colchicine Significantly Reduces Incident Cancer in Gout Male Patients: A 12-Year Cohort Study. Medicine (Baltimore) [Internet]. 2015 Dec [cited 2018 May 31];94(50):e1570. Available from: http://www.ncbi.nlm.nih.gov/pubmed/26683907

70. Robinson SP, McIntyre DJO, Checkley D, Tessier JJ, Howe FA, Griffiths JR, et al. Tumour dose response to the antivascular agent ZD6126 assessed by magnetic resonance imaging. Br J Cancer [Internet]. 2003 May 13 [cited 2018 May 31];88(10):1592–7. Available from: http://www.ncbi.nlm.nih.gov/pubmed/12771928

71. Mccarty M, Takeda A, Stoeltzing O, Liu W, Fan F, Reinmuth N, et al. ZD6126 inhibits orthotopic growth and peritoneal carcinomatosis in a mouse model of human gastric cancer. Br J Cancer [Internet]. 2004 [cited 2018 May 31];90:705–11. Available from: https://www.nature.com/articles/6601490.pdf?origin=ppub

72. Kleespies A, Köhl G, Friedrich M, Ryan AJ, Barge A, Jauch K-W, et al. Vascular Targeting in Pancreatic Cancer: The Novel Tubulin-Binding Agent ZD6126 Reveals Antitumor Activity in Primary and Metastatic Tumor Models. Neoplasia [Internet]. 2005 Oct 1 [cited 2018 May 31];7(10):957–66. Available from: https://www.sciencedirect.com/science/article/pii/S1476558605801198

73. Davis PD, Dougherty GJ, Blakey DC, Galbraith SM, Tozer GM, Holder AL, et al. ZD6126: A Novel Vascular-targeting Agent That Causes Selective Destruction of Tumor Vasculature. CANCER Res [Internet]. 2002 [cited 2018 May 31];62:7247–53. Available from: http://cancerres.aacrjournals.org/content/canres/62/24/7247.full.pdf

74. Singh B, Kumar A, Joshi P, Guru SK, Kumar S, Wani ZA, et al. Organic & Biomolecular Chemistry Colchicine derivatives with potent anticancer activity and reduced P-glycoprotein induction liability. Org Biomol Chem [Internet]. 2015 [cited 2018 May 1];13. Available from: www.rsc.org/obc

75. Kim S-K, Cho S-M, Kim H, Seok H, Kim S-O, Kwon TK, et al. The colchicine derivative CT20126 shows a novel microtubule-modulating activity with apoptosis. Exp Mol Med [Internet]. 2013 Apr 19 [cited 2018 May 16];45(4):e19. Available from: http://www.ncbi.nlm.nih.gov/pubmed/23598593

76. Desai A, Mitchison TJ. MICROTUBULE POLYMERIZATION DYNAMICS. Annu Rev Cell Dev Biol [Internet]. 1997 Nov [cited 2018 May 31];13(1):83–117. Available from: http://www.ncbi.nlm.nih.gov/pubmed/9442869

77. Carlier MF, Pantaloni D. Kinetic analysis of guanosine 5’-triphosphate hydrolysis

associated with tubulin polymerization. Biochemistry [Internet]. 1981 Mar 31 [cited 2018 May 31];20(7):1918–24. Available from: http://www.ncbi.nlm.nih.gov/pubmed/7225365

78. Brouhard GJ, Rice LM. Microtubule dynamics: an interplay of biochemistry and mechanics. Nat Rev Mol Cell Biol [Internet]. 2018 Apr 19 [cited 2018 May 31];1. Available from: http://www.nature.com/articles/s41580-018-0009-y

79. Odde DJ, Cassimeris L, Buettner HM. Kinetics of microtubule catastrophe assessed by probabilistic analysis. Biophys J [Internet]. 1995 Sep [cited 2018 May 31];69(3):796–802. Available from: http://www.ncbi.nlm.nih.gov/pubmed/8519980

80. Coombes CE, Yamamoto A, Kenzie MR, Odde DJ, Gardner MK. Evolving Tip Structures Can Explain Age-Dependent Microtubule Catastrophe. Curr Biol [Internet]. 2013 Jul 22 [cited 2018 May 31];23(14):1342–8. Available from: http://www.ncbi.nlm.nih.gov/pubmed/23831290

81. Akhmanova A, Steinmetz MO. Tracking the ends: a dynamic protein network controls the fate of microtubule tips. Nat Rev Mol Cell Biol [Internet]. 2008 Apr 1 [cited 2018 May 31];9(4):309–22. Available from: http://www.ncbi.nlm.nih.gov/pubmed/18322465

82. Howard J, Hyman AA. Microtubule polymerases and depolymerases. Curr Opin Cell Biol [Internet]. 2007 Feb [cited 2018 May 31];19(1):31–5. Available from: http://www.ncbi.nlm.nih.gov/pubmed/17184986

83. Drummond DR. Regulation of microtubule dynamics by kinesins. Semin Cell Dev Biol [Internet]. 2011 Dec [cited 2018 May 31];22(9):927–34. Available from:

http://www.ncbi.nlm.nih.gov/pubmed/22001250

84. Akhmanova A, Steinmetz MO. Control of microtubule organization and dynamics: two ends in the limelight. Nat Rev Mol Cell Biol [Internet]. 2015 Dec 12 [cited 2018 May 31];16(12):711–26. Available from: http://www.nature.com/articles/nrm4084

85. Jordan MA, Wilson L. Microtubules as a target for anticancer drugs. Nat Rev Cancer. 2004;4(4):253–65.

86. Komlodi-Pasztor E, Sackett DL, Fojo AT. Inhibitors Targeting Mitosis: Tales of How Great Drugs against a Promising Target Were Brought Down by a Flawed Rationale. Clin Cancer Res [Internet]. 2012 Jan 1 [cited 2018 May 31];18(1):51–63. Available from: http://www.ncbi.nlm.nih.gov/pubmed/22215906

87. Jordan MA, Kamath K. How do microtubule-targeted drugs work? An overview. Curr Cancer Drug Targets [Internet]. 2007 Dec [cited 2018 May 31];7(8):730–42. Available from: http://www.ncbi.nlm.nih.gov/pubmed/18220533

88. Olziersky A-M, Labidi-Galy SI. Clinical Development of Anti-mitotic Drugs in Cancer. In Springer, Cham; 2017 [cited 2018 May 31]. p. 125–52. Available from: http://link.springer.com/10.1007/978-3-319-57127-0_6

89. Jordan MA, Toso RJ, Thrower D, Wilson L. Mechanism of mitotic block and inhibition of cell proliferation by taxol at low concentrations. Proc Natl Acad Sci U S A [Internet]. 1993 Oct 15 [cited 2018 May 31];90(20):9552–6. Available from: http://www.ncbi.nlm.nih.gov/pubmed/8105478

90. Thadani-Mulero M, Nanus DM, Giannakakou P. Androgen Receptor on the Move: Boarding the Microtubule Expressway to the Nucleus. Cancer Res [Internet]. 2012 Sep 15 [cited 2018 May 31];72(18):4611–5. Available from: http://www.ncbi.nlm.nih.gov/pubmed/22987486

91. Darshan MS, Loftus MS, Thadani-Mulero M, Levy BP, Escuin D, Zhou XK, et al. Taxane-Induced Blockade to Nuclear Accumulation of the Androgen Receptor Predicts Clinical Responses in Metastatic Prostate Cancer. Cancer Res [Internet]. 2011 Sep 15 [cited 2018 May 31];71(18):6019–29. Available from: http://www.ncbi.nlm.nih.gov/pubmed/21799031

92. Zhu M-L, Horbinski CM, Garzotto M, Qian DZ, Beer TM, Kyprianou N. Tubulin-Targeting Chemotherapy Impairs Androgen Receptor Activity in Prostate Cancer. Cancer Res [Internet]. 2010 Oct 15 [cited 2018 May 31];70(20):7992–8002. Available from: http://www.ncbi.nlm.nih.gov/pubmed/20807808

93. Poruchynsky MS, Komlodi-Pasztor E, Trostel S, Wilkerson J, Regairaz M, Pommier Y, et al. Microtubule-targeting agents augment the toxicity of DNA-damaging agents by disrupting intracellular trafficking of DNA repair proteins. Proc Natl Acad Sci [Internet]. 2015 Feb 3 [cited 2018 May 31];112(5):1571–6. Available from: http://www.ncbi.nlm.nih.gov/pubmed/25605897

94. Zasadil LM, Andersen KA, Yeum D, Rocque GB, Wilke LG, Tevaarwerk AJ, et al. Cytotoxicity of paclitaxel in breast cancer is due to chromosome missegregation on multipolar spindles. Sci Transl Med [Internet]. 2014 Mar 26 [cited 2018 May

21];6(229):229ra43. Available from: http://www.ncbi.nlm.nih.gov/pubmed/24670687

95. Dutcher SK. The tubulin fraternity: alpha to eta. Curr Opin Cell Biol [Internet]. 2001 Feb [cited 2018 May 31];13(1):49–54. Available from: http://www.ncbi.nlm.nih.gov/pubmed/11163133

96. Leandro-García LJ, Leskelä S, Landa I, Montero-Conde C, López-Jiménez E, Letón R, et al. Tumoral and tissue-specific expression of the major human β-tubulin isotypes. Cytoskeleton [Internet]. 2010 Apr [cited 2018 Apr 27];67(4):214–23. Available from: http://www.ncbi.nlm.nih.gov/pubmed/20191564

97. Sullivan KF. STRUCTURE AND UTILIZATION OF TUBULIN ISOTYPES. Ann Rev Cell Bioi [Internet]. 1988 [cited 2018 Jan 10];4:687–716. Available from: http://www.annualreviews.org/doi/pdf/10.1146/annurev.cb.04.110188.003351

98. Cowan NJ, Lewis SA, Gu W, Burgoyne RD. Tubulin isotypes and their interaction with microtubule associated proteins. Protoplasma [Internet]. 1988 Jun [cited 2018 May 31];145(2–3):106–11. Available from: http://link.springer.com/10.1007/BF01349346

99. JCB: Review. Rockefeller Univ Press J Cell Biol [Internet]. [cited 2018 May 31];206(4):461–72. Available from: www.jcb.org/cgi/doi/10.1083/jcb.201406055

100. Narishige T, Blade KL, Ishibashi Y, Nagai T, Hamawaki M, Menick DR, et al. Cardiac hypertrophic and developmental regulation of the beta-tubulin multigene family. J Biol Chem [Internet]. 1999 Apr 2 [cited 2018 May 16];274(14):9692–7. Available from: http://www.ncbi.nlm.nih.gov/pubmed/10092657

101. Lezama R, Castillo A, Ludueña RF, Meza I. Over-expression of βI tubulin in MDCK cells and incorporation of exogenous βI tubulin into microtubules interferes with adhesion and spreading. Cell Motil Cytoskeleton [Internet]. 2001 Nov [cited 2018 May 31];50(3):147–60. Available from: http://doi.wiley.com/10.1002/cm.10003

102. Armas-Portela R, Parrales MA, Albar JP, Martinez-A. C, Avila J. Distribution and Characteristics of βII Tubulin-Enriched Microtubules in Interphase Cells. Exp Cell Res [Internet]. 1999 May 1 [cited 2018 May 31];248(2):372–80. Available from: https://www.sciencedirect.com/science/article/pii/S0014482799944269

103. Pazour GJ, Agrin N, Leszyk J, Witman GB. Proteomic analysis of a eukaryotic cilium. J Cell Biol [Internet]. 2005 Jul 4 [cited 2018 May 31];170(1):103–13. Available from: http://www.ncbi.nlm.nih.gov/pubmed/15998802

104. Lu Q, Moore GD, Walss C, Ludueña RF. Structural and functional properties of tubulin isotypes. Adv Struct Biol [Internet]. 1999 Jan 1 [cited 2018 May 31];5:203–27. Available from: https://www.sciencedirect.com/science/article/pii/S1064600098800124

105. Thazhath R, Liu C, Gaertig J. Polyglycylation domain of β-tubulin maintains axonemal architecture and affects cytokinesis in Tetrahymena. Nat Cell Biol [Internet]. 2002 Mar 25 [cited 2018 May 31];4(3):256–9. Available from: http://www.ncbi.nlm.nih.gov/pubmed/11862218

106. Nielsen MG, Turner FR, Hutchens JA, Raff EC. Axoneme-specific β-tubulin specialization: a conserved C-terminal motif specifies the central pair. Curr Biol [Internet]. 2001 Apr 3 [cited 2018 May 31];11(7):529–33. Available from:

https://www.sciencedirect.com/science/article/pii/S0960982201001506

107. Wang D, Villasante A, Lewis SA, Cowan NJ. The mammalian beta-tubulin repertoire: hematopoietic expression of a novel, heterologous beta-tubulin isotype. J Cell Biol [Internet]. 1986 Nov [cited 2018 May 31];103(5):1903–10. Available from: http://www.ncbi.nlm.nih.gov/pubmed/3782288

108. Italiano JE, Bergmeier W, Tiwari S, Falet H, Hartwig JH, Hoffmeister KM, et al. Mechanisms and implications of platelet discoid shape. Blood [Internet]. 2003 Feb 27 [cited 2018 Jun 1];101(>12):4789–96. Available from: http://www.ncbi.nlm.nih.gov/pubmed/12586623

109. White JG, de Alarcon PA. Platelet spherocytosis: A new bleeding disorder. Am J Hematol [Internet]. 2002 Jun [cited 2018 Jun 1];70(2):158–66. Available from: http://www.ncbi.nlm.nih.gov/pubmed/12111791

110. Schwer HD, Lecine P, Tiwari S, Italiano JE, Hartwig JH, Shivdasani RA. A lineage-restricted and divergent beta-tubulin isoform is essential for the biogenesis, structure and function of blood platelets. Curr Biol [Internet]. 2001 Apr 17 [cited 2018 Jun 1];11(8):579–86. Available from: http://www.ncbi.nlm.nih.gov/pubmed/11369202

111. Mellon MG, Rebhun LI. Sulfhydryls and the in vitro polymerization of tubulin. J Cell Biol [Internet]. 1976 Jul [cited 2018 Jun 1];70(1):226–38. Available from: http://www.ncbi.nlm.nih.gov/pubmed/945278

112. Ludueiiasq RF, Roach$ MC, Jordanv MA, Murphy11 DB. THE JOURNAL OF

BIOLOGICAL CHEMISTRY Different Reactivities of Brain and Erythrocyte Tubulins toward a Sulfhydryl Group-directed Reagent That Inhibits Microtubule Assembly*. 1985 [cited 2018 Jun 1];260(2):1257–64. Available from: http://www.jbc.org/content/260/2/1257.full.pdf

113. Bai RL, Lin CM, Nguyen NY, Liu TY, Hamel E. Identification of the cysteine residue of beta-tubulin alkylated by the antimitotic agent 2,4-dichlorobenzyl thiocyanate, facilitated by separation of the protein subunits of tubulin by hydrophobic column chromatography. Biochemistry [Internet]. 1989 Jun 27 [cited 2018 Jun 1];28(13):5606–12. Available from: http://www.ncbi.nlm.nih.gov/pubmed/2775724

114. Stengel C, Newman SP, Leese MP, Potter BVL, Reed MJ, Purohit A. Class III β-tubulin expression and in vitro resistance to microtubule targeting agents. Br J Cancer [Internet]. 2010 Jan 22 [cited 2018 May 17];102(2):316–24. Available from: http://www.nature.com/articles/6605489

115. Zhao X, Yue C, Chen J, Tian C, Yang D, Xing L, et al. Class III β-Tubulin in Colorectal Cancer: Tissue Distribution and Clinical Analysis of Chinese Patients. Med Sci Monit [Internet]. 2016 Oct 23 [cited 2018 May 9];22:3915–24. Available from: http://www.ncbi.nlm.nih.gov/pubmed/27771732

116. Katsetos CD, Legido A, Perentes E, M SJ. The New Neuroembryology Class III β-Tubulin Isotype: A Key Cytoskeletal Protein at the Crossroads of Developmental Neurobiology and Tumor Neuropathology. [cited 2018 May 9]; Available from: http://journals.sagepub.com/doi/pdf/10.1177/088307380301801205

117. Carré M, André N, Carles G, Borghi H, Brichese L, Briand C, et al. Tubulin is an inherent component of mitochondrial membranes that interacts with the voltage-dependent anion channel. J Biol Chem [Internet]. 2002 Sep 13 [cited 2018 Jun 1];277(37):33664–9. Available from: http://www.ncbi.nlm.nih.gov/pubmed/12087096

118. Reuter S, Gupta SC, Chaturvedi MM, Aggarwal BB. Oxidative stress, inflammation, and cancer: how are they linked? Free Radic Biol Med [Internet]. 2010 Dec 1 [cited 2018 Jun 1];49(11):1603–16. Available from: http://www.ncbi.nlm.nih.gov/pubmed/20840865

119. Sosa V, Moliné T, Somoza R, Paciucci R, Kondoh H, LLeonart ME. Oxidative stress and cancer: An overview. Ageing Res Rev [Internet]. 2013 Jan [cited 2018 Jun 1];12(1):376–90. Available from: http://www.ncbi.nlm.nih.gov/pubmed/23123177

120. Aletta JM. Phosphorylation of type III beta-tubulin PC12 cell neurites during NGF-induced process outgrowth. J Neurobiol [Internet]. 1996 Dec [cited 2018 Jun 1];31(4):461–75. Available from: http://www.ncbi.nlm.nih.gov/pubmed/8951104

121. Jiang YQ, Oblinger MM. Differential regulation of beta III and other tubulin genes during peripheral and central neuron development. J Cell Sci [Internet]. 1992 Nov [cited 2018 Jun 1];103 (Pt 3):643–51. Available from: http://www.ncbi.nlm.nih.gov/pubmed/1478962

122. Fanarraga ML, Avila J, Zabala JC. Expression of unphosphorylated class III beta-tubulin isotype in neuroepithelial cells demonstrates neuroblast commitment and differentiation. Eur J Neurosci [Internet]. 1999 Feb [cited 2018 Jun 1];11(2):517–27. Available from: http://www.ncbi.nlm.nih.gov/pubmed/10073918

123. Asai DJ, Remolona NM. Tubulin isotype usage in vivo: a unique spatial distribution of the minor neuronal-specific beta-tubulin isotype in pheochromocytoma cells. Dev Biol [Internet]. 1989 Apr [cited 2018 Jun 1];132(2):398–409. Available from: http://www.ncbi.nlm.nih.gov/pubmed/2647542

124. Gard DL, Kirschner MW. A polymer-dependent increase in phosphorylation of beta-tubulin accompanies differentiation of a mouse neuroblastoma cell line. J Cell Biol [Internet]. 1985 Mar 1 [cited 2018 Jun 1];100(3):764–74. Available from: http://www.ncbi.nlm.nih.gov/pubmed/2857724

125. Minoura I, Takazaki H, Ayukawa R, Saruta C, Hachikubo Y, Uchimura S, et al. Reversal of axonal growth defects in an extraocular fibrosis model by engineering the kinesin–microtubule interface. Nat Commun [Internet]. 2016 Jan 18 [cited 2018 Jun 1];7:10058. Available from: http://www.nature.com/doifinder/10.1038/ncomms10058

126. Poirier K, Saillour Y, Bahi-Buisson N, Jaglin XH, Fallet-Bianco C, Nabbout R, et al. Mutations in the neuronal β-tubulin subunit TUBB3 result in malformation of cortical development and neuronal migration defects. Hum Mol Genet [Internet]. 2010 Nov 15 [cited 2018 Jun 1];19(22):4462–73. Available from: http://www.ncbi.nlm.nih.gov/pubmed/20829227

127. Whitman MC, Andrews C, Chan W-M, Tischfield MA, Stasheff SF, Brancati F, et al. Two unique *TUBB3* mutations cause both CFEOM3 and malformations of cortical development. Am J Med Genet Part A [Internet]. 2016 Feb [cited 2018 Jun 1];170(2):297–305. Available from: http://www.ncbi.nlm.nih.gov/pubmed/26639658

128. Lus Q, Luduena RF. In Vitro Analysis of Microtubule Assembly of Isotypically Pure Tubulin Dimers. J Biol Chem [Internet]. 1994 [cited 2018 Jun 1];269(3):2041–7. Available from: http://www.jbc.org/content/269/3/2041.full.pdf

129. Rezania V, Azarenko O, Jordan MA, Bolterauer H, Ludueña RF, Huzil JT, et al. Microtubule assembly of isotypically purified tubulin and its mixtures. Biophys J [Internet]. 2008 Aug [cited 2018 Jun 1];95(4):1993–2008. Available from: http://www.ncbi.nlm.nih.gov/pubmed/18502790

130. Hari M, Yang H, Zeng C, Canizales M, Cabral F. Expression of class III ?-tubulin reduces microtubule assembly and confers resistance to paclitaxel. Cell Motil Cytoskeleton [Internet]. 2003 Sep [cited 2018 Jun 1];56(1):45–56. Available from: http://doi.wiley.com/10.1002/cm.10132

131. Mariani M, Karki R, Spennato M, Pandya D, He S, Andreoli M, et al. Class III β-tubulin in normal and cancer tissues. Gene [Internet]. 2015 Jun 1 [cited 2018 May 9];563(2):109–14. Available from: https://www-sciencedirect-com.login.ezproxy.library.ualberta.ca/science/article/pii/S0378111915003674?via%3Dihub#f0005

132. Barbuti AM, Chen ZS. Paclitaxel through the ages of anticancer therapy: Exploring its role in chemoresistance and radiation therapy. Cancers. 2015.

133. Kavallaris M. Microtubules and resistance to tubulin-binding agents. Nat Rev Cancer [Internet]. 2010 Mar 11 [cited 2018 Jan 10];10(3):194–204. Available from: http://www.nature.com/doifinder/10.1038/nrc2803

134. McCarroll JA, Gan PP, Liu M, Kavallaris M. βIII-tubulin is a multifunctional protein involved in drug sensitivity and tumorigenesis in non-small cell lung cancer. Cancer Res. 2010;

135. Yu J, Gao J, Lu Z, Li Y, Shen L. Serum levels of TUBB3 correlate with clinical outcome in Chinese patients with advanced gastric cancer receiving first-line paclitaxel plus capecitabine. Med Oncol [Internet]. 2012 Dec 6 [cited 2018 May 9];29(5):3029–34. Available from: http://link.springer.com/10.1007/s12032-012-0292-y

136. Ranganathan S, Dexter DW, Benetatos CA, Chapman AE, Tew KD, Hudes GR, et al. Increase of beta(III)- and beta(IVa)-tubulin isotopes in human prostate carcinoma cells as a result of estramustine resistance. Cancer Res [Internet]. 1996 Jun 1 [cited 2018 May 21];56(11):2584–9. Available from: http://www.ncbi.nlm.nih.gov/pubmed/8653701

137. Terry S, Ploussard G, Allory Y, Nicolaiew N, Boissière-Michot F, Maillé P, et al. Increased expression of class III β-tubulin in castration-resistant human prostate cancer. Br J Cancer [Internet]. 2009 Sep 18 [cited 2018 Jun 1];101(6):951–6. Available from: http://www.nature.com/articles/6605245

138. Leng X-F, Chen M-W, Xian L, Dai L, Ma G-Y, Li M-H. Combined analysis of mRNA expression of ERCC1, BAG-1, BRCA1, RRM1 and TUBB3 to predict prognosis in patients with non-small cell lung cancer who received adjuvant chemotherapy. J Exp Clin Cancer Res [Internet]. 2012 Mar 23 [cited 2018 May 9];31(1):25. Available from: http://jeccr.biomedcentral.com/articles/10.1186/1756-9966-31-25

139. βIII-tubulin overexpression is linked to aggressive tumor features and genetic instability in

urinary bladder cancer. Hum Pathol [Internet]. 2017 Mar 1 [cited 2017 Nov 24];61:210–20. Available from: http://www.sciencedirect.com/science/article/pii/S0046817716303513?via%3Dihub

140. Galmarini CM, Treilleux I, Cardoso F, Bernard-Marty C, Durbecq V, Gancberg D, et al. Class III -Tubulin Isotype Predicts Response in Advanced Breast Cancer Patients Randomly Treated Either with Single-Agent Doxorubicin or Docetaxel. Clin Cancer Res [Internet]. 2008 Jul 15 [cited 2018 Jun 1];14(14):4511–6. Available from: http://www.ncbi.nlm.nih.gov/pubmed/18628466

141. Aoki D, Oda Y, Hattori S, Taguchi K, Ohishi Y, Basaki Y, et al. Overexpression of class III beta-tubulin predicts good response to taxane-based chemotherapy in ovarian clear cell adenocarcinoma. Clin Cancer Res [Internet]. 2009 Feb 15 [cited 2018 Jun 1];15(4):1473–80. Available from: http://www.ncbi.nlm.nih.gov/pubmed/19228748

142. Akasaka K, Maesawa C, Shibazaki M, Maeda F, Takahashi K, Akasaka T, et al. Loss of Class III b-Tubulin Induced by Histone Deacetylation Is Associated with Chemosensitivity to Paclitaxel in Malignant Melanoma Cells. J Invest Dermatol [Internet]. 2009 [cited 2018 Jun 1];129406(10):1516–26. Available from: https://ac.els-cdn.com/S0022202X15343803/1-s2.0-S0022202X15343803-main.pdf?_tid=76ad14bf-2829-498a-a385-4db34228fad4&acdnat=1527870672_1271235ea07d498640b2033ce15a9a14

143. Edelman M, Schneider C-P, Krankenhaus DM, Tsai C-M. Randomized Phase II Study of Ixabepilone or Paclitaxel Plus Carboplatin in Patients With Non-Small-Cell Lung Cancer

Prospectively Stratified by Beta-3 Tubulin Status. Artic J Clin Oncol [Internet]. 2013 [cited 2018 May 9]; Available from: https://www.researchgate.net/publication/236186141

144. Katsetos CD, Legido A, Perentes E, Mörk SJ. Class III β-Tubulin Isotype: A Key Cytoskeletal Protein at the Crossroads of Developmental Neurobiology and Tumor Neuropathology. J Child Neurol [Internet]. 2003 Dec 2 [cited 2018 Jun 1];18(12):851–66. Available from: http://www.ncbi.nlm.nih.gov/pubmed/14736079

145. Karki R, Mariani M, Andreoli M, He S, Scambia G, Shahabi S, et al. βIII-Tubulin: biomarker of taxane resistance or drug target? Expert Opin Ther Targets [Internet]. 2013 Apr 2 [cited 2018 Jun 1];17(4):461–72. Available from: http://www.tandfonline.com/doi/full/10.1517/14728222.2013.766170

146. Ploussard G, Terry S, Maille P, Allory Y, Sirab N, Kheuang L, et al. Class III -Tubulin Expression Predicts Prostate Tumor Aggressiveness and Patient Response to Docetaxel-Based Chemotherapy. Cancer Res [Internet]. 2010 Nov 15 [cited 2018 Jun 1];70(22):9253–64. Available from: http://www.ncbi.nlm.nih.gov/pubmed/21045157

147. Brabletz T, Jung A, Reu S, Porzner M, Hlubek F, Kunz-Schughart LA, et al. Variable beta-catenin expression in colorectal cancers indicates tumor progression driven by the tumor environment. Proc Natl Acad Sci U S A [Internet]. 2001 Aug 28 [cited 2018 Mar 28];98(18):10356–61. Available from: http://www.ncbi.nlm.nih.gov/pubmed/11526241

148. Koh Y, Jang B, Han S-W, Kim T-M, Oh D-Y, Lee S-H, et al. Expression of Class III Beta-Tubulin Correlates with Unfavorable Survival Outcome in Patients with Resected Non-small Cell Lung Cancer. J Thorac Oncol [Internet]. 2010 [cited 2018 Jun 1];5:320–5.

Available from: https://ac.els-cdn.com/S1556086415323030/1-s2.0-S1556086415323030-main.pdf?_tid=4444eaaf-97e7-42c1-8951-971efba983ae&acdnat=1527871888_5f8b59a15b575f8bebb6dcfd2f86b38c

149. Katsetos CD, Del Valle L, Geddes JF, Assimakopoulou M, Legido A, Boyd JC, et al. Aberrant localization of the neuronal class III beta-tubulin in astrocytomas. Arch Pathol Lab Med [Internet]. 2001 May [cited 2018 Jun 1];125(5):613–24. Available from: http://www.ncbi.nlm.nih.gov/pubmed/11300931

150. Raspaglio G, Petrillo M, Martinelli E, Li Puma DD, Mariani M, De Donato M, et al. Sox9 and Hif-2α regulate TUBB3 gene expression and affect ovarian cancer aggressiveness. Gene [Internet]. 2014 Jun 1 [cited 2018 May 9];542(2):173–81. Available from: https://www.sciencedirect.com/science/article/pii/S0378111914003485

151. Raspaglio G, Filippetti F, Prislei S, Penci R, De Maria I, Cicchillitti L, et al. Hypoxia induces class III beta-tubulin gene expression by HIF-1α binding to its 3’ flanking region. Gene [Internet]. 2008 Feb 15 [cited 2018 Jun 1];409(1–2):100–8. Available from: https://www.sciencedirect.com/science/article/pii/S0378111907005902

152. Axelson H, Fredlund E, Ovenberger M, Landberg G, Påhlman S. Hypoxia-induced dedifferentiation of tumor cells – A mechanism behind heterogeneity and aggressiveness of solid tumors. Semin Cell Dev Biol [Internet]. 2005 Aug 1 [cited 2018 Jun 1];16(4–5):554–63. Available from: https://www.sciencedirect.com/science/article/pii/S1084952105000595

153. Chouaib S, Noman M, Kosmatopoulos K, Curran M. Hypoxic stress: obstacles and

opportunities for innovative immunotherapy of cancer. Oncogene [Internet]. 2017 [cited 2018 Jun 1];36. Available from: https://www.nature.com/articles/onc2016225.pdf?origin=ppub

154. Vaupel P. The role of hypoxia-induced factors in tumor progression. Oncologist [Internet]. 2004 Nov 1 [cited 2018 Jun 1];9 Suppl 5(Supplement 5):10–7. Available from: http://www.ncbi.nlm.nih.gov/pubmed/15591418

155. Tang Y, Rodríguez-Salarichs J, Zhao Y, Cai P, Estévez-Gallego J, Balaguer-Pérez F, et al. Modification of C-seco taxoids through ring tethering and substituent replacement leading to effective agents against tumor drug resistance mediumted by βIII-Tubulin and P-glycoprotein (P-gp) overexpressions. Eur J Med Chem [Internet]. 2017 Sep 8 [cited 2018 May 9];137:488–503. Available from: http://www.ncbi.nlm.nih.gov/pubmed/28624703

156. Ferlini C, Raspaglio G, Mozzetti S, Cicchillitti L, Filippetti F, Gallo D, et al. The Seco-Taxane IDN5390 Is Able to Target Class III β-Tubulin and to Overcome Paclitaxel Resistance. Cancer Res [Internet]. 2005 Mar 15 [cited 2018 May 9];65(6):2397–405. Available from: http://www.ncbi.nlm.nih.gov/pubmed/15781655

157. Pepe A, Sun L, Zanardi I, Wu X, Ferlini C, Fontana G, et al. No Title. 2009 Jun 15 [cited 2018 May 9];19(12). Available from: http://www.ncbi.nlm.nih.gov/pubmed/19423340

158. Cai P, Lu P, Sharom FJ, Fang W-S. A semisynthetic taxane Yg-3-46a effectively evades P-glycoprotein and β-III tubulin mediumted tumor drug resistance in vitro. Cancer Lett [Internet]. 2013 Dec 1 [cited 2018 May 9];341(2):214–23. Available from: http://www.ncbi.nlm.nih.gov/pubmed/23941826

159. Druley TE, Stein WD, Ruth A, Roninson IB. P-glycoprotein-mediumted colchicine resistance in different cell lines correlates with the effects of colchicine on P-glycoprotein conformation. Biochemistry [Internet]. 2001 Apr 10 [cited 2018 Jun 1];40(14):4323–31. Available from: http://www.ncbi.nlm.nih.gov/pubmed/11284688

160. Sood AK, Sorosky JI, Squatrito RC, Skilling JS, Anderson B, Buller RE. Cyclosporin A reverses chemoresistance in patients with gynecologic malignancies. Neoplasia [Internet]. 1999 Jun [cited 2018 Jun 1];1(2):118–22. Available from: http://www.ncbi.nlm.nih.gov/pubmed/10933045

161. Borst P, Evers R, Kool M, Wijnholds J. A Family of Drug Transporters: the Multidrug Resistance-Associated Proteins. JNCI J Natl Cancer Inst [Internet]. 2000 Aug 16 [cited 2018 Jun 1];92(16):1295–302. Available from: https://academic.oup.com/jnci/article-lookup/doi/10.1093/jnci/92.16.1295

162. David KA, Milowsky MI, Nanus DM. Chemotherapy for Non–Clear-Cell Renal Cell Carcinoma. Clin Genitourin Cancer [Internet]. 2006 Mar [cited 2018 Jun 1];4(4):263–8. Available from: http://www.ncbi.nlm.nih.gov/pubmed/16729909

163. Diamond E, Molina AM, Carbonaro M, Akhtar NH, Giannakakou P, Tagawa ST, et al. Cytotoxic chemotherapy in the treatment of advanced renal cell carcinoma in the era of targeted therapy. Crit Rev Oncol Hematol [Internet]. 2015 Dec 1 [cited 2018 Jun 1];96(3):518–26. Available from: http://linkinghub.elsevier.com/retrieve/pii/S1040842815300226

164. Yu DS, Chang SY, Ma CP. The expression of mdr-1-related gp-170 and its correlation

with anthracycline resistance in renal cell carcinoma cell lines and multidrug-resistant sublines. Br J Urol [Internet]. 1998 Oct [cited 2018 Jun 1];82(4):544–7. Available from: http://www.ncbi.nlm.nih.gov/pubmed/9806185

165. Razmik Mirzayans DM, Mirzayans R. Role of Therapy-Induced Cellular Senescence in Tumor Cells and its Modification in Radiotherapy: The Good, The Bad and The Ugly. J Nucl Med Radiat Ther [Internet]. 2013 Oct 22 [cited 2018 Jun 1];s6(01). Available from: https://www.omicsonline.org/role-of-therapy-induced-cellular-senescence-in-tumor-cells-and-its-modification-in-radiotherapy-2155-9619.S6-018.php?aid=19607

166. Ewald JA, Desotelle JA, Wilding G, Jarrard DF. Therapy-induced senescence in cancer. J Natl Cancer Inst [Internet]. 2010 Oct 20 [cited 2018 Jun 1];102(20):1536–46. Available from: http://www.ncbi.nlm.nih.gov/pubmed/20858887

167. Yang S, Hwang S, Kim M, Seo S Bin, Lee J-H, Jeong SM. Mitochondrial glutamine metabolism via GOT2 supports pancreatic cancer growth through senescence inhibition. Cell Death Dis [Internet]. 2018 Feb 19 [cited 2018 Jun 1];9(2):55. Available from: http://www.nature.com/articles/s41419-017-0089-1

168. Song Y, Baba T, Mukaida N. Gemcitabine induces cell senescence in human pancreatic cancer cell lines. Biochem Biophys Res Commun [Internet]. 2016 Aug 26 [cited 2018 Jun 1];477(3):515–9. Available from: http://www.ncbi.nlm.nih.gov/pubmed/27311854

169. Kumar R, Gont A, Perkins TJ, Hanson JEL, Lorimer IAJ. Induction of senescence in primary glioblastoma cells by serum and TGFβ. Sci Rep [Internet]. 2017 Dec 19 [cited 2018 Jun 1];7(1):2156. Available from: http://www.nature.com/articles/s41598-017-

02380-1

170. Ouchi R, Okabe S, Migita T, Nakano I, Seimiya H. Senescence from glioma stem cell differentiation promotes tumor growth. Biochem Biophys Res Commun [Internet]. 2016 Feb 5 [cited 2018 Jun 1];470(2):275–81. Available from: http://www.ncbi.nlm.nih.gov/pubmed/26775840

171. Taddei ML, Cavallini L, Comito G, Giannoni E, Folini M, Marini A, et al. Senescent stroma promotes prostate cancer progression: The role of miR-210. Mol Oncol [Internet]. 2014 Dec 1 [cited 2018 Jun 1];8(8):1729–46. Available from: https://www.sciencedirect.com/science/article/pii/S1574789114001641

172. Blute ML, Damaschke N, Wagner J, Yang B, Gleave M, Fazli L, et al. Persistence of senescent prostate cancer cells following prolonged neoadjuvant androgen deprivation therapy. PLoS One [Internet]. 2017 [cited 2018 Jun 1];12(2):e0172048. Available from: http://www.ncbi.nlm.nih.gov/pubmed/28234906

173. Besançon OG, Tytgat GAM, Meinsma R, Leen R, Hoebink J, Kalayda G V., et al. Synergistic interaction between cisplatin and gemcitabine in neuroblastoma cell lines and multicellular tumor spheroids. Cancer Lett [Internet]. 2012 Jun 1 [cited 2018 Jun 1];319(1):23–30. Available from: http://www.ncbi.nlm.nih.gov/pubmed/22182450

174. Moufarij MA, Phillips DR, Cullinane C. Gemcitabine potentiates cisplatin cytotoxicity and inhibits repair of cisplatin-DNA damage in ovarian cancer cell lines. Mol Pharmacol [Internet]. 2003 Apr [cited 2018 Jun 1];63(4):862–9. Available from: http://www.ncbi.nlm.nih.gov/pubmed/12644587

175. van Moorsel CJ, Pinedo HM, Veerman G, Vermorken JB, Postmus PE, Peters GJ. Scheduling of gemcitabine and cisplatin in Lewis lung tumour bearing mice. Eur J Cancer [Internet]. 1999 May [cited 2018 Jun 1];35(5):808–14. Available from: http://www.ncbi.nlm.nih.gov/pubmed/10505043

176. Jordan MA, Thrower D, Wilson L. Mechanism of inhibition of cell proliferation by Vinca alkaloids. Cancer Res [Internet]. 1991 Apr 15 [cited 2018 Apr 27];51(8):2212–22. Available from: http://www.ncbi.nlm.nih.gov/pubmed/2009540

177. Kim S-K, Cho S-M, Kim H, Seok H, Kim S-O, Kwon TK, et al. The colchicine derivative CT20126 shows a novel microtubule-modulating activity with apoptosis. Exp Mol Med [Internet]. 2013 [cited 2018 Apr 27];4538. Available from: https://www.nature.com/articles/emm201338.pdf

178. Silva R, Carmo H, Vilas-Boas V, Barbosa DJ, Palmeira A, Sousa E, et al. Colchicine effect on P-glycoprotein expression and activity: In silico and in vitro studies. Chem Biol Interact [Internet]. 2014 Jul 25 [cited 2018 Jun 1];218:50–62. Available from: http://www.ncbi.nlm.nih.gov/pubmed/24759273

179. Uludag A, Silan C, Atik S, Akurut C, Uludag A, Silan F, et al. Relationship Between Response to Colchicine Treatment and *MDR1* Polymorphism in Familial Mediterranean Fever Patients. Genet Test Mol Biomarkers [Internet]. 2014 Feb [cited 2018 Jun 1];18(2):73–6. Available from: http://www.ncbi.nlm.nih.gov/pubmed/24180297

180. Zhang Y-K, Wang Y-J, Gupta P, Chen Z-S. Multidrug Resistance Proteins (MRPs) and Cancer Therapy. AAPS J [Internet]. 2015 Jul 4 [cited 2018 May 21];17(4):802–12.

Available from: http://link.springer.com/10.1208/s12248-015-9757-1

181. Hasegawa ' S, Abe2 T, Naito ' S, Kotohl S, Kumazawal J, Hipfner3 D, et al. Expression of multidrug resistance-associated protein (jMRP), MDR1 and DNA topoisomerase II in human multidrug-resistant bladder cancer cell lines. i Jaon dCf cer [Internet]. [cited 2017 Nov 22];7:907–13. Available from: https://www.nature.com/articles/bjc1995177.pdf

182. Hamaguchi K, Godwin AK, Yakushiji M, O 'dwyer PJ, Ozols RF, Hamilton2 TC. Cross-Resistance to Diverse Drugs Is Associated with Primary Cisplatin Resistance in Ovarian Cancer Cell Lines1. CANCER Res. 1993;53:5225–32.

183. Acosta, J. C., & Gil, J. S. (2011). Senescence: a new weapon for cancer therapy. *Trends in Cell Biology*, *22*, 211–219. https://doi.org/10.1016/j.tcb.2011.11.006

184. Bhattacharya, S., Das, A., Datta, S., Ganguli, A., & Chakrabarti, G. (2016). Colchicine induces autophagy and senescence in lung cancer cells at clinically admissible concentration: potential use of colchicine in combination with autophagy inhibitor in cancer therapy. *Tumor Biology*, *37*(8), 10653–10664. https://doi.org/10.1007/s13277-016-4972-7

185. Ewald, J. A., Desotelle, J. A., Wilding, G., & Jarrard, D. F. (2010). Therapy-induced senescence in cancer. *Journal of the National Cancer Institute*, *102*(20), 1536–1546. https://doi.org/10.1093/jnci/djq364

186. Vicencio, J. M., Galluzzi, L., Tajeddine, N., Ortiz, C., Criollo, A., Tasdemir, E., … Kroemer, G. (2008). Senescence, apoptosis or autophagy? When a damaged cell must decide its path--a mini-review. *Gerontology*, *54*(2), 92–99. https://doi.org/10.1159/000129697

187. Shawi, M., & Autexier, C. (2008). Telomerase, senescence and ageing. *Mechanisms of Ageing and Development*, *129*(1–2), 3–10. https://doi.org/10.1016/j.mad.2007.11.007